FAULT DETECTION AND ISOLATION FOR WIND TURBINE DYNAMIC SYSTEMS

YUSHENG LIU

A thesis submitted in partial fulfilment of the requirements of the Liverpool John Moores University for the degree of Doctor of Philosophy

October 2017

ABSTRACT

This work presents two fault detection and isolation (FDI) approaches for wind turbine systems (WTS). Firstly, a non-linear mathematical model for wind turbine (WT) dynamics is developed. Based on the developed WTS mathematical model, a robust fault detection observer is designed to estimate system faults, so as to generate residuals. The observer is designed to be robust to system disturbance and sensitive to system faults. A WT blade pitch system fault, a drive-train system gearbox fault and three sensor faults are simulated to the nominal system model, and the designed observer is then to detect these faults when the system is subjected to disturbance. The simulation results showed that the simulated faults are successfully detected.

In addition, a neural network (NN) method is proposed for WTS fault detection and isolation. Two radial basis function (RBF) networks are employed in this method. The first NN is used to generate the residual from system input/output data. A second NN is used as a classifier to isolate the faults. The classifier is trained to achieve the following target: the output are all “0”s for no fault case; while the output is “1” if the corresponding fault occurs. The performance of the developed neural network FDI method was evaluated using the simulated three sensor faults. The simulation results demonstrated these faults are successfully detected and isolated by the NN classifier.

ACKNOWLEDGEMENT

Firstly, I would like to express my sincere gratitude to my supervisor **Prof. Dingli Yu** for the continuous support of my Ph.D study and related research, for his patience, motivation, and immense knowledge. His guidance helped me in all the time of research and writing of this thesis. I could not have imagined having a better advisor and mentor for my Ph.D study.

Besides **Prof. Yu**, I would like to thank my second supervisor: **Dr. David Allanson**, for his insightful comments and encouragement, but also for the hard question which motivated me to widen my research from various perspectives.

A special thanks to my **father Yongchang Liu**, my **mother Xiaojie Wu**, my dearest **wife Yuxuan Su** and my lovely **son Lucas Liu** for their endless support and motivation throughout my Ph.D study. Without their constant assurance and assistance, completion of this research would have not been possible. And as a sign of my love, gratitude and affection I dedicated this thesis to them appreciating their immense contribution towards the success of my Ph.D thesis for these years.

Thanks to you all.

Yusheng Liu

TABLE OF CONTENTS

LIST OF FIGURES

LIST OF ABBREVIATIONS

AE	Acoustic Emission
ANN	Artificial Neural Network
BFDF	Beard Fault Detection Filter
CSTR	Continuous Stirred-Tank Reactor
DES	Discrete Event System
DWT	Discrete Wavelet Transform
FBG	Fiber-optic Bragg Grating
FBS	Function-Behaviour-State
FDI	Fault Detection and Isolation
FE	Finite-Element
FFT	Faster Fourier Transform
LS	Least Squares
MAE	Mean Absolute Error
MBR	Model-Based Reasoner
MIMO	Multiple-Inputs Multiple-Outputs
MLP	Multi-Layer Perceptron
MSE	Mean Square Error
NN	Neural Network
RBF	Radial Basis Function
RLS	Recursive Least Squares
WT	Wind Turbine
WTS	Wind Turbine System

LIST OF TABLES

LIST OF SYMBOLS

A	Area covered by the rotor
R	Radius of the rotor disc
ρ	Air density
v	Speed of the wind
P_w	Available power by rotor
C_p	Power coefficient
P_r	Rotor power
λ	Tip-speed ratio
β_{ref}	Reference blade pitch angle
β	Blade pitch angle
T_r	Rotor torque
ω_n	Natural frequency of pitch actuator
ζ	Damping ratio of pitch actuator
N	Gear ratio
I_r	Moment of inertia of rotor
I_g	Moment of inertia of generator
D_s	Driveshaft dampening constant
K_s	Driveshaft spring constant
T_g	Generator torque

J	Blade inertia
b	Friction factor
c_j	RBF neural network center
σ	RBF neural network width

CHAPTER 1
INTRODUCTION

1.1 Background

The usage of wind energy or wind power by humans has a long history. The earliest design of windmill was developed in Persia about 500 – 900 A.D. for grain-grinding and water-pumping (Dodge, n. d.). In late July 1887, the first electricity generating wind turbine in the world was installed (Price, 2005). One of the biggest advantages of wind energy is that it is a renewable energy. The renewable energy is generally defined as energy from the resources which are continually replenished by nature on a human timescale such as thermal, wind, hydraulic and tides (Ellabban et al., 2014). Due to the heavy pollution production of the traditional fossil fuels, the utilisation of renewable energy for electrical production has been developed worldwide. It is estimated that about 208 GW of new electric capacity which is produced by renewable energy had been installed globally and a total of more than 1360GW of renewable energy capacity had been reached in 2011. For non-hydro renewable energy, the capacity exceeded 390GW, which is a 24% increase compared with 2010. Globally, wind power contributed nearly 40% of new renewable capacity, solar PV accounted for almost 30% and hydropower nearly 25%. By the end of 2011, more than 25% of the total global power generating capacity was renewable energy capacity and it supplied approximately 20.3% of global electricity (REN21, 2011).

Wind as a renewable energy source is a significant aspect of renewable energy and has been given more and more attention and plays an increasingly important role in the energy industry nowadays because of its inherent attribute of generating carbon-free electricity. Until 2011 there were in total 306 operational wind farms in the UK, which generated 5,737.60 MW of power to the grid (REN21, 2011). In 2013, the wind power capacity added more than 35 GW, for a total above 318 GW. In the last five years, all kinds of renewable energy were increased significantly but wind power has added the most capacity of all renewable technologies over this period. (REN21, 2014)

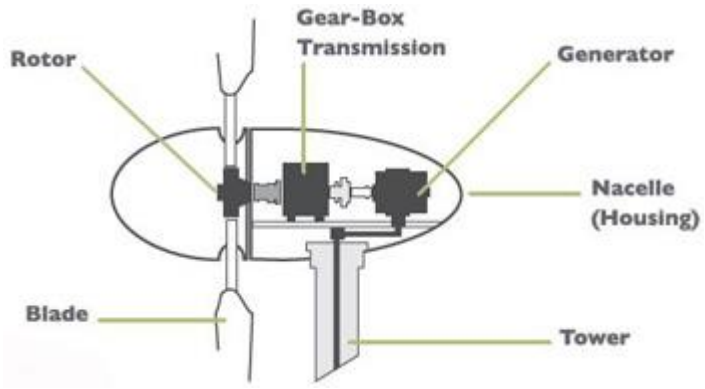

Fig. 1.1 Wind Turbine Components

The WT generates electrical power from kinetic power. Commercial production of electric power normally uses three-bladed WTs and are usually computer-controlled (Anaya-Lara et al., 2009). Generally a WT is made up by following components: foundation, tower, nacelle, rotor and blade (Manwell et al., 2010). The gear box and generator is placed in nacelle. Fig 1.1 shows the wind turbine components. The high cost of operation and maintenance for a WTS is a major issue. Most of WTs are located in remote areas with hard-to-access structures, which would increase the maintenance

cost for wind power systems. Moreover, the wind power availability is reduced directly by the poor reliability (Walford, 2006). Hence, the reliability is highly required to reduce cost. To achieve the goal, the condition monitoring and fault diagnosis are introduced. Condition monitoring and fault diagnosis are important techniques to reduce operation and maintenance cost by minimizing downtime and increasing the energy availability and the life time service of WT components (Daneshi-Far et al., 2010).

1.2 Research Motivations

The WT has attracted great attention in recent years as it contributes greatly to the global environment due to its low greenhouse gas production. One challenge from the control system viewpoint is WTS modelling. Nonlinear and non-minimum phase dynamics are the nature of WTs. The drive-train and tower modes may be excited by large cyclic disturbances. In addition, it is difficult to obtain mathematical models which can describe their dynamic behaviour accurately because of the particular operating conditions (Bianchi et al., 2007).

Many FDI methods for WT have been studied. However, those techniques are very difficult to be developed for WTs due to the fact that they have a slow speed, varying direction and torque (Yang et al., 2008, Yang et al., 2010). Another reason is that the WT technology is significantly different from synchronous generators which are widely

used by conventional power plants, and the dramatically changed dynamic characteristics lead to the different requirements for network control and operation (Anaya-Lara et al., 2009). Hence, the effective and reliable FDI methods for wind turbine system need to be studied and developed.

1.3 Aims and Objectives of the Research

The aim of this project is to develop, design and evaluate by simulation the fault detection, isolation and condition monitoring systems for wind systems. The modelling and simulation will use MATLAB/SIMULINK. The objectives of this research are:

1. Develop mathematical model for the WTS.
2. Develop simulation model of the WTS using Matlab/Simulink.
3. Develop designation of the State Observers for WTS.
4. Develop fault diagnosis for WTS using designed State Observers. Evaluate and validate the simulation results.
5. Develop fault diagnosis for WTS using Neural Networks. Evaluate and validate the simulation results.

1.4 Contributions to Knowledge

First of all, the fundamental contribution of this study is to develop a robust fault detection observer. The observer is robust to system disturbance and sensitive to fault

signals. A mathematical model of WTS which could accurately describe WT dynamics has been modelled. Based on the developed WT model, a robust observer, which is robust to system turbulence but sensitive to system faults, has been designed. This observer is used to detect faults that are simulated in the WT dynamic model. The faults simulated include one component fault, one actuator fault and three sensor faults. The main contribution of this study is the designed robust observer which is new in the WT fault diagnosis research area.

Secondly, an RBF NN model of the independent mode for the WTS has been developed. The developed RBF model is applied to detect faults for the WTS. Three sensor faults have been simulated and all three faults are successfully detected and isolated by designed RBF NN model.

1.5 Thesis Scope and Organisation

In this thesis, the structure of work to complete in achieving the above objectives is outlined as follows:

Chapter 1: Introducing the background of the study. The usage of wind energy has a very long history in human civilisation. The development of the wind energy industry has been increased rapidly in the modern age due to its environment-friendly characteristic. Many researches have been carried out to improve the performance and reliability of WT but there are still many aspects that could be improved. The aim and

objectives are also addressed in this chapter.

Chapter 2: The literature review relating to this work. This includes the brief explanation of the used methods, discussion and comparison of definitions and techniques for WT fault diagnosis.

Chapter 3: The WTS and modelling are presented here. All the sub-systems of a WT are modelled and described including aerodynamic, drive-train, pitch actuator and generator.

Chapter 4: The state observers for WT are designed. A Luenberger-type observer is proposed and the designed observer is sensitive with faults and robust with system disturbance.

Chapter 5: The different kinds of WTS faults are simulated. The simulated faults includes pitch system fault, drive-train system fault and three different sensor faults. The simulated faults are detected by using designed state observers.

Chapter 6: The theory of ANN is explained in this chapter. The structures, training algorithm and data selection are described for RBF network method. Fault diagnosis is tested by the designed ANN.

Chapter 7: Conclusion of this thesis is presented in this chapter and a proposal of future work is discussed as well to continue the research in this subject.

CHAPTER 2
LITERATURE REVIEW

2.1 Introduction

Fault detection and isolation is a subfield in control engineering. In many engineering applications, fault detection and isolation is an important and challenging task (Inseok et al., 2010). During system operation, there could be some unexpected changes in physical parameters of the system, or some malfunction of system components, actuators and sensors, which tends to degrade overall system performance. Such an unexpected change or malfunction is defined as a fault (Patton and Chen, 1991a). The determination of occurrence of a fault in the system is called fault detection. After detection, the determination of which fault occurs among all possible faults that are pre-designed is called fault isolation (Chen et al., 1996).

In the control system, fault diagnosis is one of the significant jobs (Patton et al., 1994). Fault detection and fault isolation are two important stages in the process of fault diagnosis in control systems, so fault diagnosis methods could be divided into two parts, methods for fault detection and methods for fault isolation. Due to the fast increasing complexity of recently developed control systems and growing desire for the fault tolerance, cost efficiency and reliability, the development of fault detection and diagnosis in dynamic systems has been paid considerable attention (Basseville, 1988, Willsky, 1976). There are three general categories for fault diagnosis methods, which

include the knowledge based methods, analytical model based methods and signal based methods, classified by Frank (1996). Venkatasubramanian (2003a, 2003b, 2003c) divides existing fault diagnosis methods into two categories, the model-based approach and knowledge-based approach. The quantitative analytical model of the physical system is used in model-based approaches. In knowledge-based approaches, the full analytical modelling is not necessary, the qualitative models could be used based on the available information and knowledge of a physical system. The analytical model-based methods are preferred if the system could be described by mathematical models, because the analysis could be performed more amendable (Zhou et al., 2011).

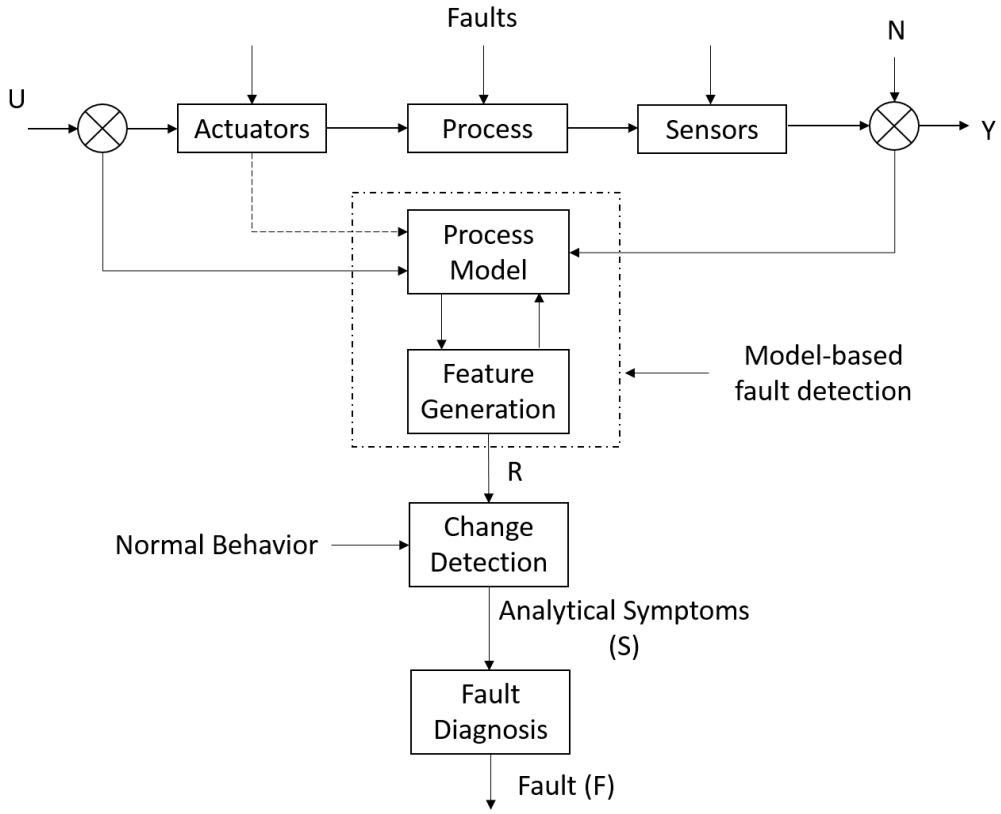

Fig. 2.1 General process scheme of model-based fault detection and diagnosis

2.2 General Fault Detection and Isolation Methods

In the fault detection and isolation field, model-based methods have been studied by many researchers. Fig. 2.1 shows the general process of model-based FDI methods. The residual (R) is generated based on input signals (U) and measured output (Y). The differences between residual (R) and normal behaviour value can be detected and diagnosed by analytical symptoms (S) (Isermann, 2005). The comparison between actual and anticipated system responses generated by mathematical models, is the basic principle for model-based fault detection and isolation (Chen et al., 1996). This difference between process plant output and the estimated model output is the system residuals. If the system is normal, the residual should be zero and when a fault occurs its value should be diverged from zero. This zero and non-zero property of the residual is used as the faults indicator (Chen and Patton, 2012). In control systems, the generation of residual signals is the core element of model-based fault detection. In both academic and applications, the model-based approach of FDI has been paid considerable attention in the last several decades (Willsky, 1976, Isermann, 1984, Patton et al., 1989, Frank, 1990, Patton and Chen, 1991a, Patton et al., 1994, Chen and Patton, 2012).

Compared with detection, fault isolation is more complicated. Designing a set of structured residual signals is one isolation approach, and another approach is to design a directional residual vector (Patton et al., 1989, Frank, 1990, Chen et al., 1996). To generate directional residual vectors, one of the most effective ways is to use the Beard

fault detection filter (BFDF) (Park and Rizzoni, 1993, White and Speyer, 1987, Beard, 1971). The FDI performance is usually affected by system uncertainties. Hence an ideal FDI scheme is sensitive to faults whilst insensitive to system uncertainties. To achieve this, a robust fault diagnosis approach, which uses the disturbance de-coupling principle, was considered the most successful. A number of techniques of robust control have been developed (Zhou and Doyle, 1998). For the fault diagnosis procedure there are typically three tasks: fault detection, fault isolation and fault identification. In the case of nonlinear uncertain systems, less attention has been paid to the fault isolation problem, compared with the fault detection problem. An FDI scheme was presented, by Zhang, Polycarpou, and Parisini (Zhang et al., 2002), for nonlinear uncertain dynamic systems. A rigorous analysis of the performance properties of the related isolation scheme was also provided.

2.2.1 Observer-based Approach

The most effective model-based faults detection and isolation approach is the observer-based approach, in which the difference between actual and estimated outputs is used as the residual vector. When the system is normal the residual is zero without considering the effects of noise and model-plant mismatch and when a fault occurs it is non-zero (Chen et al., 1996, Patton et al., 1989). There are lots of studies and researches which have been done and many different residual generation methods have been developed. Among these many approaches, the observer-based approach is the most common one (Patton and Chen, 1997). The estimation of the system output from the

measurements (or a subset of measurements) is the basic idea behind the observer-based approach. These measurements could be gained by using either Luenberger observer(s) in a deterministic setting or Kalman filter(s) in a stochastic setting and then the weighted output estimation error is used as a residual (Mehra and Peschon, 1971, Willsky and Jones, 1976). Accordingly, in the Luenberger observer approach, the observer gains are selected flexibly to minimise the noise effect on the fault detection and isolation properties. As a result, by appropriately placing the poles of the observers, the fault response dynamics could be controlled (Frank and Keller, 1980, Patton et al., 1989, Puig et al., 2002).

2.2.2 Kalman Filter Approach

The Kalman filter is a set of mathematical equations that provide a computational method which could estimate the state of a process efficiently and minimise the mean of the squared error. It could estimate the past states, present states and future states, even when the precise nature of the modelled system is unknown (Welch, 2014). The Kalman filter was developed by R. E. Kalman (1960) in 1960. In his paper, he described a recursive solution to the discrete-data linear filtering problem which is well known as the Kalman filter (Kalman, 1960). Since then, the Kalman filter has been widely applied and many studies and researches have been undertaken (Gelb, 1974, Maybeck, 1982). A multi-model strategy was developed by Diao and Passino (2002) where each particular system fault is represented by each model. More recently, in real industrial systems for fault diagnosis, some researchers have proved the effectiveness of a multi-

model approach with the assumptions that weighing functions of models are not affected by faults (Bhagwat et al., 2003, Gatzke and Doyle Iii, 2002). Some similar researches for control purposes have also been undertaken (Athans et al., 2005, Porfírio et al., 2003). A multi-model of a dynamic hydraulic system is developed by Rodrigues et al. (2008) for fault diagnosis.

2.2.3 Parity Space Approach

In a linear dynamic transformation, parity relations, also known as parity equations, are rearranged direct input-output model equations and many studies have been carried out on the parity relation based fault detection methods (Gertler, 1997, Patton and Chen, 1991b, Patton and Chen, 1994). The basis of the parity space approach is the parity check of the parity equations' consistency by using the measured actual process signals. The system equations are modified to decoupling among different faults, which could enhance their diagnostic ability. The faults could be detected from the residuals of the parity equations (Frank, 1996). From the state space model of the system, the parity equations were derived by Chow and Willsky (1984). The relations between parity equations and transfer functions were contributed by Gertler and his colleagues (1990, 1995). Mironovski (1979) has proposed a parity relation approach in which the system input-output consistency checking is the basis of residual generation. Some other researches related to transfer functions were also done by Delmaire et al. (1994) and Staroswiecki et al. (1993). Further development regarding parity relation methods were made by Ploix and Adrot (2006), also by Chen and Patton (2012). The application of

parity equations on FDI for bilinear systems with unknown inputs is studied by Yu and Shields (1995, 1997), where a wide selection of faults are detected and isolated.

2.3 Intelligent Fault Detection and Isolation Methods

Artificial Neural Network (ANN) is a well-developed artificial intelligence technique which has been used widely in modelling and control of nonlinear systems for the last two decades (Yu and Gomm, 2003). ANN is a mathematical tool which tries to represent low-level intelligence in natural organisms. It is also a flexible structure which is capable of making a nonlinear mapping between input and output spaces (Rumelhart et al., 1985). For traditional computing solutions, most of them are based on predefined rules or equations. However, in many practical cases the rules are either not known or difficult to discover. In this situation, NN is extremely useful (Rafiq et al., 2001). An accurate input-output relation could be provided by a well-designed ANN model, because of its excellent multi-dimensional mapping capability. ANNs are computational paradigms made up of massively interconnected adaptive processing units, known as neurons (Ou and Achenie, 2005). Due to the excellent performance and wide adaptability, they have been widely applied in various areas of engineering and technology, for example signal processing and control engineering.

2.3.1 Fault Detection and Isolation with Neural Networks

The potential of NNs for FDI in nonlinear system has been demonstrated in recent

years. For nonlinear systems, NNs provide an excellent mathematical tool (Narendra and Parthasarathy, 1990). This is because of the ability of the NN to model any nonlinear function, given suitable weighting factors and approximate (Patton et al., 1999). For NNs, there is no linearization required. Also there is no mathematical model of the system needed to implement NNs. Online training makes it possible to change the FDI system easily in cases where changes are made in the physical process, control system or parameters. A suitably trained NN can generalise when presented with inputs not appearing in the training data. NNs have the ability to make intelligent decisions in cases of noisy or corrupted data. They also have a highly parallel structure, which is expected to achieve a higher degree of fault tolerance than conventional schemes (Patton et al., 1999). NNs have been proposed for function approximation and classification problems. In general, for fault diagnosis, they can be classified into two aspects: (i) the architecture of the network such as sigmoid, radial basis and so on; and

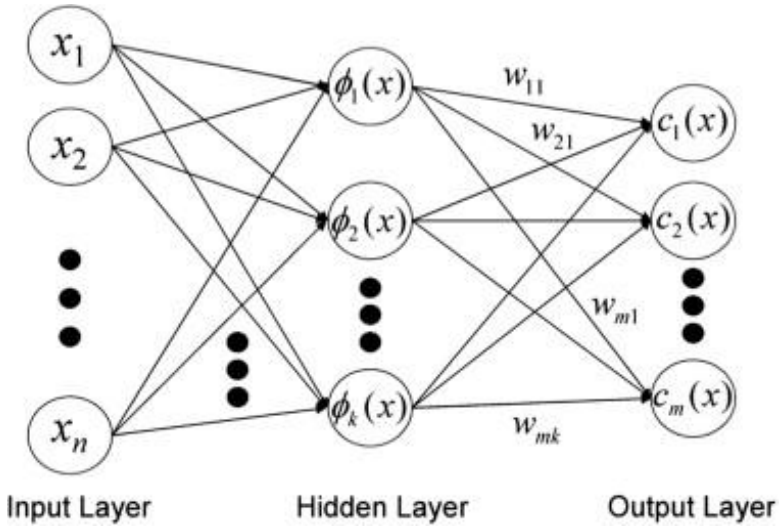

Fig. 2.2 General Structure of Radial Basis Function Networks

(ii) supervised and unsupervised learning (Venkatasubramanian et al., 2003c). There are two well-known NN architectures: multilayer perceptron networks and radial basis function networks (Sorsa et al., 1991).

2.3.1.1 Radial basis function neural network

Radial basis function (RBF) NNs have gained much popularity in recent times. This is due to their ability to approximate complex nonlinear mappings directly from the input–output data with a simple topological structure (Guang-Bin et al., 2005). RBF NNs are almost invariably and generally consist of three layers: a transparent input layer, a hidden layer with sufficiently large number of nodes, and an output layer, which is shown in Fig 2.2. The radially symmetric basis function is used as activation functions of hidden nodes. The transformation from the input nodes to the hidden nodes is nonlinear and the one from hidden nodes to the output nodes is linear (Kashaninejad et al., 2009). Yu et al. (1999) investigated fault diagnosis for a chemical reactor where the residuals for diagnosing the sensor faults are generated by RBF networks and it also has been used as a classifier which shows a satisfactory fault analysis. An RBF NN with Gaussian basis functions for novelty detection is studied by Fredrickson et al. (1994). The Continuous Stirred-Tank Reactor (CSTR) process with multiple-inputs multiple-outputs (MIMO) has also been investigated by Yu et al. (2005) using the RBF networks to model the

nonlinear CSTR systems which shows the effectiveness of the method. The RBF network has been considered successful in application to nonlinear time-series prediction. However, the performance of the RBF predictor for non-stationary signals is less satisfactory because it does not characterize temporal variability well (Chng et al., 1996).

2.3.1.2 Multilayer perceptron neural network

Multilayer perceptron is the best known and most widely used class of NNs. It is also known as Back Propagation network and its popularity in engineering problems is due to the nonlinear mapping. The MLP consists of an input layer, a hidden layer and an output layer, the structure of which is shown in Fig. 2.3. The input nodes receive the data values and pass them on to the first hidden layer nodes. Each one collects the input from all input nodes after multiplying each input value by a weight, attaches a bias to this

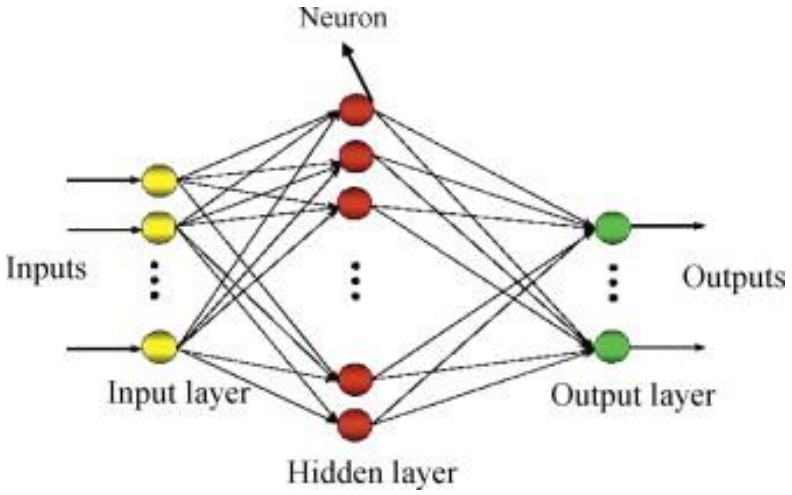

Fig. 2.3 General Structure of Multilayer Perceptron Neural Network

sum, and passes on the results through a non-linear transformation like the sigmoid transfer function (Kashaninejad et al., 2009). Yilmaz and Özer (2009) applied MLP with back propagation learning algorithm to a variable-speed WT as pitch angle controllers and the study got sufficient results. The MLP model is used and the nonlinear dynamic is simulated by Gomm et al. (1996) in a chemical process. It shows a significant improvement in the performance. An approach for nonlinear dynamic process faults detection and isolation is proposed by Patton et al. (1994). In this approach the MLP network was trained to predict the future system and a NN is used again as a classifier to isolate faults from these state prediction errors.

2.3.2 Fault Detection and Isolation with Fuzzy Logic

The theory of fuzzy logic is aimed at the development of a set of concepts and techniques for dealing with sources of uncertainty, imprecision, or incompleteness (Zadeh, 1971, Yager, 1987, Zimmerman, 1991). Fuzzy systems are particularly well suited for modelling nonlinear systems. The nature of fuzzy rules and the relationship between fuzzy sets of differing shapes are the basis of its powerful capability for incrementally modelling a system whose complexity makes traditional expert system, mathematical, and statistical approaches very difficult. In addition, fuzzy system modelling provides a more flexible, richer representational scheme than other methods such as certainty factors or Bayesian probabilities (Yi et al., 2000). Recently, fuzzy

theory is used in many technical disciplines taking care of vague descriptions. The fuzzy approach is used to build an adaptive fuzzy threshold which take cares of modelling errors, so that no increased threshold is necessary and even small faults can quickly be detected (Schneider and Frank, 1994). The fuzzy logic and NN applications for fault diagnosis are studied by Frank and Köppen-Seliger (1997). In their study, a dependent NN for residual generation and fuzzy logic for residual evaluation are used. Yi et al. (2000) proposed and investigated a fuzzy system for automotive fault diagnosis. A fuzzy model is described that learns automotive diagnostic knowledge through machine learning techniques.

2.3.3 Fault Detection and Isolation with Expert Systems

An expert system is a software system that captures human expertise for supporting decision-making which is useful for dealing with problems involving incomplete information or large amounts of complex knowledge. In the control field, the expert systems are very useful, particularly for on-line operations. This is due to the fact that they incorporate symbolic and rule-based knowledge that relates situation and actions, and they also have the ability to explain and justify a line of reasoning (Chiang et al., 2012). Fault diagnosis is a common application of expert system technology in control engineering. Typically, there are three basic components of an expert system: a knowledge base, an inference engine and user interface. The knowledge base contains either shallow knowledge based on heuristics, or deep knowledge based on structural, behavioural or mathematical models (Chiang et al., 2012). The expert system can use

different types of knowledge representation schemes, including production rules, frames and semantic networks (Xia and Rao, 1999). Since performance of the expert system is highly dependent on the correctness and completeness of the information stored in the knowledge base, updates to the knowledge base is necessary should the industrial process change. The inference engine provides inference mechanisms to direct use of the knowledge, and the mechanisms typically include backward and forward chaining, hypothesis testing, heuristic search methods, and meta-rules (Prasad et al., 1998, Norvilas et al., 2000, Rao et al., 2000). Finally, the user interface translates user input into a computer understandable language and presents conclusions and explanations to the user. Early applications of expert systems primarily focused on medical diagnosis (Clancey and Shortliffe, 1984). Currently, expert systems have been adopted in many industrial applications, including equipment maintenance, diagnosis and control, plant safety, and other areas in engineering.

2.4 Fault Detection and Isolation for Wind Turbine

WTs are complex, nonlinear, dynamic systems forced by stochastic wind disturbances. Fault occurrence therefore is inevitable in this system. On the other hand, extracting accurate models for the system is complex and challenging. Therefore, FDI is not a straight forward process. There are many fault detection schemes for different parts of WTS in the literature. Signal-based approaches are usually used for condition monitoring and predictive maintenance purposes. Vibration analysis of rotating devices, acoustic emission

analysis of mechanical parts and temperature analysis are examples of the frequently used methods in this group. Additional sensors are needed in most of the proposed methods (Bin et al., 2009, Z. Hameed, 2009, Amirat et al., 2007). The implementation of a fault detection system is critical for an early detection of faults and getting necessary time for a maintenance schedule to arrange spare parts and related logistics (Z. Hameed, 2009). All possible faults or other abnormal conditions could be divided into three categories: cautions, warnings and alarms. A caution indicates that a particular monitored quantity is outside of its normal operating range and indicates a need for service and/or adjustment of the affected component. A warning indicates that a particular monitored quantity is outside of acceptable operating limits and the continued operation could lead to component damage and/or power system failure. An alarm indicates a severe malfunction that poses an immediate danger to personnel and/or equipment and the system responds by immediately disconnecting and shutting down the affected component (Caselitz et al., 1994).

There are numbers of techniques which are available for identification of faults and these are listed below: System identification approach is a model-based approach using system identification techniques. Parameter estimation methods are well established and widely used in control systems and it has been successfully applied to fault detection problems as well. In the observer-based approach based on state observers and Kalman filters, the residual is the observation error. The observer can be designed with reduced sensitivity against model uncertainties and structural external

disturbances. It is still a very accurate model for essential process (Frank, 1993, Patton et al., 1989). In the signal analysis approach fault indicators are derived from process measurements and signal analysis methods are not as fast as model-based approaches in detecting abrupt changes. But they can be applied to very complex systems (Caselitz et al., Pau, 1981). In the expert system and artificial intelligence approach, Fuzzy techniques and NN have been investigated in this context. However, these two methods are still under research (Caselitz et al., 1994).

A WT is a complex electromechanical system consisting of hundreds of components and subsystems, including rotor hub, blades, gearbox, generator, power electronics, etc. Each component of the WT has its own failure modes and contribution to the downtime of the WT (Qiao and Lu, 2015). There are many research works which have been reported in wind turbine subsystems' condition monitoring and fault diagnosis areas.

2.4.1 FDI for WT Gearbox and Bearing Subsystem

Gearbox fault is widely perceived as the leading issue for WT drive train condition monitoring among all subsystems (Hyers et al., 2006, Z. Hameed, 2009, Amirat et al., 2007, Tavner et al., 2006, Wilkinson et al., 2007). Gear and bearing are the two main components in a gearbox. Most gearbox failures are caused by gear and bearing failures. Various factors, such as design and material defects, manufacturing and installing errors, misalignment, torque overloads, surface wear, and fatigue, contribute to WT gearbox

faults (Qiao and Lu, 2015). In particular, it was pointed out that the gearbox bearings tend to fail at different rates. Among all bearings in a planetary gearbox, the planet bearings, the intermediate shaft-locating bearings and high-speed locating bearings tend to fail at the fastest rate, while the planet carrier bearings, hollow shaft bearings and non-locating bearings are most unlikely to fail (Bin et al., 2009).

Vibration measurement and spectrum analysis are typical choices for gearbox monitoring and diagnostics. For instance, Huang et al. (2008) presented a study on vibration spectrum analysis based gearbox fault classification using wavelet NN. For variable-speed WT operation, wavelet analysis has been recently accepted for feature extraction, as compared to faster Fourier transform (FFT) and envelop analysis tools developed earlier (Hatch, 2004, Z. Hameed, 2009).

The relatively slow speed of the WT sets a limitation in early fault diagnosis using vibration monitoring method. Therefore, acoustic emission (AE) sensing, which detects the surface stress waves generated by the rubbing action of failed components, has recently been considered a suitable enhancement to the classic vibration based methods for a multi-sensor based monitoring scheme for gearbox diagnosis, especially for early detection of pitting, cracking or other potential faults (Bin et al., 2009). Chen et al. (2005) set up a finite-element (FE) simulation study for the stress wave based diagnosis for the rolling-element bearing of WT gearbox. Wavelet analysis was applied to the output signals and to identify the artificial faults introduced to both the inner and outer

race of the ball bearings in the simulated case. It is noteworthy that FE analysis is a good complementary tool to the experimental based study, with which the physical insight of various levels of faults can be investigated. Notice that AE measurement features very high frequencies compared to other methods, so the cost of data acquisition systems with high sampling rates needs to be considered.

A more comprehensive study on diagnosis for the drive train of the WTs with synchronous generators is presented by Yang et al. (2009). Wavelet transforms were applied to deal with the variable-speed operation. In particular, the discrete wavelet transform (DWT) was employed to deal with the noise-rich signals from WT measurements. The electrical analysis was investigated for mechanical faults of the drive train. Diagnosis of gear eccentricity was studied using current and power signals. It is noteworthy that the data were obtained from a WT emulator, on which the properties of both natural wind and the turbine rotor aerodynamic behaviour were incorporated. Although the level of turbulence simulated was not described, the demonstrated performance was still promising for practical applications. The significant computational efforts of wavelet analysis were notified as a potential limitation.

Torque measurement has also been utilized for drive train fault detection. The rotor faults may cause either a torsional oscillation or a shift in the torque-speed ratio. Such information can be used to detect rotor faults, e.g. mass imbalance (Wilkinson et al.,

2007). Also, shaft torque has a potential to be used as an indicator for decoupling the fault-like perturbations due to higher load. However, inline torque sensors are usually highly expensive and difficult to install. Therefore, using torque measurement for drive train fault diagnosis and condition monitoring is still not practically feasible.

2.4.2 FDI for WT Rotor, Blades and Hydraulic Subsystem

WT rotor is a very critical part and its health monitoring techniques reveals some failure mode indications. There are many methods of fault detection system developed for rotor, which is listed below: Transmittance functions; Operational deflection shapes; resonant comparison; Variance analysis; Wavelet pattern recognition analysis and Thermo elastic stress analysis (Ghoshal et al., 2000, Sundaresan et al., 2002, Dutton, 2004).

Most of the failures are subject to creep fatigue and corrosion fatigue which creates cracks in the composite blades. Non-uniform build-up of ice, dirt, moisture or collected damage to the rotor blades. Due to corrosion, frosting, insects etc, the blade surface roughness may increase which results in loss in energy capture efficiency. Blade fault diagnostics has been studied based on strain measurement techniques such as Fiber-optic Bragg Grating (FBG) and AE (Amirat et al., 2007, Hyers et al., 2006, Amjady and Rezaey, 2012, Uraikul et al., 2007, Garcia et al., 2006). For the blades of small WT, Yuji et al. (2006) used a piezoelectric impact sensor, while Bouno et al. (2005) used AE sensor for fault detection.

Blade pitch control system is critical for turbine operation, as pitching is an important action for enhancing energy capture, mitigating operational load, stalling and aerodynamic braking. Under very strong wind in particular, it is used as an aerodynamic brake to stop the turbine. Avoiding pitching failure is thus important for the overall system operation. Pitching motion is typically driven by hydraulic actuators or electric motors. Electric motor driven pitching systems have larger bandwidth, which is more desirable for faster actions such as individual pitching. Hydraulic pitching systems have slower response, but bearing much larger stiffness, little backlash and higher reliability. For large to extreme aerodynamic loading situations, hydraulic systems are considered more fail-safe. Hydraulic actuation system failure takes a remarkable portion among different factors of WT failure (Bin et al., 2009).

Some faults of hydraulic systems may lead to operation instability. For instance, the effective bulk modulus of hydraulic fluid can be greatly reduced due to even a very small amount of air contamination. Reduction of fluid bulk modulus leads to the reduction of plant bandwidth, and thus reducing the stability robustness of the corresponding closed-loop system. Similar issues occur for significant leakage in the hydraulic system (Watton, 2007).

2.4.3 FDI for WT Generator Subystem

The vibration analysis of WT generator system could effectively use the fault

diagnosis method which is based on frequency spectrum analysis and wavelet analysis. The frequency and temperature field analysis and magnetic field analysis based on limited element analysis can be applied in the fault mechanism analysis of the gearbox and generator. The intelligent fault diagnosis method based on NN and fuzzy theorem has significant application prospects in the fault diagnosis of the WT generator system (Zhang et al., 2008).

2.4.4 System-Level Fault Detection and Isolation

WT and even its subsystems include many components, and thus the system- or subsystem-level FDI presents quite some complexity. Fault detection methodologies can be applied on any subsystem. The advantages are that with one approach you can detect faults and there is no need to apply a separate method for each component in a subsystem. Some approaches are listed below: The general objective of artificial intelligence is to reproduce human reasoning and more generally any human cognitive mode of comprehension, perception, representation and decision making, as faithfully as possible. There are two kinds of reasoning for solving diagnostic tasks: normal-operation-oriented reasoning and abnormal-operation-oriented reasoning (Gentil et al., 2004). The fault detection and isolation community is especially concerned with industrial process modelling and control. Models are quantitative and dynamic. Two basic representations can be used: state space models and input-output relations (Frank, 1996). The Recursive isolation relies on both a qualitative causal representation of the process and on quantitative local models. The interest of recursive isolation is to prevent

combinatorial explosion (Gentil et al., 2004).

Fault isolation also requires more systematic analysis. Relationship between component-level faults and system-level faults need to be established efficiently. The framework of Discrete Event System (DES) is considered a suitable choice. As the finite-state machines suffered from the so-called combinational explosion for complex systems, Petri Nets has been studied for WT system-level decision making for fault diagnosis. Rodriguez et al. (2008) used the coloured Petri Nets to diagnose a lubrication and cooling system for WT.

Echavarria et al. (2007, 2008) developed a qualitative physics based approach in order to develop an intelligent maintenance system for WT. The fault diagnosis system was developed based on a model-based reasoner (MBR) and functional redundancy designer (FRD). Both design tools used a function-behaviour-state (FBS) model. The advantages of using MBR and qualitative physics were claimed to be capability of reasoning with little information, no need to solve a complex system of equations, reusability of easy access of knowledge, and robustness in fault prediction. The disadvantage of a reasoning system is the ambiguity in setting up the thresholds. A preliminary framework of a multi-agent fault detection system developed for WT fault detection and identification is presented by Zaher and McArthur (2007). The development of an Anomaly Detection Agent, Power Curve Agent and Downtime Classifier Agent was briefly described. Multi-agent deserves more study due to its re-

configurability and scalability for system development.

Whelan et al. (2008) applied a sensor network to wind plant condition monitoring. Christensen et al. (2009) studied remote condition monitoring of WTs. It was pointed out that many vibration monitoring systems on the market today overwhelm the user with alarms, of which many are caused by transients, or numerous alarms all related to the same faults. It is critical to convert data into information in order to make the condition monitoring system more efficient and robust. Wiggelinkhuizen et al. (Wiggelinkhuizen et al., 2008) presented the assessment of several condition monitoring techniques in the EU-CONMOW project carried out from 2002 to 2007. Vibration data along with other SCADA measurements were used for fault detection. The usefulness and capabilities of condition monitoring systems were analysed, including algorithms for identifying early failures. The economic consequences of applying condition monitoring systems have been quantified and assessed.

2.5 Summary

In this chapter, the researches and studies related to fault detection and isolation are reviewed. There are three general categories for fault diagnosis methods, which include the knowledge based methods, analytical model based methods and signal based methods. The comparison between actual and anticipated system responses generated by mathematical models, is the basic principle for model-based fault

detection and isolation. The most effective model-based faults detection and isolation approach is the observer-based approach, in which the difference between actual and estimated outputs is used as the residual vector. The Kalman filter is a set of mathematical equations that provide a computational method which could estimate the state of a process efficiently and minimise the mean of the squared error. The basis of the parity space approach is the parity check of the parity equations' consistency by using the measured actual process signals. For intelligent fault detection and isolation methods, there mainly three methods: neural networks, fuzzy logic and expert systems.

CHAPTER 3
WIND TURBINE DYNAMIC MODEL

3.1 Introduction

The WT is a complex electromechanical system that extracts the kinetic power of wind and converts it into mechanical power and it is then converted into electrical power by a generator. Because of the difference between the rotor speed and generator speed, normally a gearbox is used to couple the rotor shaft and generator shaft (Slootweg et al., 2001).

A WTS generally consists of the following sub-systems: aerodynamics, pitch actuator and drive-train system (Association, n. d.). Such a complex electromechanical

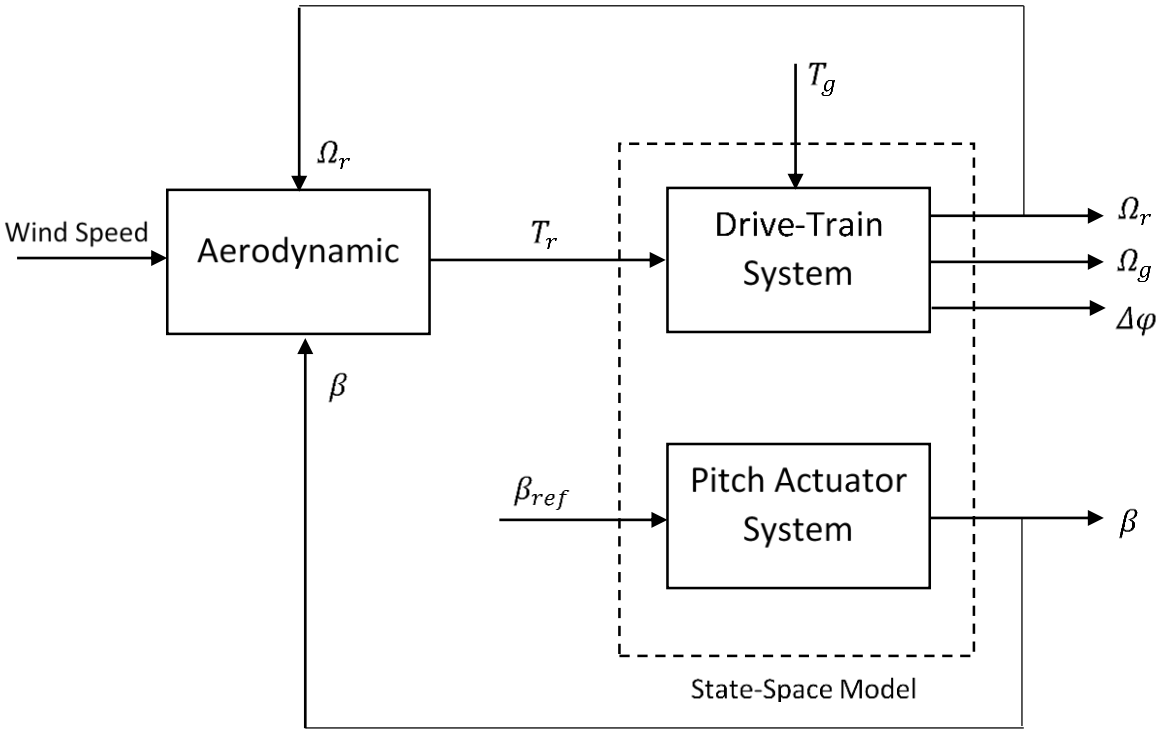

Fig. 3.1 Wind Turbine System Structure

system converts the kinetic power of wind into electrical power. A general structure of WT is shown in Fig. 3.1.

3.2 Aerodynamics

Aerodynamics is a science and study of physical laws of the behaviour of motion of air, particularly the forces that are produced when it interacts with a solid object (Joselin Herbert et al., 2007). The interaction between the rotor and the wind is the major aspect of the WT power production, in which the wind is considered as the mean wind speed. From experience, the aerodynamic force generated by the mean wind speed is the key factor of the wind performance (Manwell et al., 2010). Many studies have been undertaken to analyse the optimum blade shape and aerodynamic performance of the WT rotors. Betz and Glauert (1935) developed the classical analysis of the WT in the 1930s. Subsequently, Wilson and Lissaman (1974), Wilson et al. (1976) and Vries (1979) expanded the momentum theory and blade element theory and combined them into a strip theory, in which the performance characteristics of an annular section of the rotor could be calculated and the entire rotor could be obtained by integrating the values from each of the annular sections.

Practical horizontal axis WTs transform the kinetic energy in the wind into useful energy. The following equations can be used to represent the aerodynamics of a WT

(Burton et al., 2011). The available power of the wind which crosses the blades swept area is given by,

$$P_w = \frac{1}{2}\rho A v^3 = \frac{1}{2}\rho \pi R^2 v^3 \tag{3.1}$$

where ρ is the air density, R is the radius of the rotor disc, v is the speed of the wind and A is the area covered by the rotor ($A = \pi R^2$).

Only a limited power could be converted from the available power P_w by rotor. This limitation ratio is called the power coefficient $C_p(\lambda, \beta)$. Hence the rotor power P_r could be expressed as

$$P_r = C_p(\lambda, \beta) P_w \tag{3.2}$$

The power coefficient $C_p(\lambda, \beta)$ has a maximum value of $16/27 \approx 0.593$ known as Betz limit (Chen and Patton, 2012). This fact can be understood as the wind energy cannot be completely drained, otherwise the wind speed would reduce to zero and the rotor would stop. The modern WTs have a high power coefficient of about 0.5, which is considered that a maximum C_p is obtained (Nelson, 2009, Shen et al., 2007).

The value of C_p depends on the tip-speed ratio λ and the blade pitch angle β. It can be expressed as in, (Slootweg et al., 2001)

$$\begin{cases} C_p(\lambda,\beta) = 0.22\left(\frac{116}{\lambda_i} - 0.4\beta - 5\right)e^{-12.5/\lambda_i} \\ \frac{1}{\lambda_i} = \frac{1}{\lambda+0.08\beta} - \frac{0.035}{\beta^3+1} \end{cases} \tag{3.3}$$

where the tip-speed ratio $\lambda = \frac{R}{v}$.

According to the equations above, the non-linear rotor equation for rotor torque, T_r, is concluded as,

$$T_r = \frac{P_r}{\Omega_r} = \frac{\rho\pi R^2 v^3 C_p(\lambda,\beta)}{2\Omega_r} \tag{3.4}$$

Fig. 3.2 shows the wind turbine rotor aerodynamics variables.

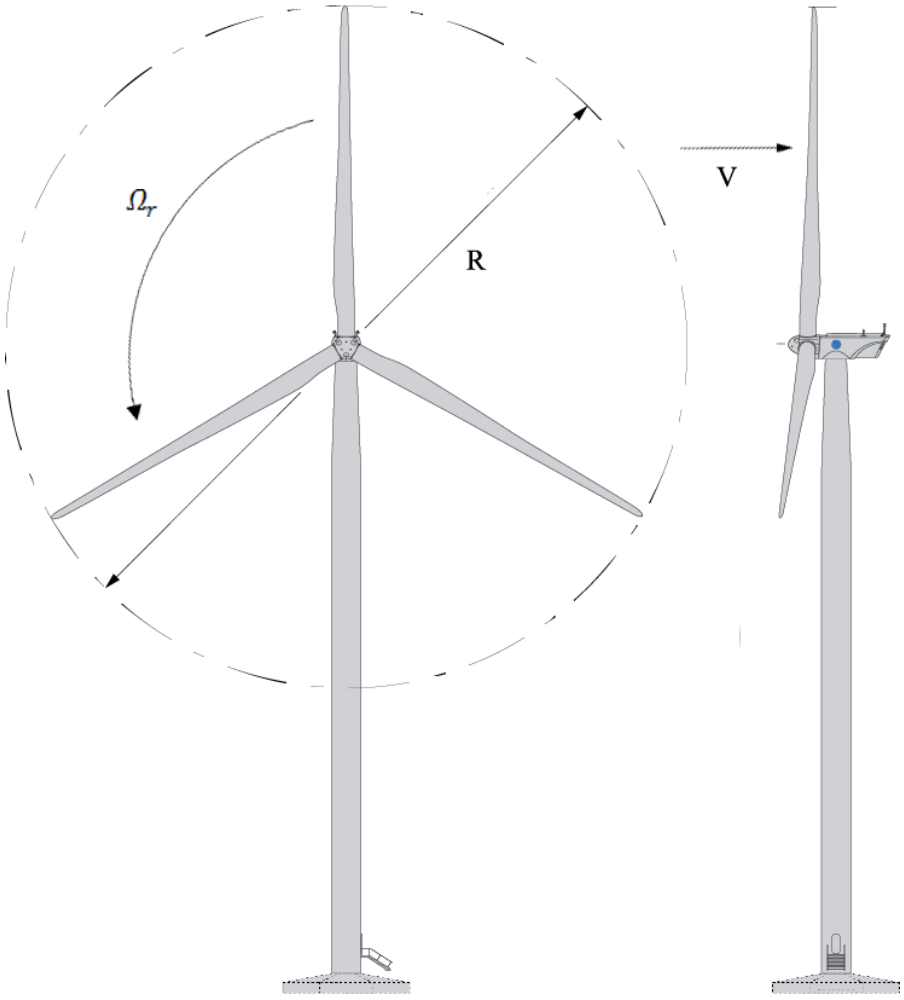

Fig. 3.2 Wind Turbine Rotor Aerodynamic

3.3 Pitch Actuator

The pitch of the rotor blade is controlled by a hydraulic or electric motor which the WT blades could turn along their longitudinal axis. The actuator model describes the dynamic behaviour between the measured pitch angle β and its reference β_{ref} (Hwas and Katebi, 2014). The dynamics of the blades are non-linear with saturation limits on both pitch angle and pitch rate. This saturation is caused by high frequency components of the pitch demand spectrum, via measurement noise, and spectral peaks induced by rotational sampling (Feng et al., 2008).

In principle, the pitch actuator of the WT blade could be seen as a piston servo system(Odgaard et al., 2009). It can be described and modelled well by a second-order transfer function (Rezaei and Johnson, 2013):

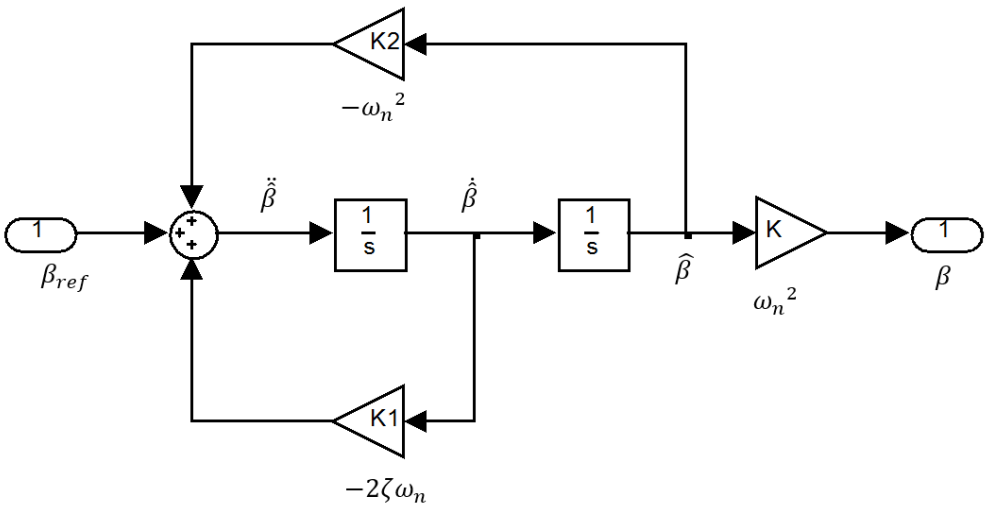

Fig. 3.3 Simulink Model for Pitch Actuator

$$\omega_n{}^2\beta_{ref} = \ddot{\beta} + 2\zeta\omega_n\dot{\beta} + \omega_n{}^2\beta \tag{3.5}$$

where β_{ref} is the desired pitch angle and β is the actual pitch angle, ω_n is the natural frequency of pitch actuator. ζ is damping ratio of pitch actuator. Pitch actuator model is showed in Fig. 3.3.

3.4 Drive-train System

The mechanical power generated by wind is transferred through the drive-train from the rotor to the generator. The drive-train part is often considered in first place compared with other mechanical models of the WT, because this part of the WT has the most significant influence on the power fluctuations (Hansen et al., 2005). In analysis, only rotor, low speed shaft, gearbox, high-speed shaft and generator are considered and other parts of WTs, e.g. tower and flap bending modes can be reasonably neglected (Ming et al., 2007). In most studies of WT modelling, four types of drive-train models are usually used: six-mass drive-train model, three-mass drive-train model, two-mass drive-train model and one-mass drive-train model (Muyeen et al., 2008). The selection of a correct drive-train model depends on the interest of study. For example, when the study focuses on the interaction between wind farms and AC grids, one-mass drive-train model could be selected for the sake of time efficiency and acceptable precision (Ming et al., 2007). In addition, it shows that significant errors in the critical clearing time that defines stability limit of the WTs could be introduced if the drive-train model is over

simplified (Salman and Teo, 2003). Normally, a two-mass model is sufficient to represent the characteristic of drive-train while modelling (Okedu, 2012).

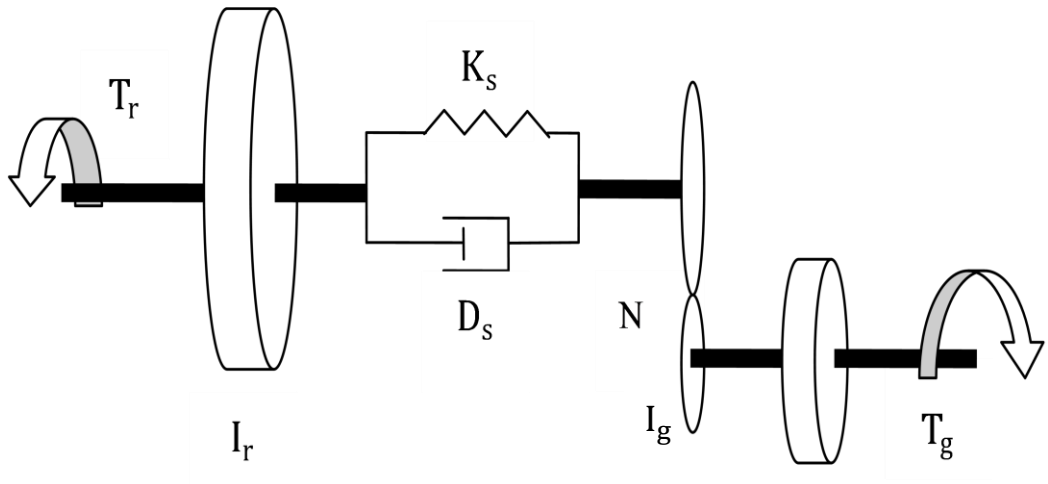

Fig. 3.4 Mass-Spring-Damper Model for Drive-train

In this study, the drive-train is modelled as a rotational 2-mass, 1-spring, 1-damper system as shown in Fig. 3.2. The shaft on the rotor side is assumed flexible and the shaft on the generator side is assumed rigid. Furthermore, the gear box contributes only a relatively small fraction and hence inertia of the gear box is often neglected and only the transformation ratio of the gear system is included (Ackermann, 2012). The gear ratio between the rotor and the generator is a constant *N*. The differential equation, which describes the system, is shown below,

$$T_r - T_g N = I_r \ddot{\varphi}_r - I_g N \ddot{\varphi}_g + \left(\dot{\varphi}_r - \frac{\dot{\varphi}_g}{N}\right) D_s + \left(\varphi_r - \frac{\varphi_g}{N}\right) K_s \qquad (3.6)$$

where $\Omega_r = \dot{\varphi}_r$ and $\Omega_g = \dot{\varphi}_g$.

By defining $\Delta\varphi = \varphi_r - \frac{\varphi_g}{N}$, a 4th order differential equation is reduced to 3rd order to simplify the model. The equation is rewritten as below.

$$\dot{\Omega}_r = \ddot{\varphi}_r = \frac{T_r - T_g N + I_g N \ddot{\varphi}_g - (\dot{\Delta\varphi}) D_s - (\Delta\varphi) K_s}{I_r} \tag{3.7}$$

$$\dot{\Omega}_g = \ddot{\varphi}_g = \frac{T_r - T_g N - I_r \ddot{\varphi}_r + (\dot{\Delta\varphi}) D_s + (\Delta\varphi) K_s}{I_g N} \tag{3.8}$$

It should be noted that $T_g N = I_g N \ddot{\varphi}_g$ and $T_r = I_r \ddot{\varphi}_r$. Equations (3.7)-(3.8) could be further simplified,

$$\dot{\Omega}_r = \ddot{\varphi}_r = \frac{T_r - (\dot{\Delta\varphi}) D_s - (\Delta\varphi) K_s}{I_r} \tag{3.9}$$

$$\dot{\Omega}_g = \ddot{\varphi}_g = \frac{-T_g N + (\dot{\Delta\varphi}) D_s + (\Delta\varphi) K_s}{I_g N} \tag{3.10}$$

Rewrite the above equations (3.9) (3.10), we get

$$\dot{\Omega}_r = \ddot{\varphi}_r = -\frac{D_s}{I_r}\dot{\varphi}_r + \frac{D_s}{I_r N}\dot{\varphi}_g - \frac{K_s}{I_r}\Delta\varphi + \frac{1}{I_r}T_r \tag{3.11}$$

$$\dot{\Omega}_g = \ddot{\varphi}_g = \frac{D_s}{I_g N}\dot{\varphi}_r - \frac{D_s}{I_g N^2}\dot{\varphi}_g + \frac{K_s}{I_g N}\Delta\varphi - \frac{1}{I_g}T_g \tag{3.12}$$

with

$$\dot{\Delta\varphi} = \dot{\varphi}_r - \frac{\dot{\varphi}_g}{N} \tag{3.13}$$

3.5 Combination of Blade Pitch Dynamics and Drive-train Dynamics

The equations for WT blade pitch dynamics and drive-train dynamics are,

$$\dot{\beta} = \dot{\beta} \tag{3.14}$$

$$\dot{\Omega}_r = -\frac{D_s}{I_r}\Omega_r + \frac{D_s}{I_r N}\Omega_g - \frac{K_s}{I_r}\Delta\varphi + \frac{1}{I_r}T_r \tag{3.15}$$

$$\dot{\Omega}_g = \frac{D_s}{I_g N}\Omega_r - \frac{D_s}{I_g N^2}\Omega_g + \frac{K_s}{I_g N}\Delta\varphi - \frac{1}{I_g}T_g \tag{3.16}$$

$$\dot{\Delta\varphi} = \Omega_r - \frac{\Omega_g}{N} \tag{3.17}$$

$$\ddot{\beta} = -{\omega_n}^2\beta - 2\zeta\omega_n\dot{\beta} + {\omega_n}^2\beta_{ref} \tag{3.18}$$

The differential equations (14)-(18) can be combined to form a state space model,

$$\dot{x} = Ax + Bu + Ed + Ff_a + Gf_c \tag{3.19a}$$

$$y = Cx + Qf_s \tag{3.19b}$$

with

$$x^T = \begin{bmatrix}\beta & \Omega_r & \Omega_g & \Delta\varphi & \dot{\beta}\end{bmatrix}$$

$$u^T = [T_r \quad T_g \quad \beta_{ref}]$$

$$y^T = [\beta \quad \Omega_r \ \Omega_g \quad \Delta\varphi]$$

$$A = \begin{bmatrix} 0 & 0 & 0 & 0 & 1 \\ 0 & -\frac{D_s}{I_r} & \frac{D_s}{I_r N} & -\frac{K_s}{I_r} & 0 \\ 0 & \frac{D_s}{I_g N} & -\frac{D_s}{I_g N^2} & \frac{K_s}{I_g N} & 0 \\ 0 & 1 & -\frac{1}{N} & 0 & 0 \\ -{\omega_n}^2 & 0 & 0 & 0 & -2\zeta\omega_n \end{bmatrix}$$

$$B = \begin{bmatrix} 0 & 0 & 0 \\ \frac{1}{I_r} & 0 & 0 \\ 0 & -\frac{1}{I_g} & 0 \\ 0 & 0 & 0 \\ 0 & 0 & {\omega_n}^2 \end{bmatrix} \quad \mathrm{C} = \begin{bmatrix} 1 & 0 & 0 & 0 & 0 \\ 0 & 1 & 0 & 0 & 0 \\ 0 & 0 & 1 & 0 & 0 \\ 0 & 0 & 0 & 1 & 0 \end{bmatrix}$$

where $x \in \mathbb{R}^n$, $u \in \mathbb{R}^m$, $y \in \mathbb{R}^p$ are the system state, input and output vectors. d, f_c, f_a, f_s represent the unknown inputs, component and actuator faults and sensor faults, respectively. *A, B, C, E, G, Q* are known matrices. It is assumed that $rank\{C\} = p$, $rank\{E\} = l$, $rank\{G\} = q$ and $rank\{Q\} = g$.

3.6 Summary

In this chapter, the mathematical dynamic model of wind turbine system and subsystems have been developed. The wind turbine subsystems contain aerodynamics, pitch actuator and drive-train system. The aerodynamics reflects the interaction between the wind turbine rotor and the wind as the major aspect of the wind turbine power production. The pitch actuator system controls the rotor blade pitch by a hydraulic or electric motor. The dynamics of the blades are non-linear with saturation limits on both pitch angle and pitch rate. The mechanical power generated by wind is transferred through the drive-train from the rotor to the generator and normally a two-mass model is sufficient to represent the characteristic of drive-train while modelling. In this study, the drive-train is modelled as a rotational 2-mass, 1-spring, 1-damper system. A state space model is formed by combination of the differential equations of wind turbine blade pitch dynamics and drive-train dynamics.

CHAPTER 4
ROBUST OBSERVER DESIGN

4.1 Introduction

A state observer is a software system that could estimate or observe the state variables. It includes full-order state observer and reduced-order state observer. Non-measurable states are estimated from system input/output data. The residual can be constructed from the information provided by the state estimation errors that are obtained by comparing the system output and the estimated output (Ogata, 2010). A nonlinear observer is a dynamic filter which estimates the states or outputs of the system based on a mathematical model, sensor measurements and input commands. Hwas and Katebi (2012) designed and applied a linear observer for the case where the rotor speed varies slowly. However, in the real case, wind speed and a generator's rotor speed are both variables, and the behaviour of a WT is nonlinear, which should be considered in the FDI design.

4.2 Observer Structure

For the system above (3.19a-b), a Luenberger-type (Frank, 1990) of observer is proposed with the following structure,

$$\dot{z} = \hat{A}z + \hat{B}y + Hu \tag{4.1a}$$

$$\varepsilon = L_1 z + L_2 y \tag{4.1b}$$

where $z \in \mathbb{R}^d$ is a linear combination of the estimates of x

$$z = Tx \tag{4.2}$$

and $\varepsilon \in \mathbb{R}^\phi$ is called the residual vector. The observer order *d* and residual vector order ϕ are chosen in the design. $L_1 \in \mathbb{R}^{\phi \times d}$, $L_2 \in \mathbb{R}^{\phi \times p}$ are constant matrices to be designed. The structure of the robust observer is shown in Fig. 4.1.

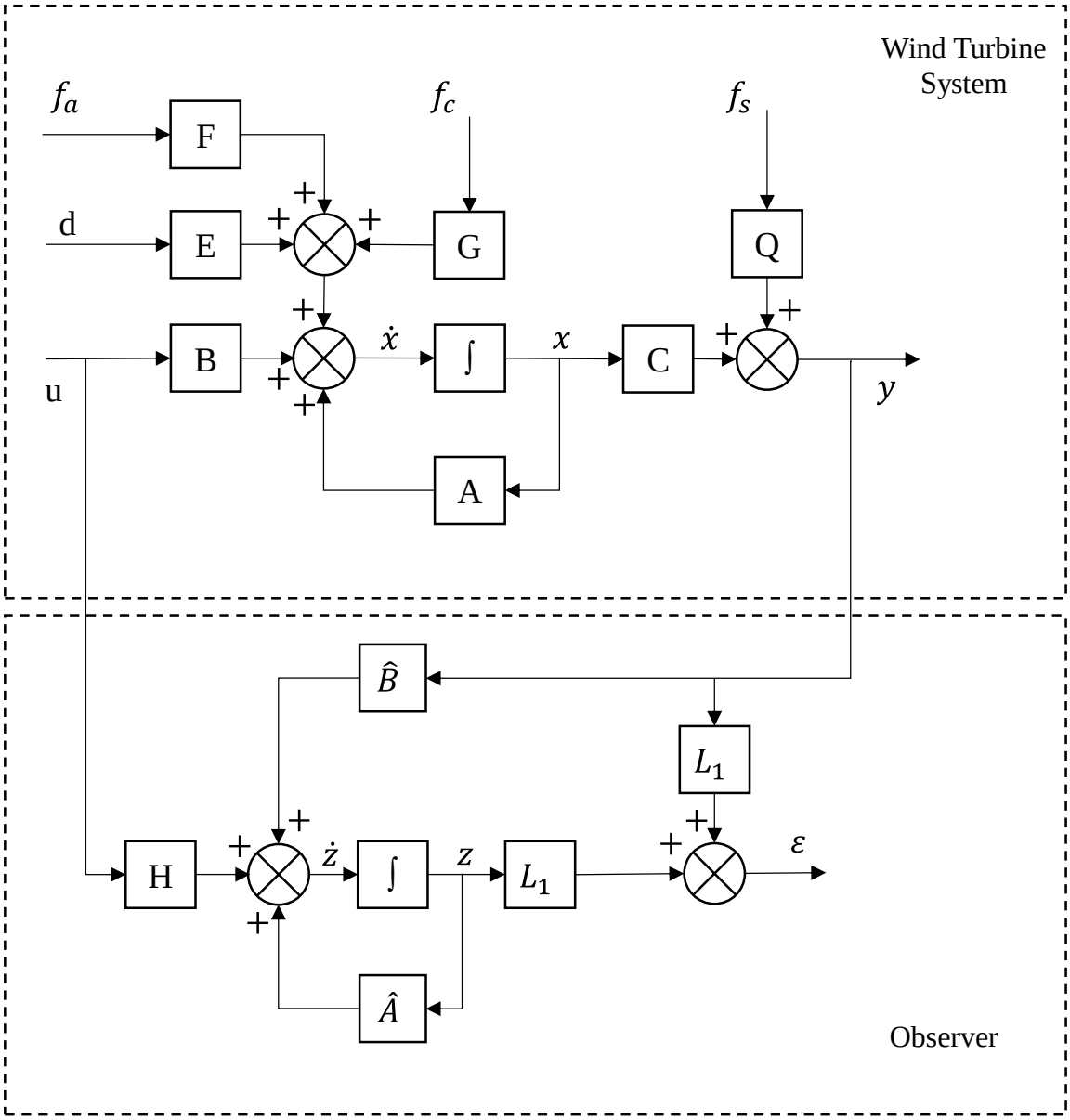

Fig. 4.1 Wind Turbine Robust Observer Structure

The fault detection observer for the system (3.19) has following definition. For any u, d, x and z, and for $f_a = 0$ and $f_c = 0$

$$\lim_{i\to\infty} e = \lim_{i\to\infty}(z - Tx) = 0 \tag{4.3a}$$

$$\lim_{i\to\infty} \varepsilon = 0 \tag{4.3b}$$

Condition (4.3a) ensures that the observer is stable while the fault is zero. Condition (4.3b) ensures the residual is decoupled from the unknown input (disturbance). Therefore, only faults could cause the system to record a non-zero steady-state response of the observer. However, any fault is not guaranteed to be detected due to the design and structure of the faults. For example, the effects of different faults on the residual may cancel each other out. In this case the residual could not reflect the faults.

From the observer structure (4.1), state estimation error could be presented in the form of,

$$e = z - Tx \tag{4.4}$$

The state error dynamics is derived,

$$\begin{aligned} \dot{e} &= \dot{z} - T\dot{x} \\ &= \hat{A}e + \left(\hat{A}T + \hat{B}C - TA\right)x + (H - TB)u \\ &-TGf_c - TFf_a + \hat{B}Qf_s - TEd \end{aligned} \tag{4.5}$$

To satisfy condition (4.1a-4.1b), the following equations must hold.

$$TA - \hat{A}T = \hat{B}C \tag{4.6a}$$

$$H = TB \tag{4.6b}$$

$$TE = 0 \tag{4.6c}$$

$$L_1 T + L_2 C = 0 \tag{4.6d}$$

Thus, the state function estimation error,

$$\dot{e} = \hat{A}e - TGf_c - TFf_a + \hat{B}Qf_s \tag{4.7}$$

is asymptotically stable for $f_c = 0$, $f_a = 0$, $f_s = 0$ and $\hat{A}$ is designed stable.

4.3 The Design of the Observer

The design of the observer is to determine matrices T, $\hat{A}$, $\hat{B}$, H, L_1 and L_2 to satisfy condition (4.6a-4.6d). Supposing $C = [I_p \quad 0]$, the system state equation can be partitioned into

$$\dot{x} = [A_1 \quad A_2]x + Bu + Ed + Gf_a \tag{4.8a}$$

$$y = Cx + Qf_s \tag{4.8b}$$

where $A_1 \in \mathbb{R}^{n\times p}$ and $A_2 \in \mathbb{R}^{n\times(n-p)}$. The matrix T is correspondingly partitioned into the form,

$$T = [T_1 \quad T_2] \tag{4.9}$$

where $T_1 \in \mathbb{R}^{d\times p}$ and $T_2 \in \mathbb{R}^{d\times(n-p)}$. Then, (4.6a) is also partitioned into the form,

$$TA_1 - \hat{A}T_1 = \hat{B} \tag{4.10a}$$

$$TA_2 - \hat{A}T_2 = 0 \tag{4.10b}$$

and equation (4.6c) is written as,

$$TE = 0 \tag{4.11}$$

From equation (4.11), the solution of matrix T is

$$[T_1 \quad T_2] = MU_{z2}^T \tag{4.12}$$

where $U_{z2} \in \mathbb{R}^{n \times r}$ is from the SVD of *E* as

$$E = [U_{z1} \quad U_{z2}] \begin{bmatrix} \Sigma_{z1} \\ 0 \end{bmatrix} [V_{z1} \quad V_{z2}]^T \tag{4.13}$$

and *M* is an arbitrary $d \times r$ matrix. The *r* is the order of the left null space for *E*, being given as

$$r = n - rank\{E\} \tag{4.14}$$

From equation (4.12), it is known that the maximum number of independent rows of *T* is *r*. therefore, $d=r$ is chosen as the observer order. And the matrix *M* then has dimensions which maximize the possible rank of *T*. Partition U_{z2}^T into two matrices:

$$U_{z2}^T = [N_1 \quad N_2] \tag{4.15}$$

where $N_1 \in \mathbb{R}^{r \times p}$ and $N_2 \in \mathbb{R}^{r \times (n-p)}$

Thus, equation (4.12) could be written as

$$T_1 = MN_1 \tag{4.16a}$$

$$T_2 = MN_2 \tag{4.16b}$$

where U_{z2} could be calculated from (4.13), and T_1 and T_2 could be calculated as well.

Now, it can be seen that if the condition $TA_2(I_n - T_2^+T_2) = 0$ or the following equivalent

$$MU_{z2}^T A_2(I_n - (MN_2)^+(MN_2)) = 0 \tag{4.17}$$

Is satisfied, the observer matrix $\hat{A}$ has the following general form to satisfy condition (4.10b).

$$\begin{aligned}\hat{A} &= MU_{z2}^T A_2(MN_2)^+ + W(I_d - MN_2(MN_2)^+) \\ &= A^* + WC^*\end{aligned} \tag{4.18}$$

where W is a $d \times d$ arbitrary matrix. If the pair $\{A^*, C^*\}$ is detectable, the W could be properly selected to design the stable observer matrix $\hat{A}$. Moreover, if the pair $\{A^*, C^*\}$ is observable, any desirable observer dynamics can be achieved by assigning eigenvalues of $\hat{A}$.

The next step is to design matrices L_1 and L_2 such that (25d) is satisfied. Equation (4.6d) could be partitioned into

$$L_1T_1 + L_2 = 0 \tag{4.19a}$$

$$L_1T_2 = 0 \tag{4.19b}$$

where $L_1 \in \mathbb{R}^{\phi \times d}$, $T_2 \in \mathbb{R}^{d \times (n-p)}$. Equation (4.6d) holds true if L_1 is chosen to satisfy (4.19b) and L_2 is chosen to satisfy (4.19a). To satisfy equation (4.17), a sufficient condition is that *M* is such that $T_2 = MN_2$ has full-column rank *n-p*. Hence a non-zero L_1 exists if only $d > n - p$. L_1 and L_2 can be solved respectively as

$$L_1 = W_1 U_{n2}^T \tag{4.20}$$

$$L_2 = -L_1 T_1 \tag{4.21}$$

where U_{n2} is given in the SVD of T_2

$$T_2 = [U_{n1} \quad U_{n2}] \begin{bmatrix} \Sigma_n \\ 0 \end{bmatrix} [V_{n1} \quad V_{n2}]^T \tag{4.22}$$

and W_1 is a $\phi \times r_n$ arbitrary matrix with

$$r_n = d - rank\{T_2\} \geq d - (n - p) \tag{4.23}$$

As the same reason of choice of *d*, the dimension of the residual vector is chosen as

$$\phi = r_n \tag{4.24}$$

4.4 Calculation of Designed Observer

The variables of designed observer *T*, $\hat{A}$, $\hat{B}$, *H*, L_1 and L_2 could be calculated to satisfy the equations (4.6a)-(4.6d) by substitute WTS parameters into system equations (3.19a) and (3.19b). The WTS parameters(Jonkman et al., 2009) are shown in Table 4.1.

Symbol	Variable	Value
N	Gear ratio	97
I_r	Moment of inertia of rotor	$5.9154 \times 10^7 \ kg\ m^2$
I_g	Moment of inertia of generator	$500 \ kg\ m^2$
D_s	Driveshaft dampening constant	$6.215 \times 10^6 \ N/rad\ s$
K_s	Driveshaft spring constant	$8.6763 \times 10^8 \ N/rad$
ζ	Damping of pitch actuator	0.9
ω_n	Natural frequency of pitch actuator	$0.88 \ rad/s$

Table 4.1 Wind Turbine System Parameters

Firstly, N_1 and N_2 could be calculated from equation (4.13), (4.15)

$$N_1 = \begin{bmatrix} 1 & 0 & 0 & 0 \\ 0 & 0 & 1 & 0 \\ 0 & 0 & 0 & 1 \\ 0 & 0 & 0 & 0 \end{bmatrix} \qquad N_2 = \begin{bmatrix} 0 \\ 0 \\ 0 \\ 1 \end{bmatrix}$$

Matrix *M* is selected as identity matrix *I*. Then, T_1, T_2, T and *H* could be solved by equation (4.16a), (4.16b) and (4.6b)

$$U_{z2} = \begin{bmatrix} 1 & 0 & 0 & 0 \\ 0 & 0 & 0 & 0 \\ 0 & 1 & 0 & 0 \\ 0 & 0 & 1 & 0 \\ 0 & 0 & 0 & 1 \end{bmatrix} \quad T_1 = \begin{bmatrix} 1 & 0 & 0 & 0 \\ 0 & 0 & 1 & 0 \\ 0 & 0 & 0 & 1 \\ 0 & 0 & 0 & 0 \end{bmatrix} \quad T_2 = \begin{bmatrix} 0 \\ 0 \\ 0 \\ 1 \end{bmatrix}$$

$$T = [T_1 \quad T_2] = \begin{bmatrix} 1 & 0 & 0 & 0 & 0 \\ 0 & 0 & 1 & 0 & 0 \\ 0 & 0 & 0 & 1 & 0 \\ 0 & 0 & 0 & 0 & 1 \end{bmatrix}$$

$$H = TB = \begin{bmatrix} 0 & 0 & 0 \\ 0 & -0.002 & 0 \\ 0 & 0 & 0 \\ 0 & 0 & 0.7744 \end{bmatrix}$$

From equation (4.18), A^*, C^* could be designed

$$A^* = \begin{bmatrix} 0 & 0 & 0 & 1 \\ 0 & 0 & 0 & 0 \\ 0 & 0 & 0 & 0 \\ 0 & 0 & 0 & -1.5840 \end{bmatrix} \quad C^* = \begin{bmatrix} 1 & 0 & 0 & 0 \\ 0 & 1 & 0 & 0 \\ 0 & 0 & 1 & 0 \\ 0 & 0 & 0 & 0 \end{bmatrix}$$

Then check the observability of the pair $\{A^*, C^*\}$

$$Rank\{M_o\} = Rank\{\begin{bmatrix} C^* \\ C^*A^* \\ C^*A^{*2} \\ C^*A^{*3} \end{bmatrix}\} = 4$$

The W could be properly selected to design the stable observer matrix $\hat{A}$.

By choosing the observer poles as,

$$\mathrm{p} = \begin{bmatrix} -10 \\ -12 \\ -16 \\ -18 \end{bmatrix}$$

The W is designed as

$$\mathrm{W} = \begin{bmatrix} -24.416 & 0 & 0 & 0 \\ 0 & -18 & 0 & 0 \\ 0 & 0 & -12 & 0 \\ -121.3251 & 0 & 0 & 0 \end{bmatrix}$$

so observer matrix

$$\hat{A} = A^* + WC^* = \begin{bmatrix} -24.416 & 0 & 0 & 1 \\ 0 & -18 & 0 & 0 \\ 0 & 0 & -12 & 0 \\ -121.3251 & 0 & 0 & -1.584 \end{bmatrix}$$

Put $\hat{A}$ into equation (4.10a),

$$\hat{B} = TA_1 - \hat{A}T_1 = \begin{bmatrix} 24.416 & 0 & 0 & 0 \\ 0 & 128.14 & 16.679 & 17889.28 \\ 0 & 1 & -0.01 & 12 \\ 120.55 & 0 & 0 & 0 \end{bmatrix}$$

From equation (4.19a)(4.19b), L_1 and L_2 could be solved as,

$$L_1 = \begin{bmatrix} 0 & 1 & 0 & 0 \\ 0 & 0 & 1 & 0 \\ 1 & 0 & 0 & 0 \end{bmatrix}$$

$$L_2 = \begin{bmatrix} 0 & 0 & -1 & 0 \\ 0 & 0 & 0 & -1 \\ -1 & 0 & 0 & 0 \end{bmatrix}$$

With the values of T, $\hat{A}$, $\hat{B}$, H, L_1 and L_2 are all calculated, the WT model with robust observer could be built up and tested in simulation.

4.5 Summary

In this chapter, a robust state observer is designed for wind turbine dynamic system to detect system faults. A Luenberger-type observer is developed. The observer is stable while the fault is zero and the residual is decoupled from the system disturbance. Only the faults could cause the system to record a non-zero steady-state response of the observer.

CHAPTER 5
FAULT DETECTION WITH ROBUST OBSERVER

According to Daneshi-Far et al. (2010), WTs are subjected to different sorts of failures. Some of them are more frequent than others but in order to compare them it is necessary to consider the downtime they could force for the whole system. Therefore, WT failures statistics should be studied by considering both failure frequencies and downtimes.

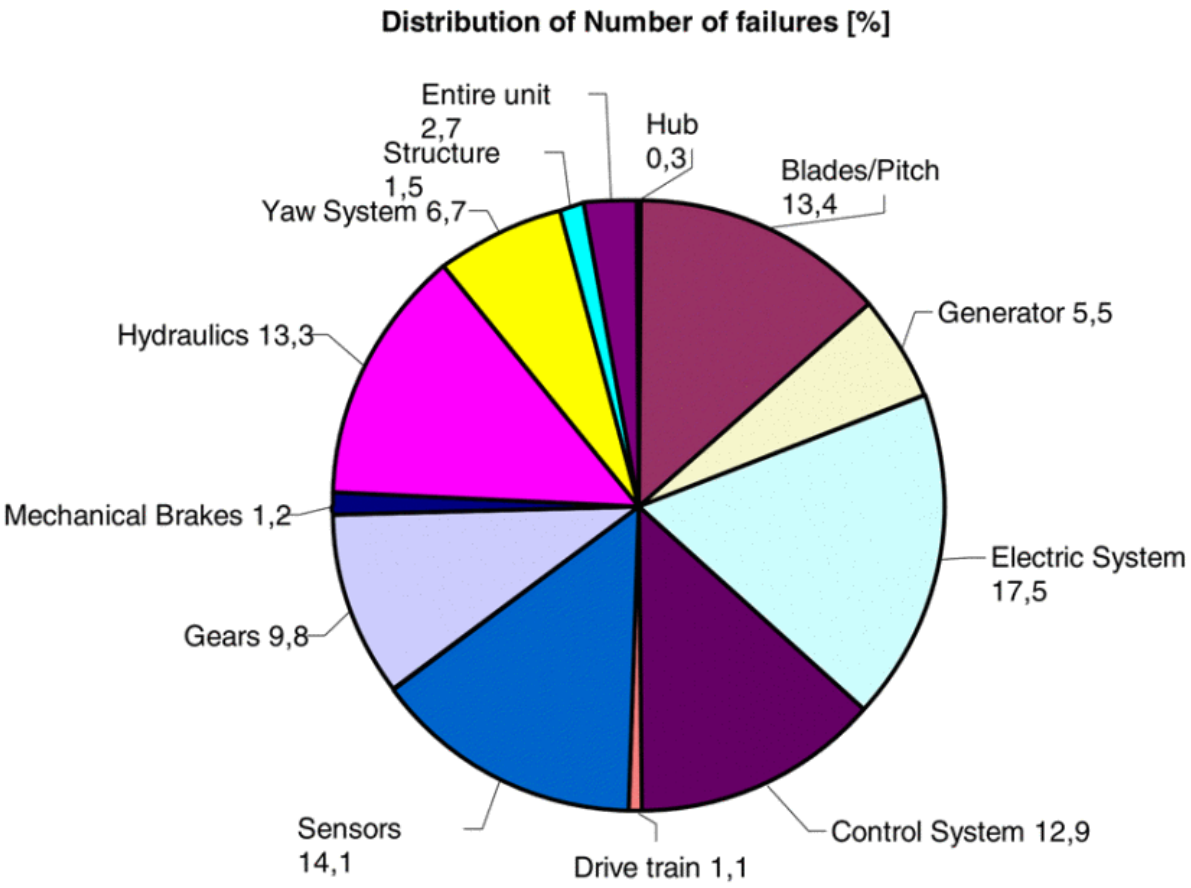

Fig 5.1 Distribution of Number of Failures

Fig 5.1 shows the percentage breakdown of failures that occurred during the years 2000–2004. Most failures were linked to the electric system followed by sensors, and blades/pitch components (Ribrant and Bertling, 2007). Their report also pointed out that the most troublesome component is the gearbox, closely followed by the control system, and the electric system. This means that the gearbox has the longest downtime compared to the other components. In this paper different kinds of possible faults in the WTS are considered. These faults include WT blade pitch system faults, drive-train system gearbox fault and three sensor faults.

5.1 Simulating Faults

5.1.1 Pitch System Fault

The WT pitch actuator fault is a kind of actuator component fault which is a multiplicative fault, where the term “multiplicative” refers to the way in which the fault enters the state equations, i.e. with state dependency. Multiplicative fault estimation is not as straightforward as that for additive faults (Shi and Patton, 2014). Some research in the area of multiplicative fault detection and estimation is available using sliding model observers (Chee Pin and Edwards, 2004), adaptive observers for linear (Gao et al., 2011), and nonlinear systems (Zhang et al., 2010), fuzzy observers (Blake and Brown, 2007), or augmented state observers.

The pitch system of the WTs is normally hydraulic or electric (Bin et al., 2009). It could be described by equation:

$$J\ddot{\beta}(t) + b\dot{\beta}(t) = T_m(t) - T_L(t) \tag{5.1}$$

where J is blade inertia, b is friction factor. From the equation (5.1) we can get,

$$\begin{aligned} G(s) = \frac{B(s)}{T_m(s)} &= \frac{1}{Js^2 + bs + T_L} \\ &= \frac{\frac{1}{J}}{s^2 + \frac{b}{J}s + \frac{T_L}{J}} \\ &= \frac{K\omega_n^2}{s^2 + 2\zeta\omega_n s + \omega_n^2} \end{aligned}$$

According to the equation above, $\omega_n = \sqrt{\frac{T_L}{J}}$ and $= \frac{b}{2\sqrt{JT_L}}$.

It is assumed that during the WT operation, the blade pitch actuator suffered a loss of lubrication which means the friction b is increased to 2 times original value, which means the damping ratio ζ is also increased by 2 times. Thus the component fault matrix $G = [0 \quad 0 \quad 0 \quad 0 \quad -2\omega_n]^T$.

5.1.2 Drive-train System Gearbox Fault

The main drive-train of a WT is commonly equipped with a gearbox connected with an electric generator, such as a single-, two-, or three-stage gearbox connected with a permanent magnet synchronous generator or a three-stage gearbox connected

with a wound rotor induction generator (Ng and Ran, 2016, Cao et al., 2012). Statistic studies from Igba et al. (2015) and Ribrant and Bertling (2007) have shown that the downtime per gearbox failure is more than 18 days, and the downtime caused by gearbox failures share about 20% of the total downtime of WTs, making gearbox failures the leading factor causing the downtime of WTs. Gear faults are a major category of failure modes in WT gearboxes. The common gear faults include tooth breakage, crack, surface wear, etc. They are caused by various factors such as manufacturing and installing errors, surface wear, fatigue, etc. A gear fault will lead to performance degradation of the WT drivetrain and may cause a catastrophic failure of the gearbox or even failures of other components in the WT drivetrain (Lu et al., 2017).

The drive-train system gearbox fault is assumed to occur on generator torque T_g in the time period 20s to 30s. The value of T_g has increased by 10%. The actuator fault matrix $F = [0 \quad 0 \quad -1/I_g \quad 0 \quad 0]^T$

5.1.3 Wind Turbine Sensor Faults

In WTS, sensors are important components; their roles are to measure the system outputs including active power, generator angular speed and so on. Any sensor fault must be detected accurately as early as possible to prevent serious accident (Jihong et al., 2008). There are several types of fault in the WT sensors. Icing and lighting strike are the major faults. Salt corrosion is another cause of fault for offshore WTs.

Furthermore, there is a large risk of offset error in the wind speed sensors (Odgaard et al., 2009).

Three different sensor faults are considered in this study. The first sensor fault is the pitch angle measurement. It is assumed that the fault appeared on the pitch angle sensor during the test time 40s to 50s. Fig. 5.3 shows the measured pitch angle changed to 2 times the original value. The pitch angle sensor fault matrix is $= [1 \quad 0 \quad 0 \quad 0]^T$. The second sensor fault is the rotor speed sensor. In the simulation, the measured rotor speed value drops 50% during time 60s to 70s, which is shown in Fig. 5.4. The rotor speed sensor fault matrix is $Q = [0 \quad 1 \quad 0 \quad 0]^T$. The last sensor fault is the measurement of generator speed. Fig. 5.4 shows the generator speed sensor gives the incorrect value during 80s to 90s. The generator speed sensor fault matrix is $Q = [0 \quad 0 \quad 1 \quad 0]^T$.

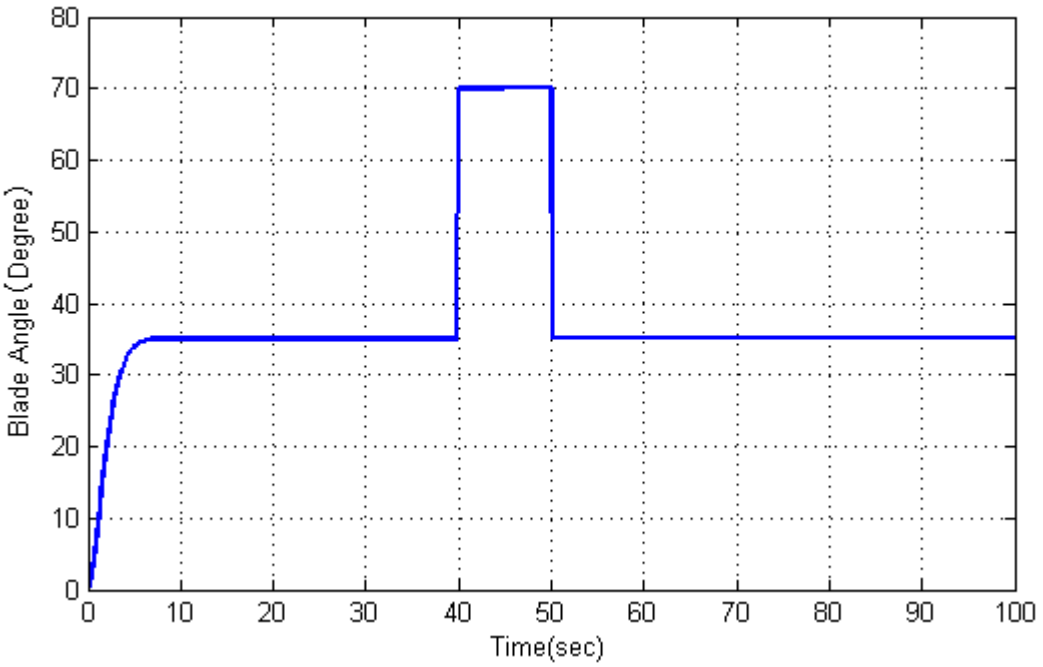

Fig. 5.2 Sensor Fault on Pitch Angle Measurement

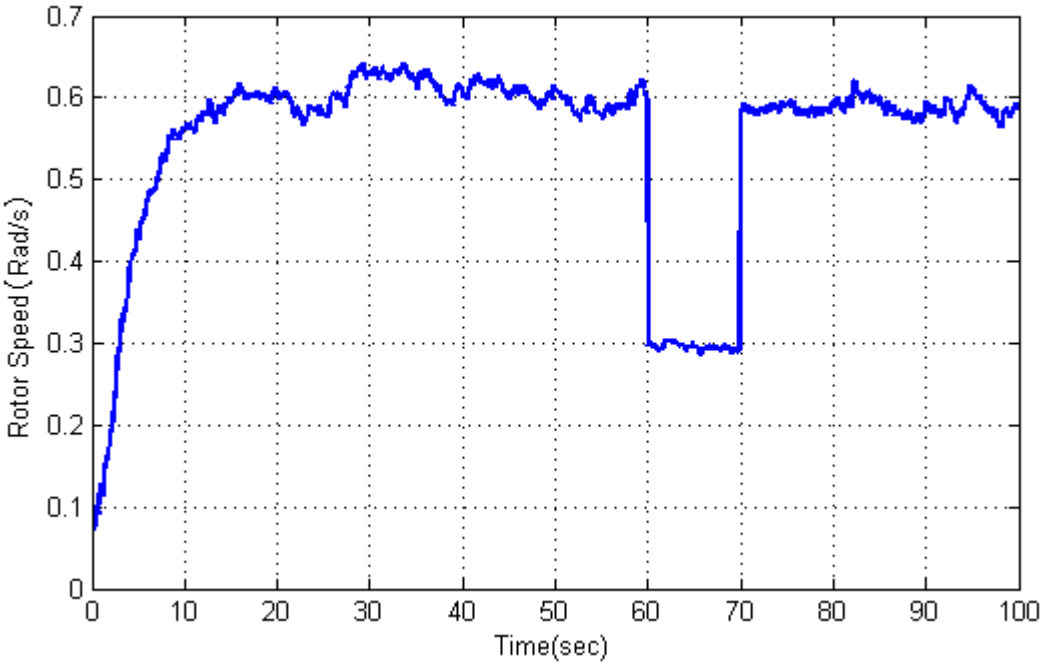

Fig. 5.3 Sensor Fault on Rotor Speed Measurement

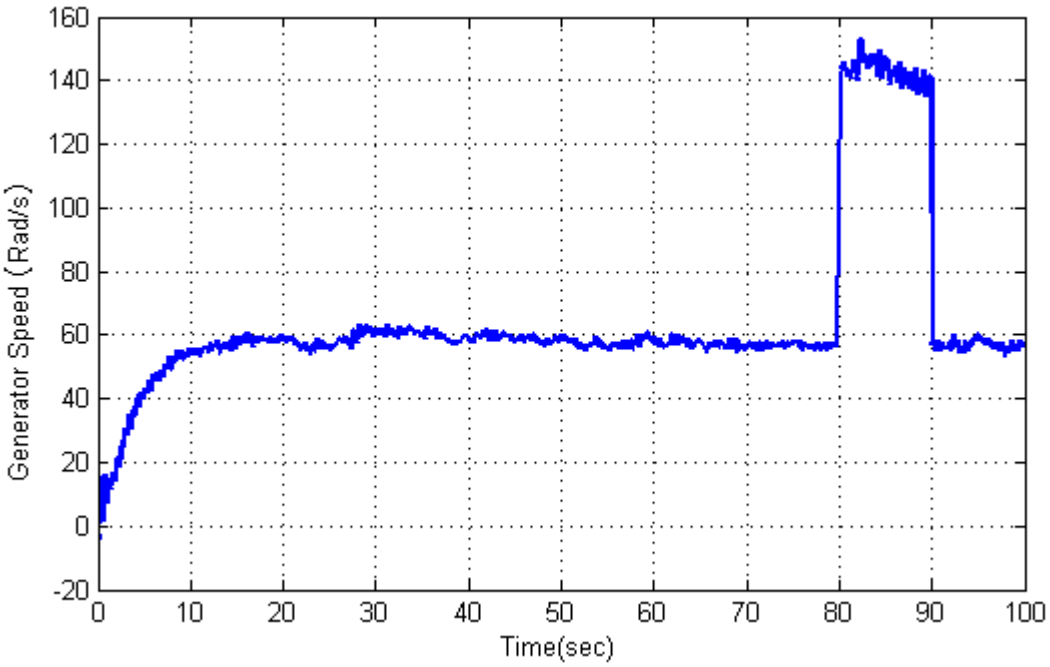

Fig. 5.4 Sensor Fault on Generator Speed Measurement

5.2 Fault Detection

The designed WT pitch system fault, drive-train system fault and sensor faults are simulated by Matlab/Simulink. When the system operates in normal condition, which means no faults occur, the residuals and state errors should remain zero. When the faults

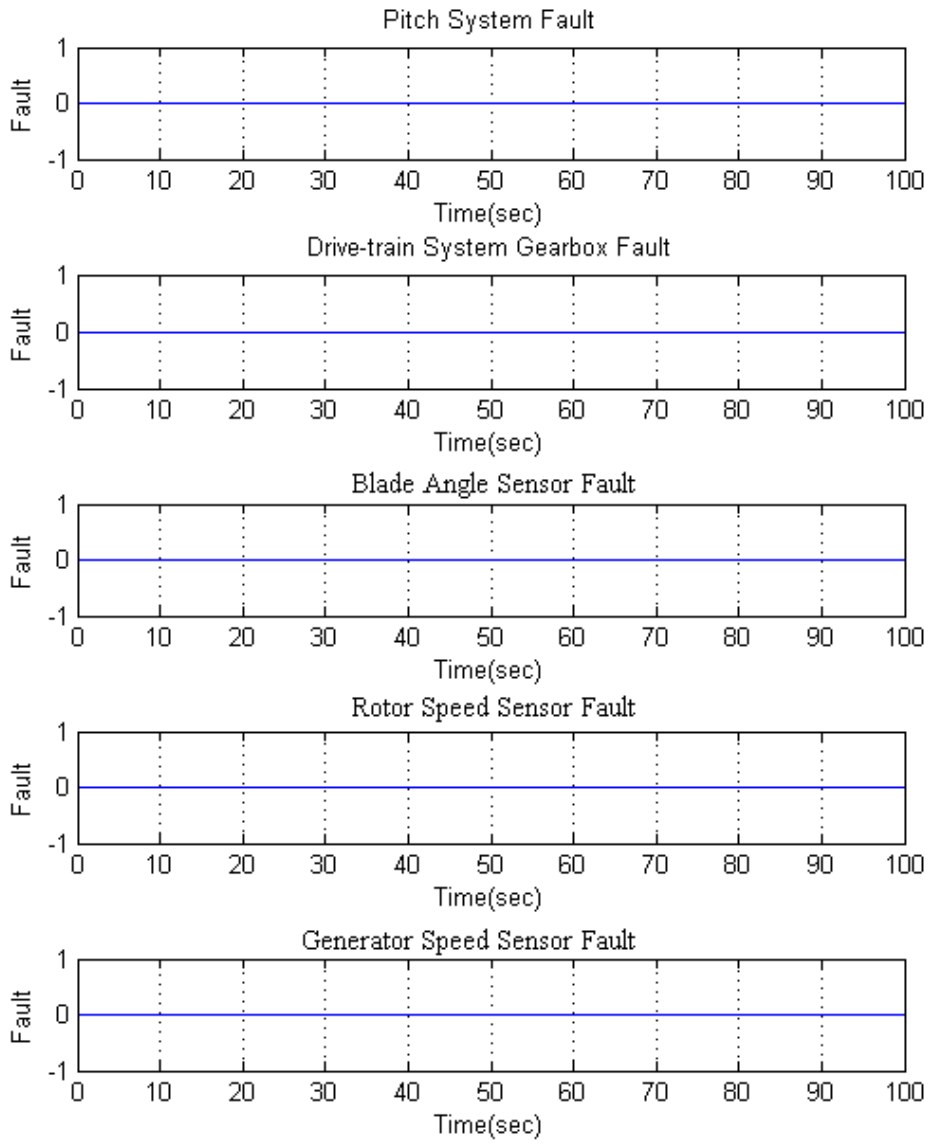

Fig. 5.5 Wind Turbine System Operating without Faults

occur during the system operation, the residuals and errors will be non-zero. After the fault disappears, the residuals and errors go back to zero.

5.2.1 Fault Detection with No Faults Occurring

Firstly the WTS is operated in normal condition with no faults being simulated (Fig. 5.5). The observer residual is zero because the observer is designed to be robust to the disturbances which is shown in Fig 5.6. The disturbance matrix $E = [0 \quad 1/I_r \quad 0 \quad 0 \quad 0]^T$.

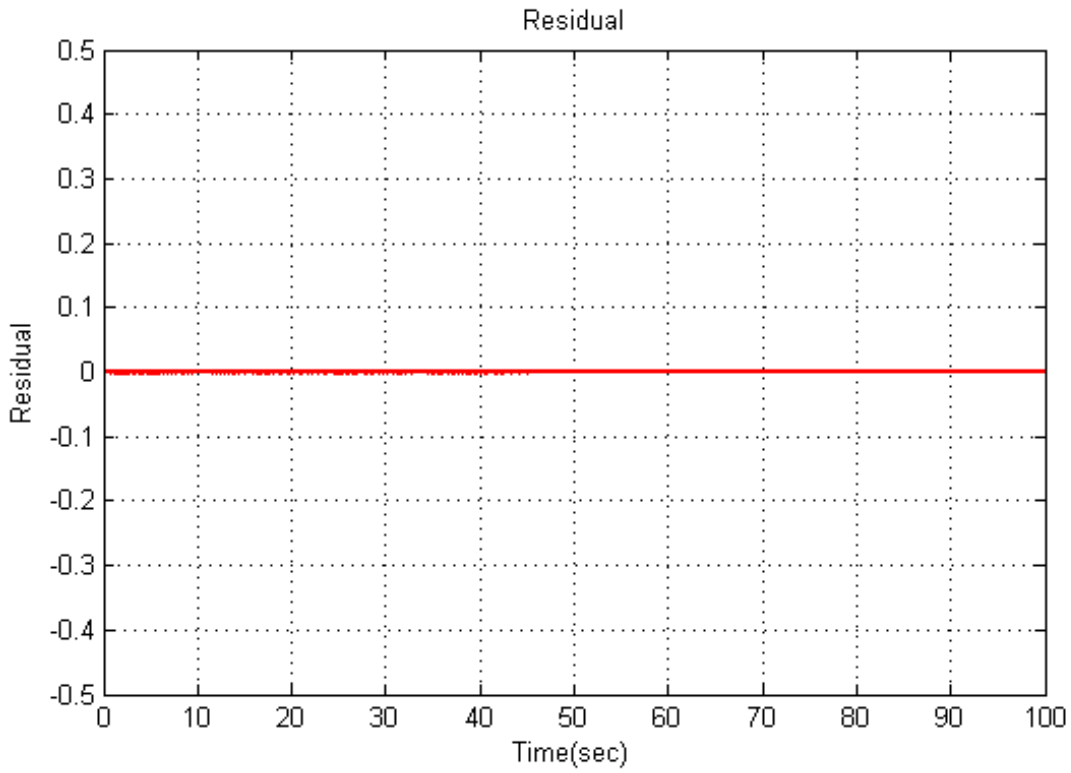

Fig. 5.6 Residual with No Faults

5.2.2 Fault Detection for Pitch System

For the pitch system fault, Fig. 5.7 shows increased damping ratio ζ in pitch system during the time period 10 sec to 20 sec. At the time of 10 second, the fault value is raised from zero and remains non-zero until 20 seconds. When the fault occurs, the residual is raised as well and lasts until the fault disappears at 20 second.

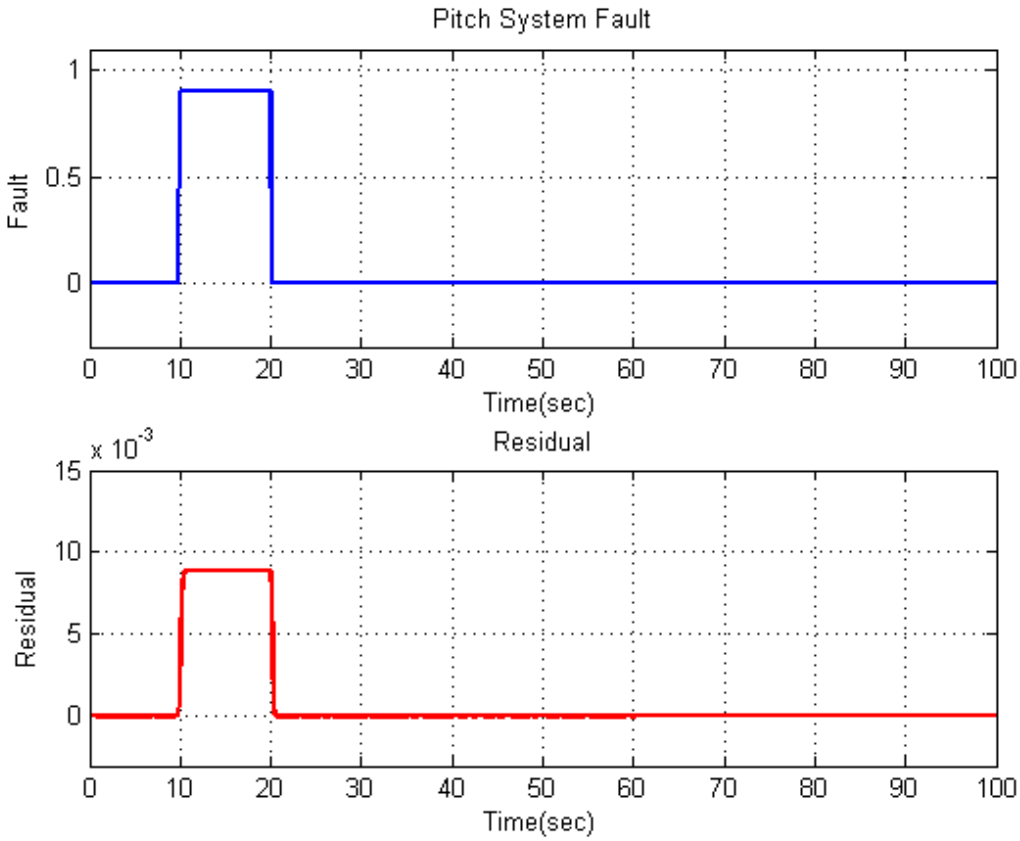

Fig. 5.7 Wind Turbine Pitch System Fault and Residual

5.2.3 Fault Detection for Drive-train System Gearbox Fault

Fig. 5.8 shows the drive-train system gearbox fault. The changed value of the generator torque T_g starts from 20 seconds and last for 10 seconds. It can be clearly seen

that the residual is increased at the same time and returns to zero when the fault signal finishes.

5.2.4 Fault Detection for Sensor Faults

Three different sensor faults for blade angle, rotor speed and generator speed are simulated here. In Fig. 5.9, the blade angle sensor fault signal starts from 40 seconds to 50 seconds. The designed observer could detect the fault and generate non-zero residual during the fault. The sensor fault and residual for rotor speed is shown in Fig. 5.10. The rotor speed sensor fault lasts for 10 seconds from time 60 seconds to 70 seconds. The

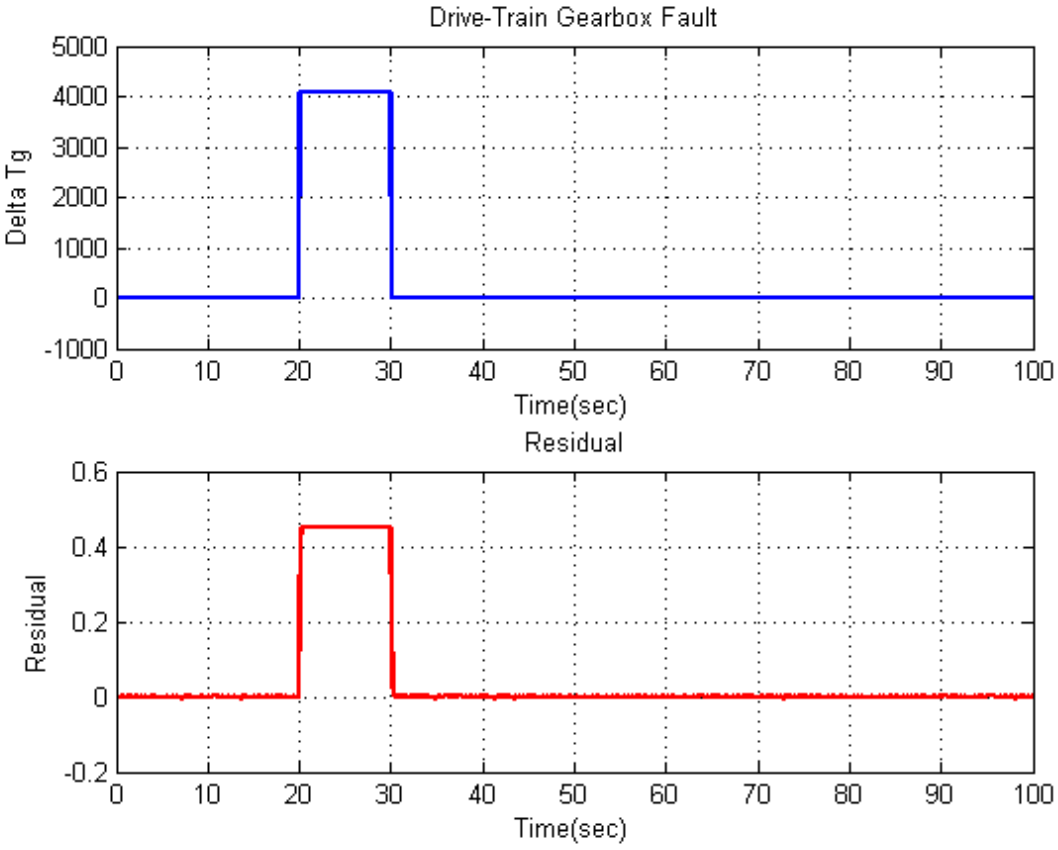

Fig. 5.8 Wind Turbine Drive-train System Gearbox Fault and Residual

residual signal generated synchronously with the sensor fault. The last sensor fault is the generator speed sensor fault. Fig. 5.11 shows the fault simulated from 80 seconds to 90 seconds. The simulated sensor fault could be reflected by the residual signal.

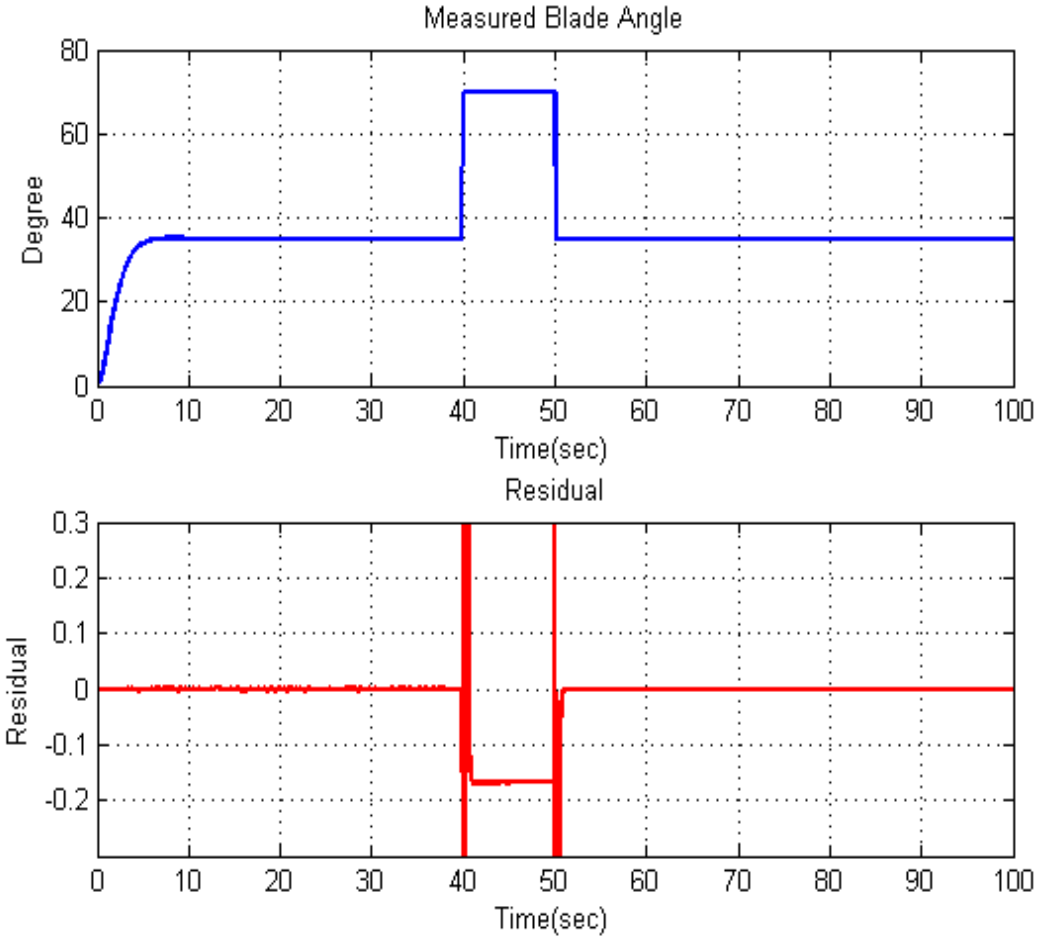

Fig. 5.9 Wind Turbine Blade Angle Sensor Fault and Residual

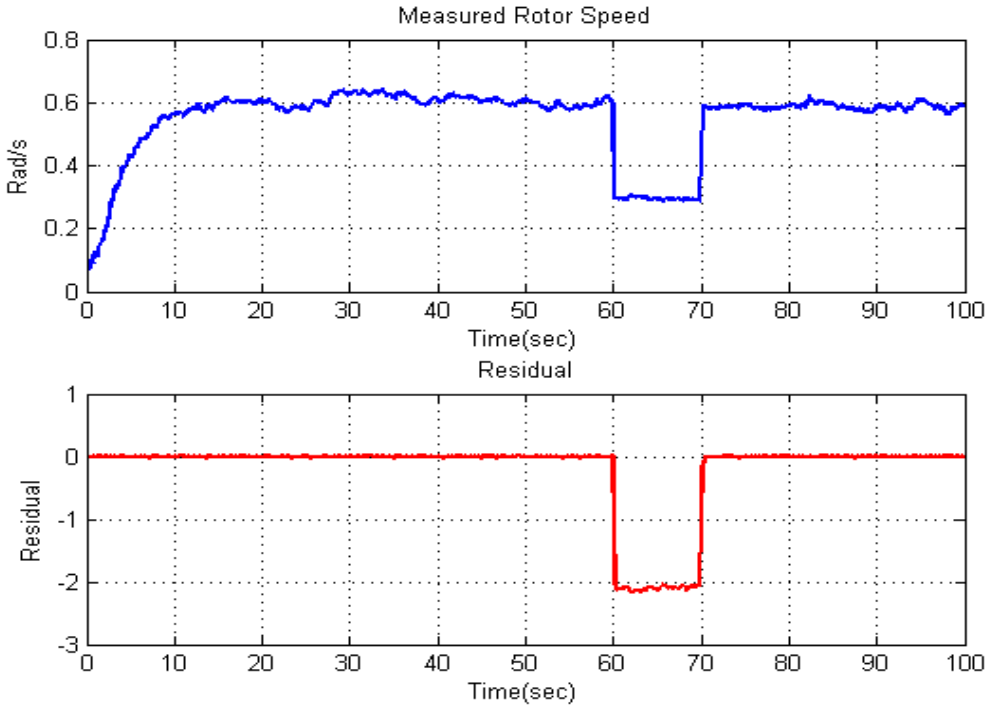

Fig. 5.10 Wind Turbine Rotor Speed Sensor Fault and Residual

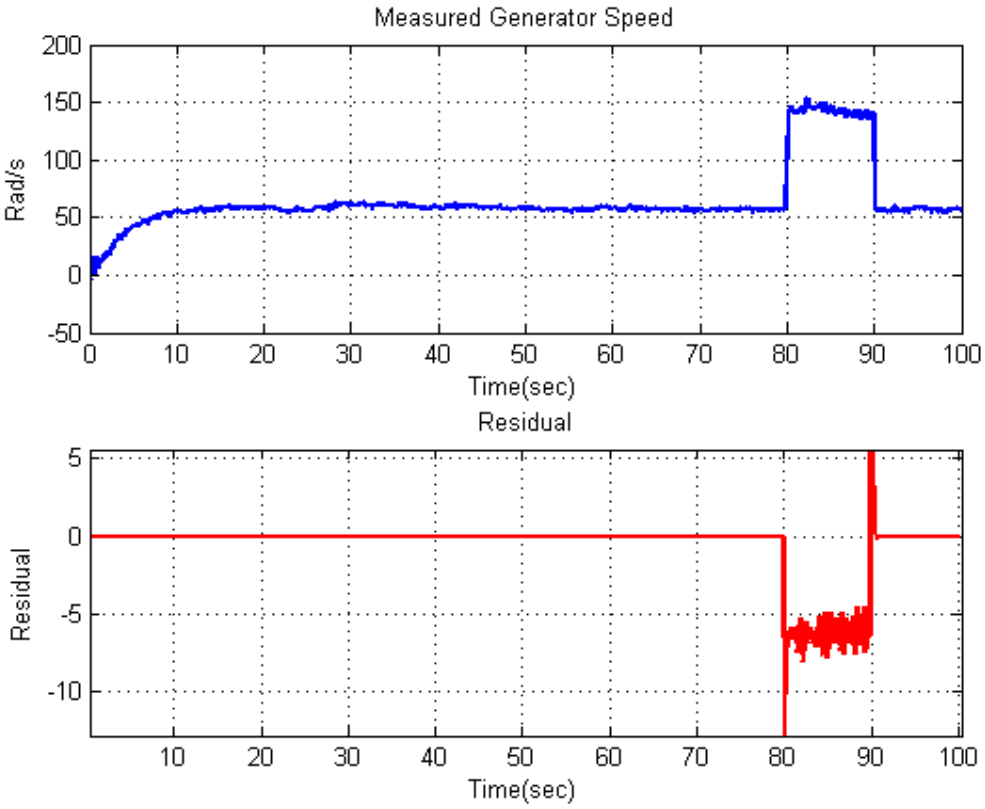

Fig. 5.11 Wind Turbine Generator Speed Sensor Fault and Residual

5.3 Summary

In this chapter, different types of faults are simulated to test the designed robust observer. In total five faults are simulated which includes pitch actuator component fault, drive-train system gearbox fault, blade angle sensor fault, rotor speed sensor fault and generator speed sensor fault. The pitch system of the WTs is normally hydraulic or electric, it is assumed that during the WT operation, the blade pitch actuator suffered a loss of lubrication which result in the fault condition. Drive-train system gearbox faults are a major category of failure modes and will lead to performance degradation of the wind turbine drive-train. Wind turbine sensor faults are another major fault type in wind turbine operation. The early detection could prevent serious accident. By referring Fig. 5.1, these three types of fault covers 38.4% of all wind turbine failure types and they could be detected by designed robust observer effectively and accurately.

CHAPTER 6
ARTIFICIAL NEURAL NETWORK MODELLING

6.1 Introduction

ANN is a mathematical model designed to train, visualise, and validate NN model (Nazari and Ersoy, 1992). Chang and Islam (2000) described the ANN as a model-free estimator because it does not rely on an assumed form of the underlying data. The NN model can be defined as a data structure that can be adjusted to produce a mapping from a given set of input data to features of or relationships among the data. The data collected from a given source is used as input to adjust and train the model and it is typically referred to as the training set. When the model is successfully trained, the NN will be able to perform classification, estimation, prediction or simulation on new data from the same or similar sources (Moustafa et al., 2011). Due to the limits of using mathematical models in complex modelling and to make FDI algorithm practical for real systems, an approach to the simulation of the WT dynamics was applied using NN modelling techniques, such as RBF and MLP. An NN provides a general way to model a nonlinear system with memory and it has been used by many researchers to describe the relationship between the input and output of monitored systems (Kamal and Yu, 2011).

6.2 Radial Basis Function Neural Network

The RBF NN network is chosen because its characteristic has the ability to approximate a nonlinear input system to a linear output. Compared with other NNs, the training process of RBF NN is faster and better. It is capable of approximating any continuous function with a certain precision level and therefore, can be used in dynamic system modelling and control (Li et al., 2009).

6.2.1 The Structure of RBF Network

The RBF NN has three layers, an input layer, a hidden layer and an output layer. Fig. 6.1 shows the RBF NN architecture. The neurons in the hidden layer contain the RBF whose outputs are inversely proportional to the distance from the centre of the

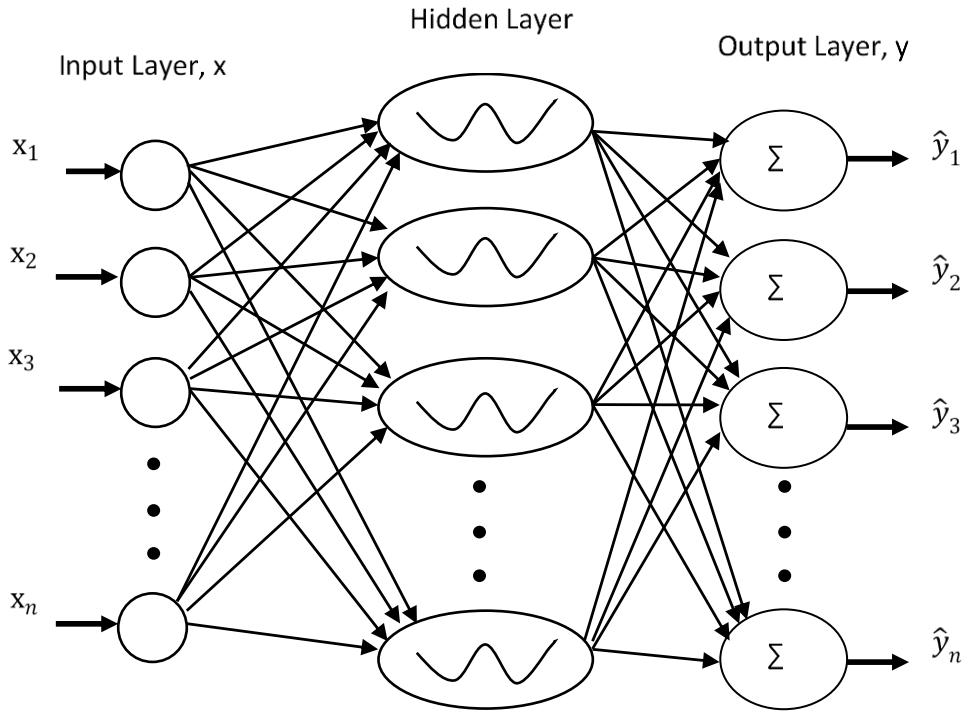

Fig. 6.1 The RBF Network Structure

neutron. The output units implement a weighted sum of outputs from the hidden unit to form their outputs.

The nonlinear system can be modelled by the multivariable NARX model of the following form,

$$y(k) = f\left[y(k-1), \ldots, y\left(k-n_y\right), u(k-1-d), \ldots, u(k-n_u-d)\right] + e(k) \quad (6.1)$$

where $u \in \Re^m$, $y, e \in \Re^p$ are the process input, output and noise vectors respectively with m and p being the number of inputs and outputs; n_y and n_u are the maximum lags in the outputs and inputs respectively, d is a dead-time vector representing delayed time to different control variables, $f(*)$ is a vector-valued nonlinear function. Suppose that the RBF network model precisely models the system; the model can then be represented by:

$$\hat{y}(k) = f\left[\hat{y}(k-1), \ldots, \hat{y}\left(k-n_y\right), u(k-1-d), \ldots, u(k-n_u-d)\right] + e(k) \quad (6.2)$$

The RBF NN consists of three layers which are the input layer, hidden layer and output layer. Each hidden node contains a centre c_j, which is a cluster centre on the input vector x defined by $\left\|x(t) - c_j(t)\right\|$ with x given as:

$$x(k) = \left[y(k-1), \ldots, y\left(k-n_y\right), u(k-1-d), \ldots, u(k-n_u-d)\right] \quad (6.3)$$

Then the output of the hidden layer node is a nonlinear function of the Euclidean distance. In this work the Gaussian function is chosen as the nonlinear function.

$$\varphi_i = e^{-\frac{\|x-c_i\|^2}{\sigma^2}}, i = 1, \ldots, n_h \quad (6.4)$$

where $\sigma \in \Re^{n_h}$ is a positive scalar called width, which is a distance scaling parameter to determine over what distance in the input space the unit will have a significant output. $c_i, x \in \Re^{n_h}$ are centre vector and input vector. The network output is then the sum of the weighted output of all hidden nodes and bias. Besides the Gaussian basis function, there are many types of function that can be used such as thin plate spline. However, the Gaussian basis function was used because it is selective and has response to the inputs that fall into the area (Nelles, 2002). Gaussian functions are suitable for describing many processes in mathematical, science and engineering. It can be used to approximate many nonlinear continuous functions defined on a compact set with any required accuracy. More details about Gaussian functions can be studied in (Nelles, 2002)

6.2.2 Network Modelling Modes

There are two different types of modes of modelling a dynamic system using NNs. By Narendra and Parthasarathy (1990), one is defined as independent mode and the other is dependent mode. The structures of dependent mode and independent mode are shown in Fig. 6.2 and Fig 6.3 respectively. From Fig. 6.2, it can be seen that in the dependent mode, the process output is used as part of the network inputs. Then, the model is dependent on the process and cannot run alone. If the dependent model runs alone, after predicting for one-step-ahead the plant output would not be available. Therefore, this dependent mode cannot do multi-step-ahead prediction and cannot run independently. The advantage of the dependent model is that it is easy to be trained for

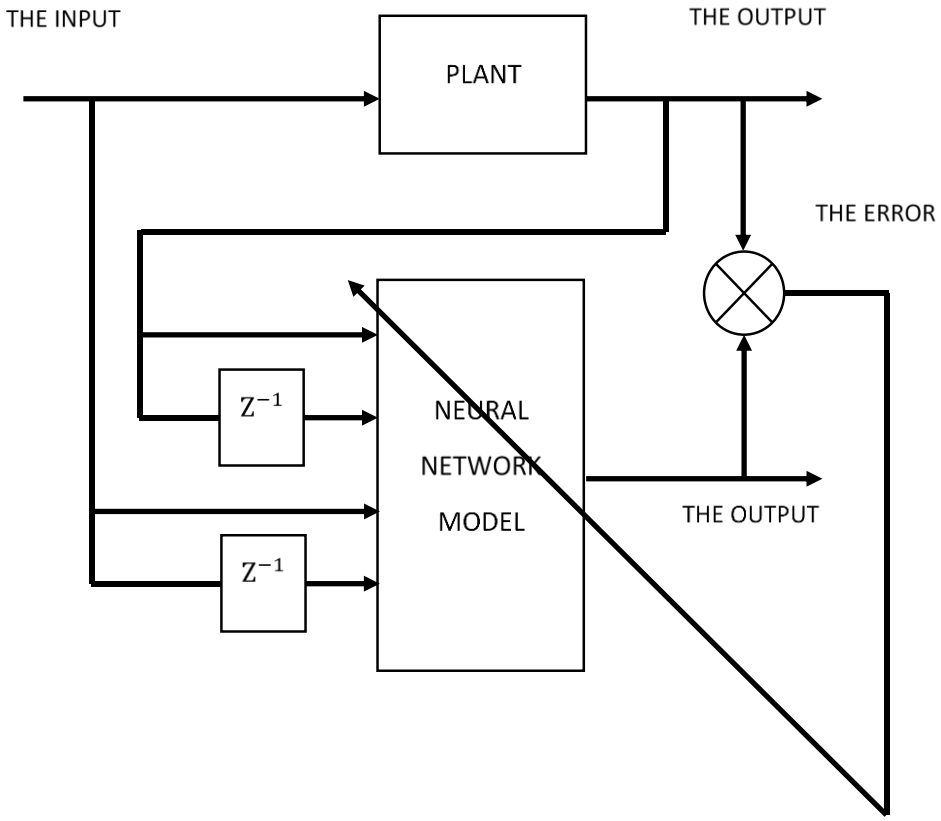

Fig. 6.2 The Dependent Model Structure

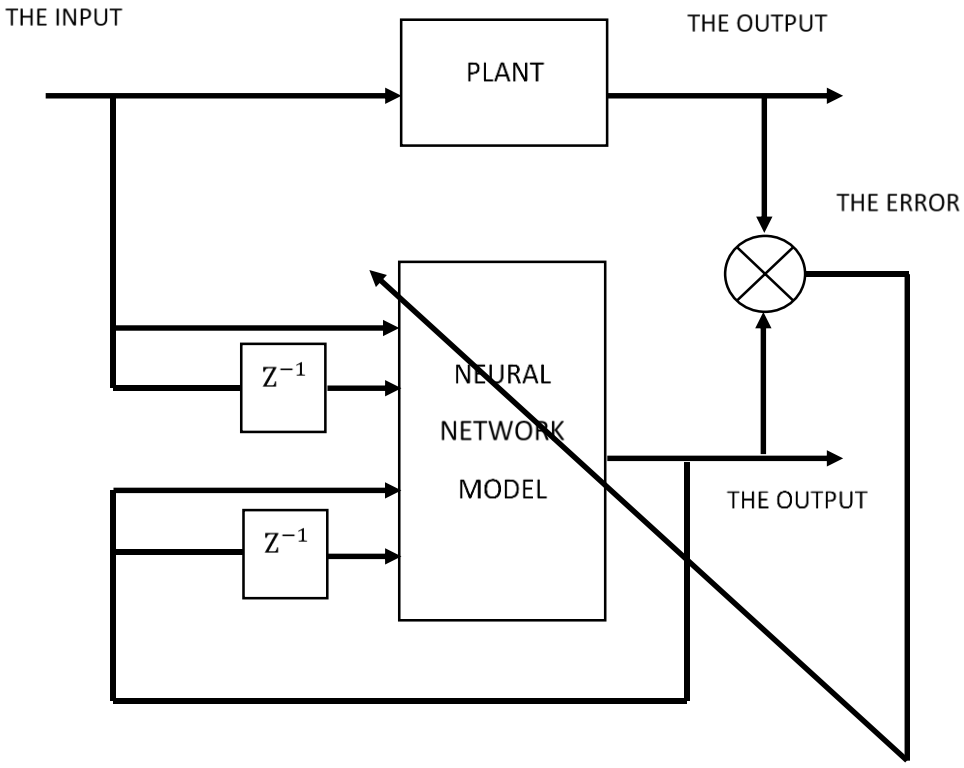

Fig 6.3 The Independent Model Structure

accurate one-step-ahead prediction, but one-step-ahead prediction is very limited for applications.

For the independent mode, the model output is used, instead of the process output, as part of the process. The model of the dependent mode can predict the process output for one-step-ahead only, while the independent model can predict for an infinite number of steps as long as the input is available. The independent model, though it is difficult to train, can be used as a simulation model or used in model prediction control for multi-step-ahead prediction. The features above have been experienced by (Yu et al., 1999). The difference between independent mode and dependent mode is significant when the two different modes of model are used for fault detection. When a fault occurs to the plant and affects the plant output, the independent model will not be affected by the occurring fault as the model is independent from the plant. For the same situation, the dependent model output will be affected through the plant output being used as the model input. Consequently, the error between the process and model output as the residual will not be sensitive to the occurrence of the fault. In this study, an independent model is selected.

6.2.3 The Training Algorithm

Training an RBF network is optimizing parameters including the hidden layer centres and the widths in Gaussian functions and network weights, to achieve

minimum model prediction error. Fig. 6.4 shows the flow chart of training the nural network.

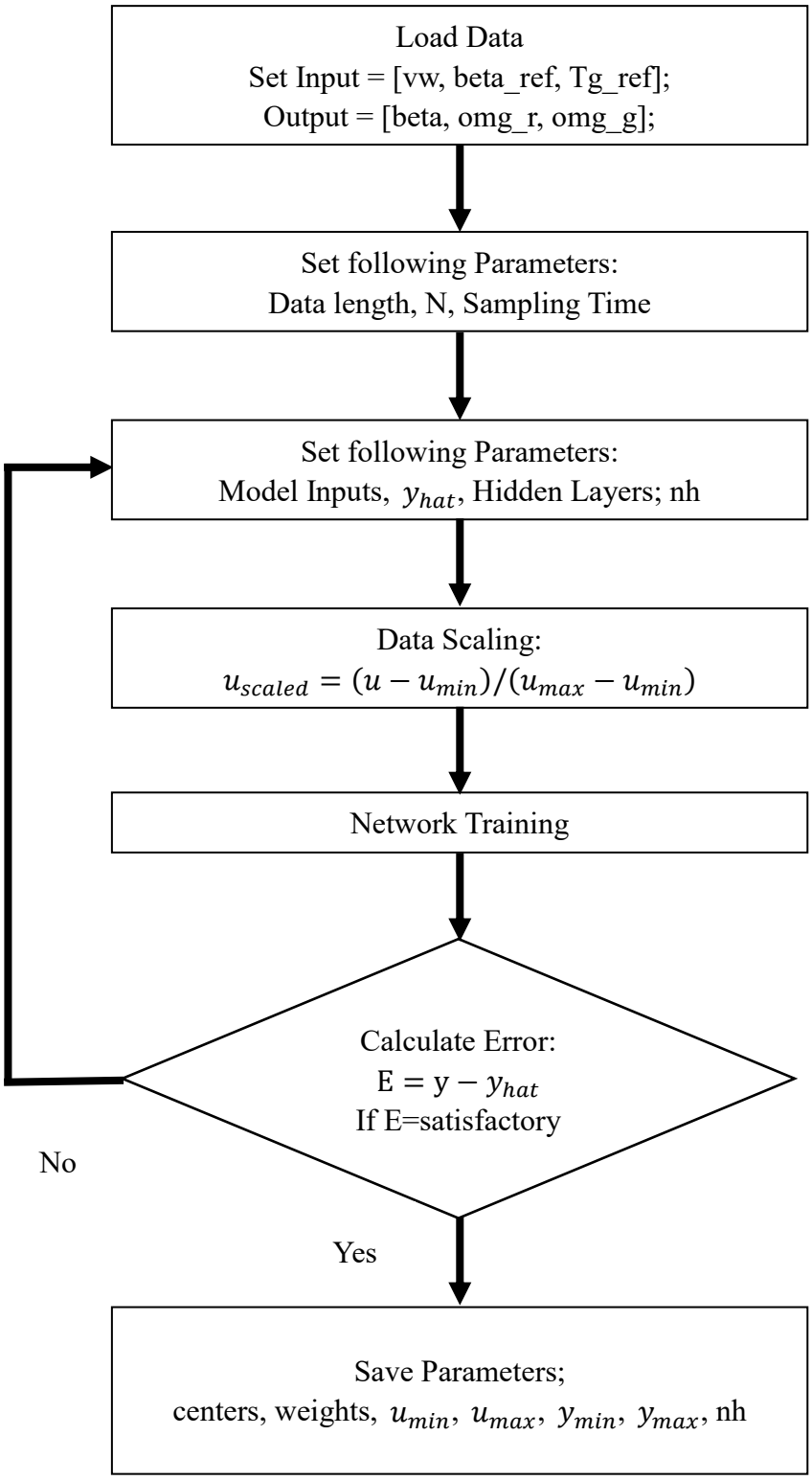

Fig. 6.4 The Flow Chart of Training the NN Network

The K-means clustering algorithm is selected for network centres in this work, so that the sum squared distance of each input data from the centre of the data group, to which it belongs, is minimized. The widths of the Gaussian functions are chosen using the p-nearest centre algorithm (Yu et al., 1999), to achieve that any input data is properly sampled by a few near centres. The weights between the hidden layer and the output are trained using the recursive least squares (RLS) as it is a numerically robust algorithm (Kamal et al., 2014). All three algorithms for the RBF network training are described in Wang et al. (2006).

6.2.3.1 Recurisve K-means algorithm

The centres are set by the K-means clustering method whose objective is to minimize the sum squared distances from each input data to its closest centre so that the data is adequately covered by the activation functions $\Phi_j(t)$ (Nelles, 2002, Zhai and Yu, 2008) The K-means clustering method proceeds as follows:

1. Choose q initial cluster centres $c_1(1), c_2(1), \dots, c_q(1)$.
2. At the t time step, distribute the sample (x) into $S_j(t)$ among the q cluster domains. $S_j(t)$ denotes the set of samples whose cluster is $c_j(t)$

$$x \in S_j(t) \quad if \left\|x(t) - c_j(t)\right\| < \|x(t) - c_i(t)\|$$

where, $j = 1, 2, \dots, q$ and $i = 1, 2, \dots, j-1, j+1, q$.

3. Update the cluster centres.

$$c_j(t+1) = \frac{1}{N_j}\sum_j^{N_j} S_j(t) \tag{6.5}$$

where, N_j is the number of elements in $S_j(t)$.

4. Repeat step 2 and step 3 until $c_j(t+1) = c_j(t)$.

6.2.3.2 *p*-nearest neighbours method

The *p*-nearest neighbours method is used to compute RBF NN width σ of each unit. The guideline is that the excitation of each node should overlap with some other nodes, usually the closest, so that a smooth surface interpolation between nodes is obtained. To achieve this each hidden node must activate at least one other hidden node to a significant degree. Therefore, the width is selected so that σ is greater than the distance to the nearest unit centre.

$$\sigma_i = \left[\frac{1}{p}\sum_{j=1}^{p}\left\|c_i - c_j\right\|^2\right]^{1/2} \tag{6.6}$$

where $i = 1, 2, \ldots, q$, and c_j is the *p*-nearest neighbours of c_i. For nonlinear function approximation *p* depends on the problem and requires experimentation.

6.2.3.3 Recursive Least Squares Algorithm

The RLS algorithm is a recursive form of the Least Squares (LS) algorithm. For each new sample it newly evaluates the parameter matrix *W*. The basic idea of the RLS algorithm is to compute the new parameter estimate *W(t)* at discrete time steps *t* by adding some correction information to the previous parameter estimate *W(t-1)* at time instant *t-1*. It is used to find the RBF network weights *W*, which can be summarized as follows (Zhi et al., 2001, Zhai and Yu, 2008)

$$Y_p(t) = Y_c(t) - W(t-1)h(t)$$

$$g_z(t) = \frac{P_{z(t-1)h(t)}}{\mu + h^T(t)P_Z(t-1)h(t)}$$

$$P_z(t) = \mu^{-1}[P_z(t-1) - g_z(t)h^T(t)P_Z(t-1)]$$

$$W(t) = W(t-1) + g_z(t)Y_p(t)$$

where W and h represent the RBF network weights and activation function outputs respectively. Y_c is the process output vector, Y_p is the prediction error, that is, the difference between the measured process output and the predicted output. P_z and g_z are middle terms. μ is called the forgetting factor ranging from 0 to 1 and is chosen to be 1 for off-line training. The parameters g_z, w and P_Z are updated orderly for each sample with the change in the activation function output h.

6.3 Wind Turbine Modelling using RBF Neural Network

ANNs have been intensively studied during the last two decades and successfully applied to dynamic system modelling as well as to fault detection and isolation. NNs provide an interesting and valuable alternative to classical methods such as Autoregressive Moving Average, Moving Average, Autoregressive with Exogenous, etc. (Nelles, 2002) because they can deal with the most complex situations which are not sufficiently defined for deterministic algorithms to execute (Patan, 2008). A Radial Basis function NN is used to model the WT dynamics in this study. It is because it provides an excellent mathematical tool for dealing with non-linear problems. Also the weights of RBF are linearly related to the objective function, so that any linear

optimization algorithm can be used to train the network weights and the training is very fast.

6.3.1 Data Collection

Collecting and preparing a suitable training data set is the first step in designing an RBF NN. As the training data will influence the accuracy of the NN modelling performance, the objective of experiment design on training data is to make the measured data become maximally informative, subject to constraints that may be at hand. As such the input signals are required to excite the dynamic modes of the process at different frequencies while also ensuring that the training data adequately cover the specified operating region. Lightbody and Irwin (1997) proposed a hybrid excitation signal for NN training. A persistently exciting input signal may be sufficient in linear system identification, but this is not the only consideration for the identification of nonlinear systems.

The process modelling of a NN model consists of two parts, part one is the capturing of the dynamics of the process and part two is the approximation of the underlying nonlinear vector function. For the WTS, the inputs are wind speed (vw), reference blade pitch angle (β_{ref}) and reference generator torque (T_g). A set of random amplitude signals (RASs) was generated and used as WTS input signals. The signals are generated randomly is to cover the whole range of frequencies and entire operating space of amplitude in the WTS. Random amplitude signals of wind speed, reference blade pitch angle and generator torque are show in Fig 6.5, Fig. 6.6 and Fig. 6.7 respectively. The RAS signals have been injected to the WTS as shown in Fig. 6.8.

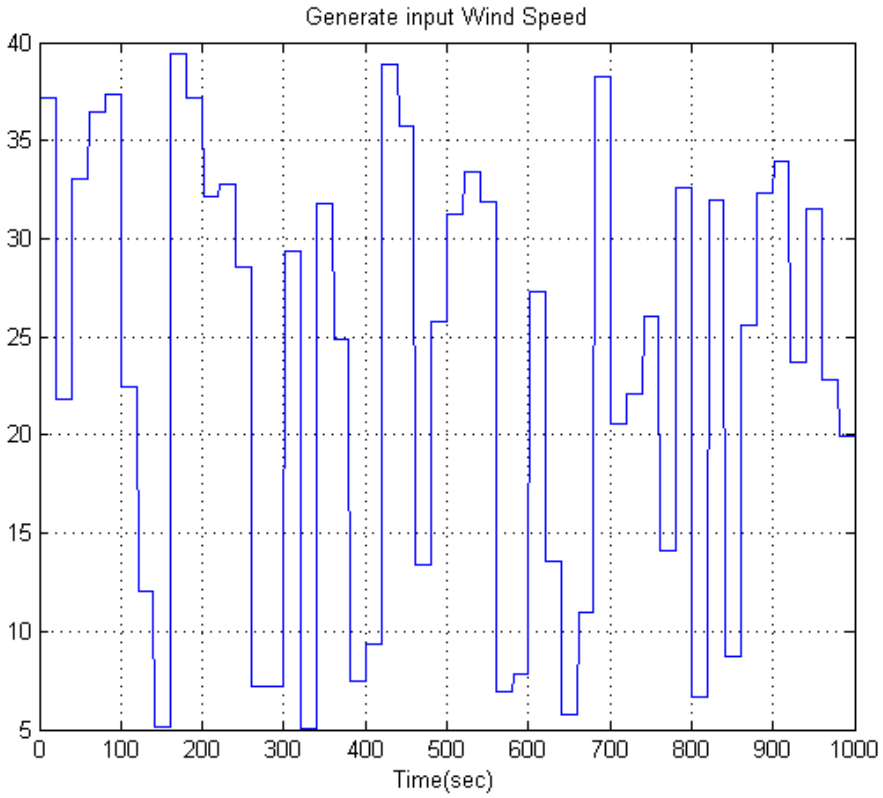

Fig. 6.5 Random Amplitude Signal of Wind Speed

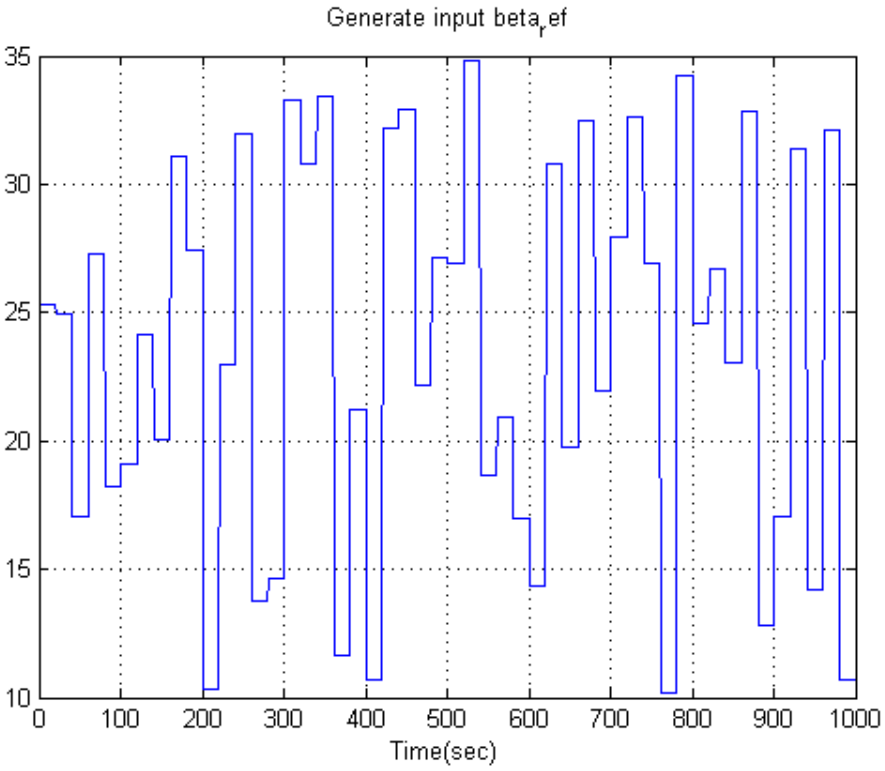

Fig. 6.6 Random Amplitude Signal of Reference Blade Pitch Angle

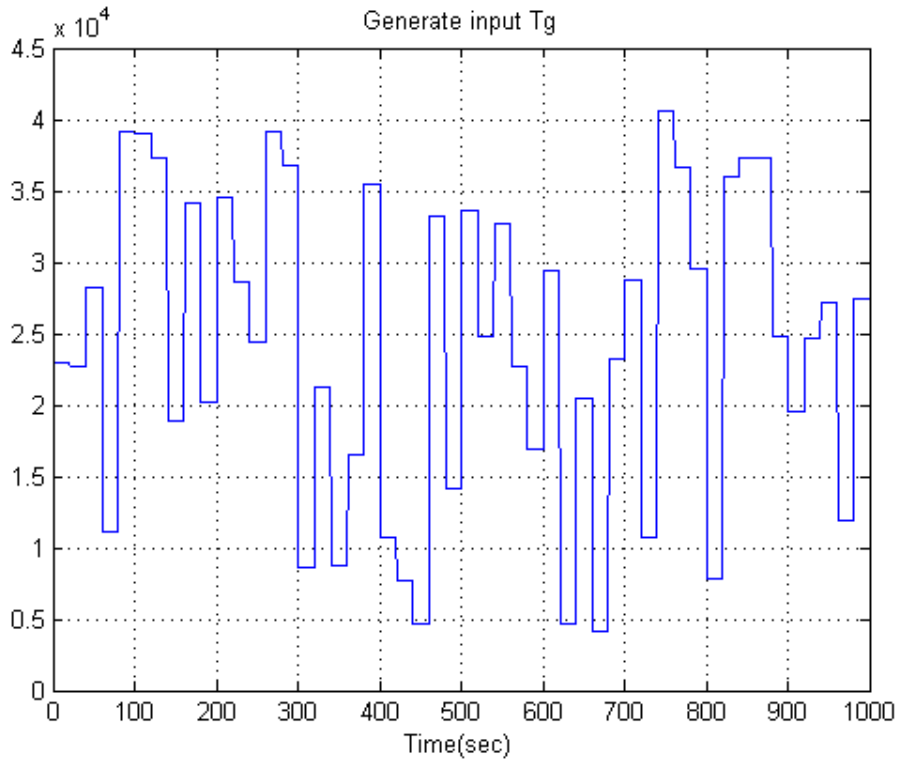

Fig. 6.7 Random Amplitude Signal of Generator Torque

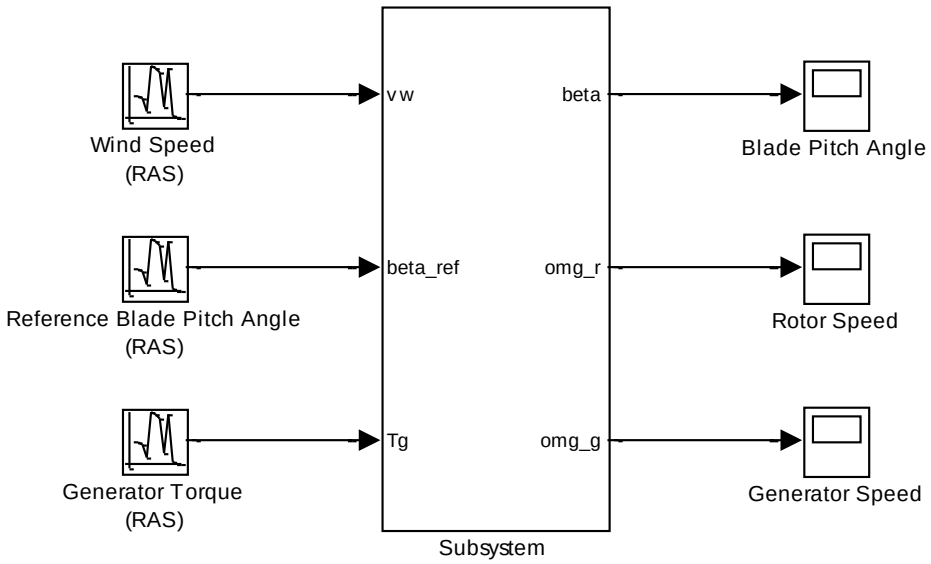

Fig. 6.8 Simulink Model of RAS Input Signals

After data collection and before the training and testing procedure, all the raw data samples have been normalized into the range of [0, 1] in order to increase the accuracy of the NN and decrease the error. The linear scale was done using the following equations:

$$u_{scale}(k) = \frac{u(k) - u_{min}}{u_{max} - u_{min}}$$

$$y_{scale}(k) = \frac{y(k) - y_{min}}{y_{max} - y_{min}}$$

Where u_{min}, u_{max}, y_{min} and y_{max} are the minimum and maximum inputs-outputs of data set, while u_{scale} and y_{scale} are the scaled input and outputs respectively.

The mean absolute error (MAE) is used rather than mean square error (MSE) because MAE can truly reflect the amplitude of the error, while the MSE reflects the squared error not the error itself. The MAS is given as the following

$$e_{MAE} = \frac{1}{N}\sum_{t=1}^{N}|f(t) - y(t)| = \frac{1}{N}\sum_{t=1}^{N}|e(t)|$$

The MAE is an average of the absolute error $e(t) = f(t) - y(t)$. $f(t)$ is the prediction by the NN model and $y(t)$ is the output of the WTS.

6.3.2 Model Structure Selection

The next step is to determine the input variables of the RBF model. The WTS to be modelled has three inputs: the wind speed (vw), reference blade pitch angle (β_{ref}) and

generator torque (T_g); and three outputs: blade pitch angle (β), rotor speed (Ω_r) and generator speed (Ω_g). The selection of RBF model structure is based on modelling trials where the model structure generates the smallest modelling errors. Different orders and time delay of these variables have been tried in the model training and the one giving the minimum training error was chosen. The equation is:

$$\hat{y}(k) = f[\hat{y}(k-1), \hat{y}(k-2), \hat{y}(k-3), u(k-1), u(k-2), u(k-3)] + e(k)$$

The selected structure of RBF network consists of 18 inputs and 3 outputs. It is shown in Fig. 6.9. The hidden layer nodes have been selected as 10. The centre is calculated using the K-means clustering algorithm, and the width σ was chosen using

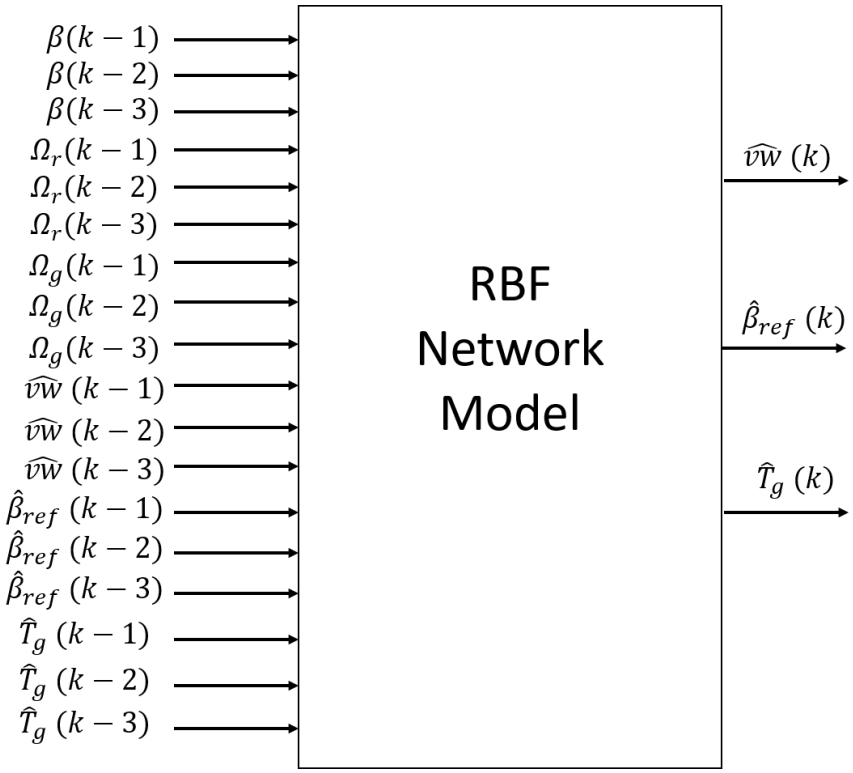

Fig. 6.9 The Structure of RBF Network Model

the p-nearest neighbours algorithm. The Gaussian functions in the 10 hidden layer nodes used the same width. The training of this algorithm was applied using the RLS algorithm developed by Zhai and Yu (2008) and the following initial values were used: $\mu = 0.999,\ w(0) = 1.0 \times 10^{-6} \times U_{(n_h \times 3)},\ P(0) = 1.0 \times 10^{8} \times I_{(n_h)}$, where μ is the forgetting factor, I is an identity matrix, U is the matrix with all element unity, and n_h is the number of hidden layers.

6.3.3 Model Training and Validation

A total of 1000 samples of data set was collected. These data were divided into two sets, the first set of 700 samples was used for RBF network training while the other 300

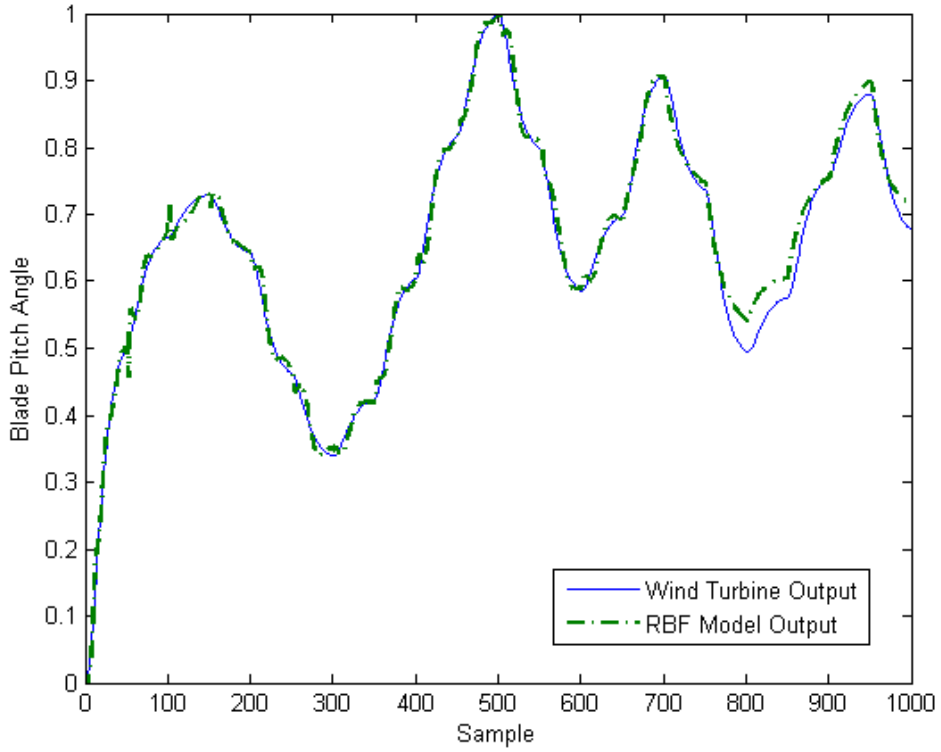

Fig. 6.10 Wind Turbine Output and RBF Model Output of Blade Pitch Angle

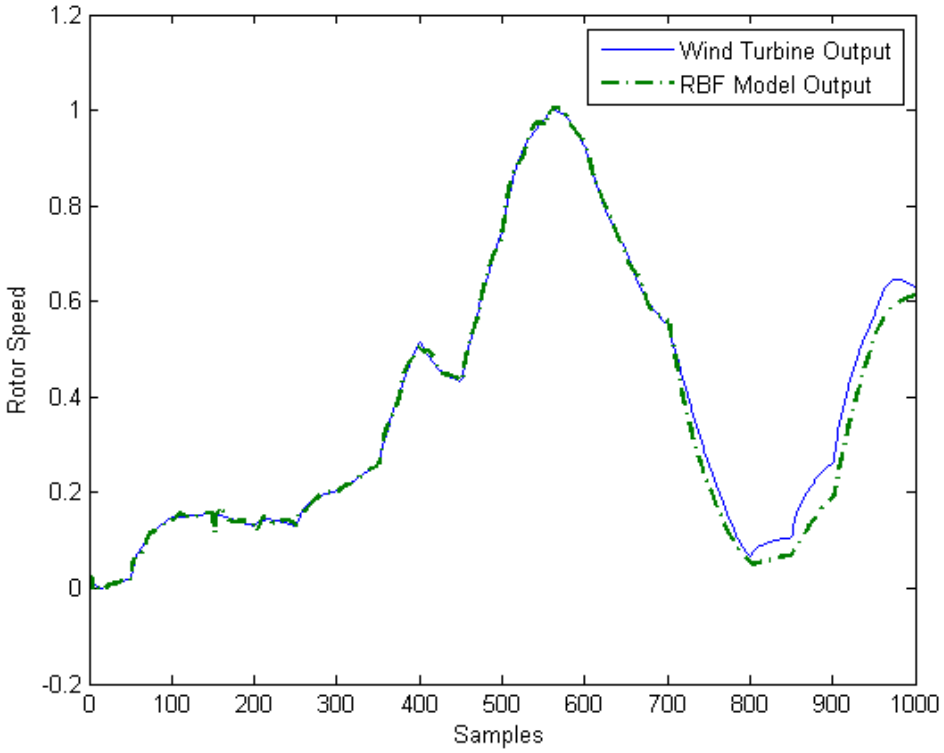

Fig. 6.11 Wind Turbine Output and RBF Model Output of Rotor Speed

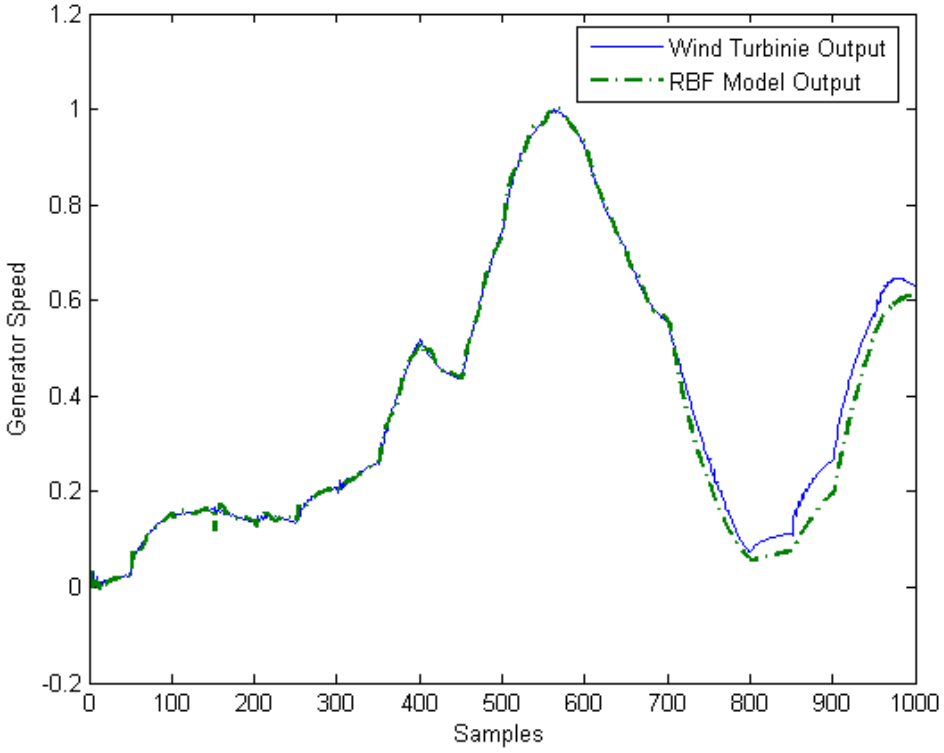

Fig. 6.12 Wind Turbine Output and RBF Model Output of Generator Speed

Outputs	MAE
Blade Pitch Angle	0.0127
Rotor Speed	0.0159
Generator Speed	0.0160

Table 6.1 MAE Value between WT Model Output and RBF Model Output

were used for testing. Fig. 6.10-6.12 show the model training and validation results of blade pitch angle, rotor speed and generator speed, respectively. It can be seen that there is a good match between the WT output and RBF model output with a small error. The mean absolute error index is used to evaluate the modelling effects. For this model, the MAE values of blade pitch angle, rotor speed and generator speed are 0.0127, 0.0159 and 0.0160 respectively, and they are shown in Table 6.1. The simulation results of training and testing the RBF NN model by using 10 hidden nodes were very good and a good prediction between the WT output and the RBF NN output was achieved.

6.4 FDI Methods and Fault Simulation

6.4.1 Fault Detection and Isolation Methods

Firstly an independent NN model is trained with data collected from the WT with no fault, which is called the healthy condition. Then, the model is used parallel to the WT in on-line mode to predict WT output. The modelling error between the WT output and model prediction will be used as the residual signal. Thus, when no fault occurs in

the WTS, the residual is just modelling error caused by noise and model-plant mismatch. When the fault occurs, the WT output will be affected by the fault and will deviate from the nominal values, while the model prediction will not be affected by the fault. So the faults will be reflected by the residual which have a significant deviation from zero caused by faults.

The fault isolation step is important in the FDI process due to its ability to classify the type of faults at that particular time when faults occurred. The fault isolation in this study is achieved by an additional RBF NN as a classifier (Kamal and Yu, 2012). The modelling error vector includes information of all faults, and different faults will affect each element in the modelling error vector in different ways. Thus, the modelling error vector will be used as the input to the classification RBF network. The RBF classifier is trained in the following way. Collect WT data for each of the faults occurring only, and then feed these data into the classifier with the target of the non-fault output being all “0”s, and indicated fault output being “1”. Thus, when the classifier is used to isolate faults in on-line mode, any output which turns to “1” indicates that the associated fault occurs. By using this characteristic the faults can be isolated clearly if all possible faults have different characteristics and no more than two faults are occurring at the same time. In this research, a total of three sensor faults have been tested, so that the classifier has three inputs and four outputs with three associated with the three sensor faults and one for no fault case.

6.4.2 Faults Detection and Isolation Using Neural Network

The three sensor faults are considered as 20% to 50% changes on the outputs of WT blade angle, rotor speed and generator speed sensors. The faults are simulated from sample time 1001 to 1500, 2501 to 3000 and 4001 to 4500 respectively, see Fig. 6.13. The faulty data for the sensors is generated using multiplying factors (MFs) of 1.2, 1.3 and 1.5 respectively, see Fig. 6.14.

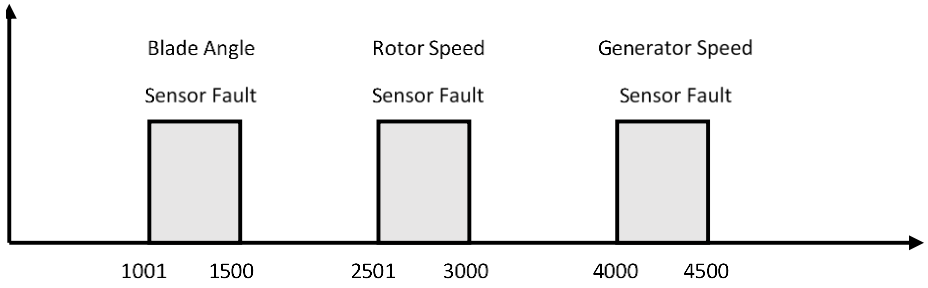

Fig. 6.13 Distribution of the Simulated Faults

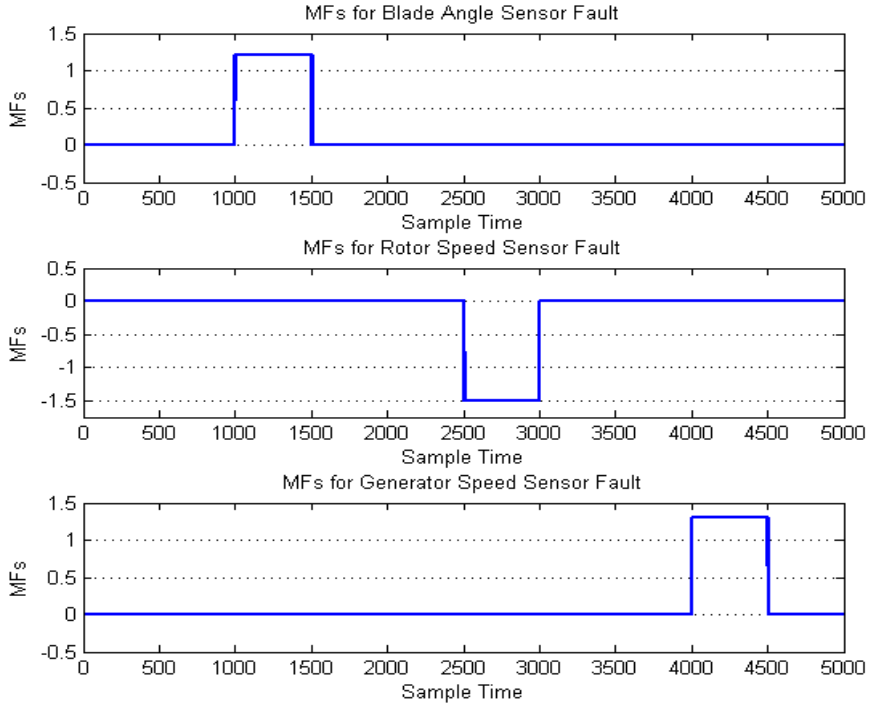

Fig. 6.14 MFs for Three Sensor Faults

6.4.2.1 Fault Detection using RBF Neural Network

Firstly, the WT model is fed with the random amplitude sequences for wind speed, reference blade pitch angle and generator torque. The collected three WT outputs, together with the three inputs and their delayed values are used to train the RBF model. After training, all three faults are simulated with the WT model. The three sensor faults are simulated as shown in Fig. 6.13. The first model prediction error of blade pitch angle is shown in Fig. 6.15. And the second model prediction error of rotor speed sensor fault and third model prediction error of generator sensor fault are shown in Fig 6.16 and Fig 6.17 respectively.

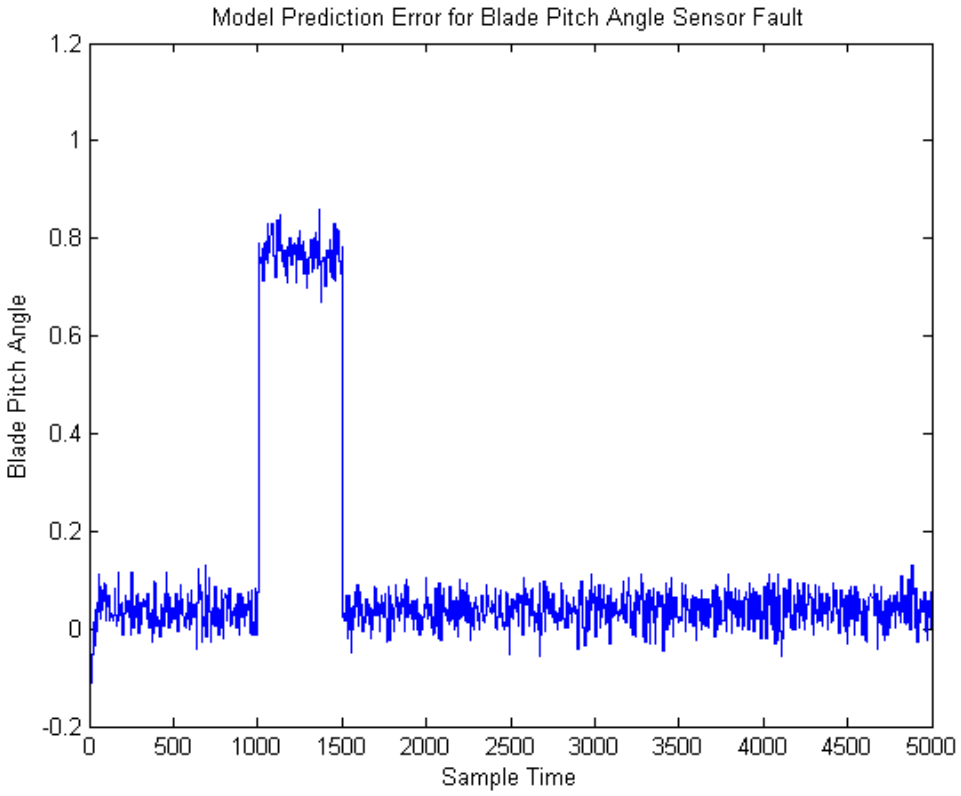

Fig. 6.15 Model Prediction Error for Blade Angle Sensor Fault

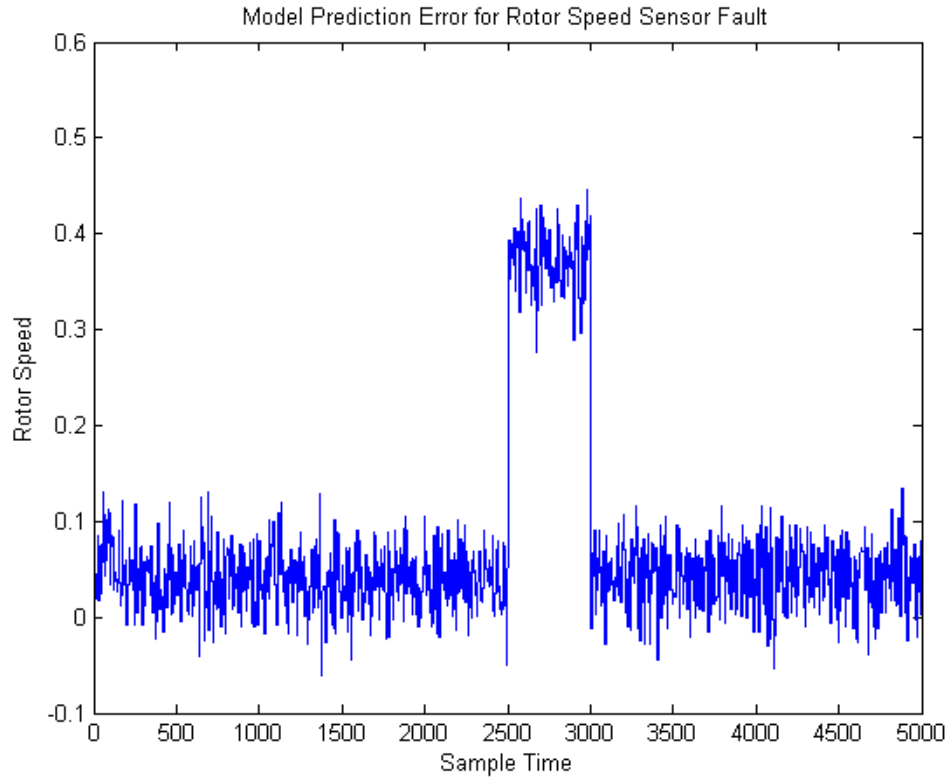

Fig. 6.16 Model Prediction Error for Rotor Speed Sensor Fault

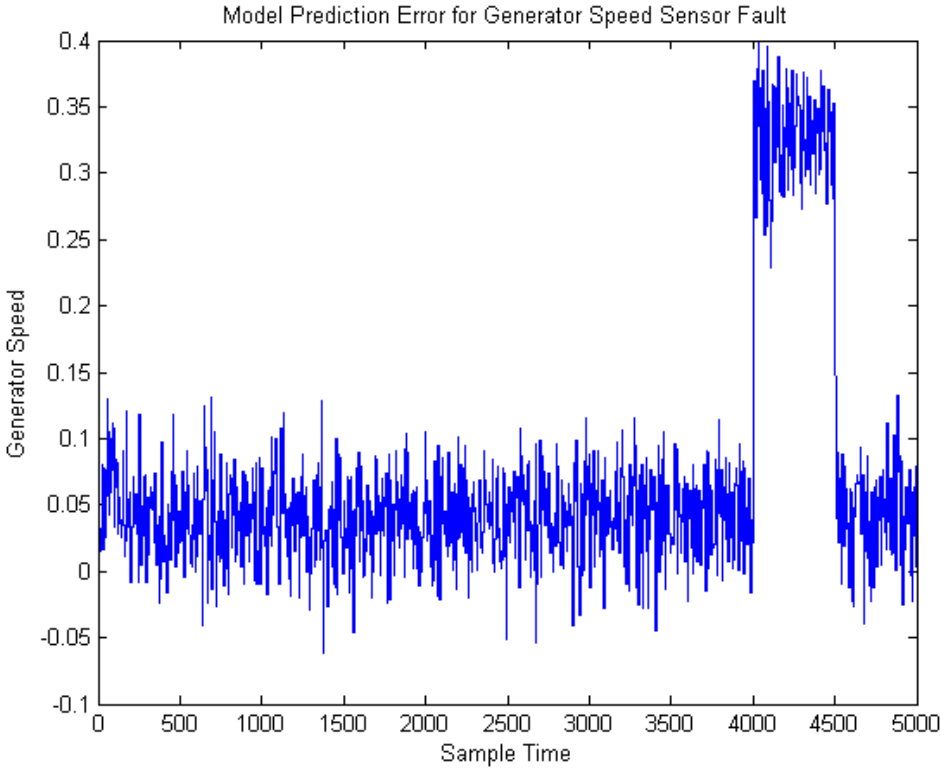

Fig. 6.17 Model Prediction Error for Generator Speed Sensor Fault

6.4.2.2 Fault Isolation using RBF Neural Network

In this study, to achieve a clear isolation among all possible faults, another RBF NN model is designed as a classifier because the RBF NN is well known for its powerful ability to classify components with different features from a mixed signal. The classifier has three inputs, each receiving one of the three modelling errors. There are four outputs for the classifier, with one representing the “no fault case” and the other three indicating the three different sensor faults.

The classifier is trained in the following way. Collect four sets of data, the first set without fault and the other three sets, each with one fault only. For each data set of the four, the target of the training for the output corresponding to the contained fault is set to “1”, while the targets for the other outputs are set to “0”. In total 6000 data samples were collected. They were split into four equal data sets so each containing a total of 1500 samples. The first data set comprised 1500 no faults samples, then the three faults were separated into three other data sets. The training targets given as described above.

After training, the classifier is tested with a similar arrangement of data. 3500 data samples are used for testing. The first 500 samples are no fault samples, followed by 500 data samples for blade pitch angle sensor fault. After blade pitch angle sensor fault, 500 fault-free samples are insert before 500 data samples of rotor speed sensor fault. This is to observe the residual rising time and disappearing time. For the same

reason, there are two sets of 500 fault-free samples before and after 500 generator speed sensor fault samples. The data samples with associated fault type are listed in Table 6.2. Similar to the fault detection RBF NN, the centres and widths are also selected using the K-means clustering algorithm and the *p*-nearest centre method. The network weights are trained using the RLS algorithm with its parameters set as $\mu = 0.999$, $w(0) = 1.0 \times 10^{-6} \times U_{(n_h \times 3)}$, $P(0) = 1.0 \times 10^{8} \times I_{(n_h)}$, where μ is the forgetting factor, I is an identity matrix, U is the matrix with all element unity, and n_h is the number of hidden layers. The number of hidden layer nodes was tried with several numbers and the one giving the minimum training error was chosen as 4. Fig 6.18-6.20 show the test results of the designed RBF classifier.

Data Samples	Fault Type
1-500	No Fault
501-1000	Blade Pitch Angle Sensor Fault
1001-1500	No Fault
1501-2000	Rotor Speed Sensor Fault
2001-2500	No Fault
2501-3000	Generator Speed Sensor Fault
3001-3500	No Fault

Table 6.2 Data Samples and Fault Type

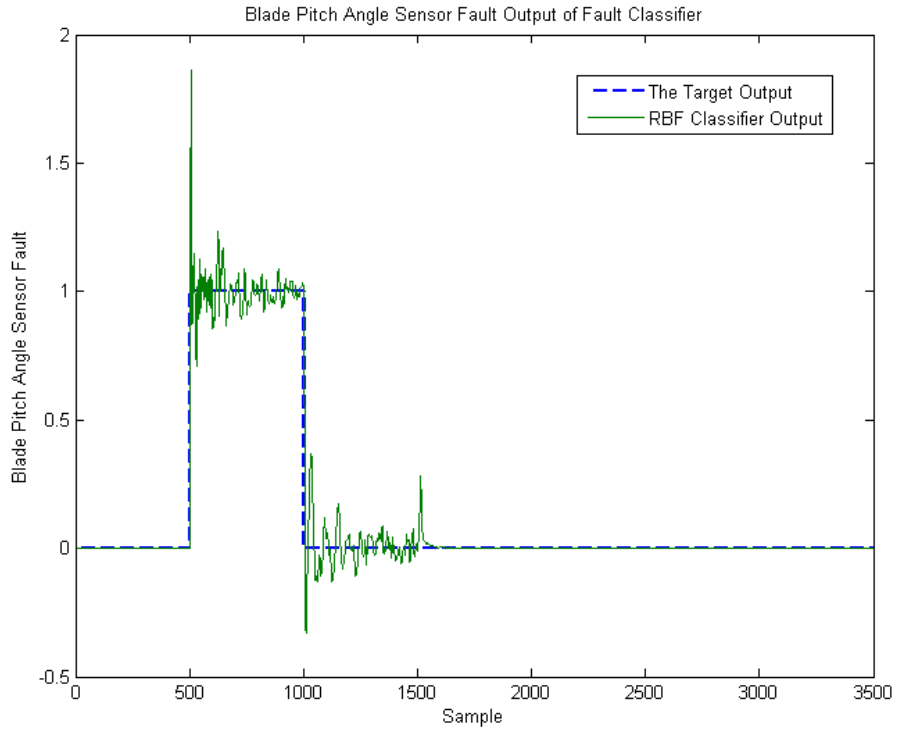

Fig. 6.18 Blade Pitch Angle Sensor Fault Output of Fault Classifier

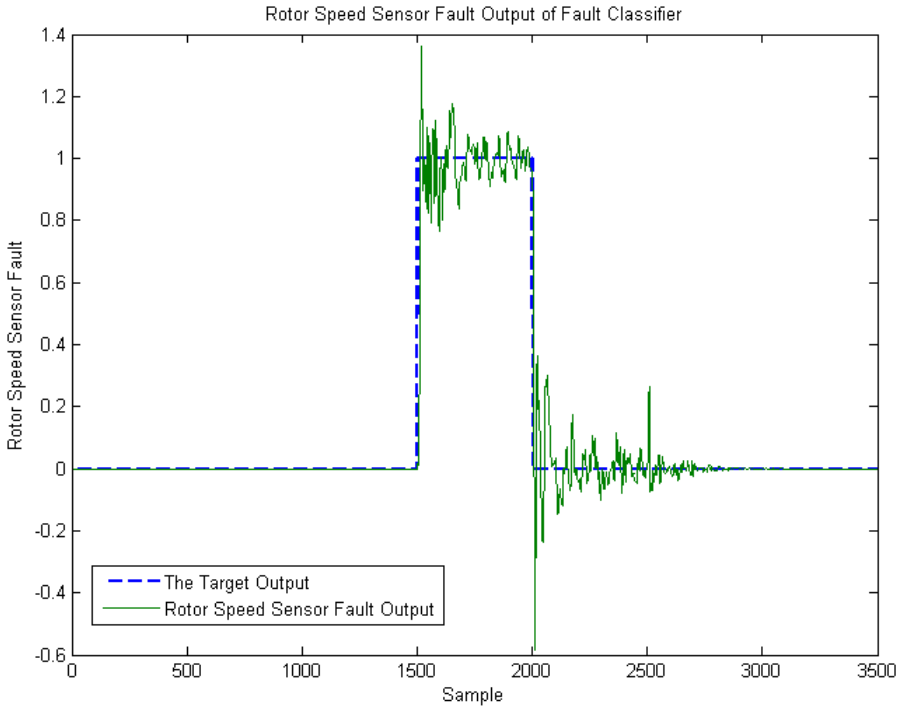

Fig. 6.19 Rotor Speed Sensor Fault Output of Fault Classifier

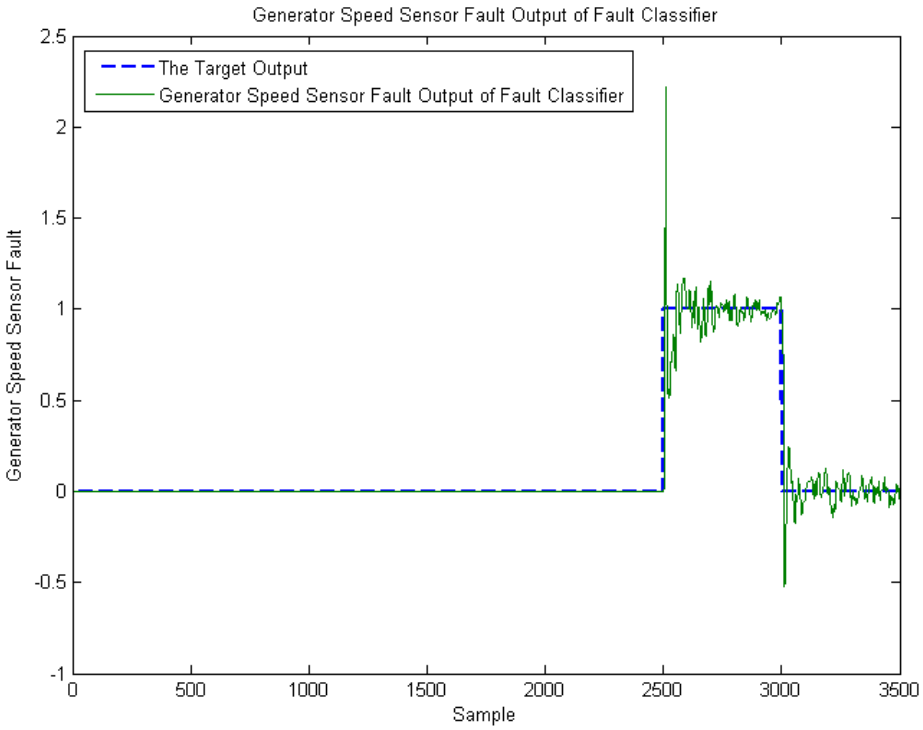

Fig. 6.20 Generator Speed Sensor Fault Output of Fault Classifier

6.4.3 Fault Detection and Isolation Results Analysis

For the wind turbine fault detection by designed RBF neural network, the model prediction errors generated from three outputs measurement based on the difference between the plant outputs and the RBF neural network model. In Fig. 6.15, the blade angle sensor fault is occurred from time 1000 to 1500, the fault is indicated by the model prediction error. Fig. 6.16 shows the model prediction error for rotor speed sensor fault. During the time 2500 to 3000, the error raised by fault in is period. Again in Fig. 6.17, the generator speed sensor fault during time 4000 to 4500 is also reflected by the raise of the model prediction error. It can be clearly seen, the three sensor faults could be detected by the designed RBF neural network.

For fault isolation with RBF network, an additional RBF neural network is designed as a classifier to isolation different faults. After training, the designed classifier is able to classify faults according to their occurrence. By referring Fig. 6.18-6.20, the outputs of the classifier are ‘1’ when there is a fault, and when there is no fault the signal is ‘0’. The all three faults could be isolated by designed RBF classifier.

6.5 Summary

In this chapter, artificial neural network fault detection and isolation method for wind turbine system is studied. The neural network model can be defined as a data structure that can be adjusted to produce a mapping from a given set of input data to features of or relationships among the data. In this study, a radial basis function neural network is chosen because its characteristic has the ability to approximate a nonlinear input system to a linear output. Compared with other NNs, the training process of RBF NN is faster and better. To design the RBF model, it is found 10 hidden layer nodes is most suitable for the task in this study. As far as accuracy of prediction is concerned, the performance of the RBF model using k-means clustering technique is satisfactory. After the well design and training of RBF neural network for wind turbine, three different sensor faults are simulated to test the fault detection and isolation. The developed model is sensitive to these three faults. All three sensor faults could be detected and isolated successfully.

CHAPTER 7
CONCLUSION AND FURTHER WORK

7.1 Conclusion

In this research, a WT dynamic system is modelled. A WTS generally consists of three sub-systems: aerodynamics, pitch actuator and drive-train system. The aerodynamics is about conversion of wind kinetic power into mechanical power, which is a major aspect of the wind power production. Pitch actuator controls the angle of the WT blade angle to extract the most power from the wind. The drive-train system transfers the mechanical power from rotor to generator. In this study, a 2-mass, 1 spring, 1-damper model has been selected for the drive-train system. Then a combined state space model has been developed. After the development of the mathematical model for WTS, a robust observer has been designed. A state observer is a software system that could estimate or observe the state variables. The designed observer is a Luenberger-type and it is robust to the system noise and sensitive to the system fault signals.

After the observer design, five different WTS faults are simulated to test the designed observer. The simulated faults are WT pitch system fault, drive-train system gearbox fault and three system output sensor faults which are the pitch angle sensor, rotor speed sensor and generator speed sensor respectively. For the pitch system fault, it is assumed that during the WT operation, the blade pitch actuator suffered a loss of lubrication which means the friction is increased to 2 times original value, which means

the damping ratio is also increased by 2 times. The gearbox faults are a major category of failure modes in WT drive-train systems. They are caused by various factors such as manufacturing and installing errors, surface wear, fatigue, etc. A gear fault will lead to performance degradation of the WT drivetrain and may cause a catastrophic failure of the gearbox or even failures of other components in the WT drivetrain (Lu et al., 2017). The drive-train system gearbox fault is assumed to occur on generator torque and the value has increased by 10%. The faults above are simulated to test the designed observer. When the system operates in the no fault condition, the residuals and state errors remain zero. When the five faults are simulated, the observer could detect those faults, by raising the residual to non-zero.

Beside the design of the robust observer, an ANN FDI method is studied. The NN is selected as a RBF NN. The characteristic of RBF NN has the ability to approximate a nonlinear input system to a linear output. Compared with other NNs, the training process of RBF NN is faster and better. After comparing two different types of modes of modelling a dynamic system using NNs, dependent mode and independent mode, the independent mode is chosen. This is because the model of the dependent mode can predict the process output for one-step-ahead only, while the independent model can predict for an infinite number of steps as long as the input is available. When a fault occurs to the plant and affect the plant output, the independent model will not be affected by the occurring fault as the model is independent from the plant. For the same situation, the dependent model output will be affected through the plant output being

used as the model input. Consequently, the error between the process and model output as the residual will not be sensitive to the occurrence of the fault.

After selecting the mode of RBF NN, a set of random amplitude signals of wind speed, reference blade pitch angle and generator torque are generated. The signals are generated randomly is to cover the whole range of frequencies and entire operating space of amplitude in the WTS. All the raw data samples have been normalized into the range of [0, 1] in order to increase the accuracy of the NN and decrease the error. The hidden layer nodes of the RBF network model have been selected as 10. The centre is calculated using the K-means clustering algorithm, and the width σ was chosen using the p-nearest neighbours algorithm. The Gaussian functions in the 10 hidden layer nodes used the same width. The training of this algorithm was applied using the recursive least squares (RLS) algorithm. The designed RBF NN model has been tested and the result shows there is a good match between the WT output and RBF model output.

After the development of the RBF NN model, it is used for fault detection and isolation. The basic fault detection strategy is as follows. Firstly an independent NN model is trained with data collected from the WT with no fault, which is called the healthy condition. Then, the model is used parallel to the WT in on-line mode to predict WT output. The modelling error between the WT output and model prediction will be used as the residual signal. Thus, when no fault occurs in the WTS, the residual is just a modelling error caused by noise and model-plant mismatch. When the fault occurs,

the WT output will be affected by the fault and will deviate from the nominal values, while the model prediction will not be affected by the fault. So the faults will be reflected by the residual which have a significant deviation from zero caused by faults. The fault isolation is achieved by an additional RBF NN as a classifier. The modelling error vector will be used as the input to the classification RBF network. The RBF classifier is trained in the following way. Collect WT data for each of the faults occurring only, and then feed these data into the classifier with the target of the non-fault output being all "0"s, and indicated fault output being "1". Thus, when the classifier is used to isolate faults in on-line mode, any output which turns to "1" indicates that the associated fault occurs. Three sensor faults are simulated and the faults are considered as 20% to 50% changes on the outputs of WT blade angle, rotor speed and generator speed sensors. The designed RBF classifier is trained in the following way. Collect four sets of data, the first set without fault and the other three sets, each with one fault only. After training, the classifier is tested with a similar arrangement of data. Similar to the fault detection RBF NN, the centres and widths are also selected using the K-means clustering algorithm and the *p*-nearest centre method. The simulation results show that the classifier could isolate all three faults successfully.

7.2 Further Works

This work forms the basis for developing a robust observer and an independent NN model for fault detection and isolation for WTS. The basic idea behind model-based

fault diagnosis is the generation of residuals, consisting of the difference between the process plant and the estimated model. It is well known that the core element of model-based fault detection in control systems is the generation of residual signals.

For the developed FDI approach, the reliability and the effectiveness need to be tested in real-time applications. The proposed models need further tests in a larger environment before being deployed for practical applications in the real world. For future work the following suggestions need to be considered:

1. The proposed FDI method needs to be tested with a real test rig. This is because in the real application, the situation will be more complicated than the simulation.
2. The fault isolation with designed robust observer could be studied. The fault isolation is another important part of fault diagnosis. The fault detection only indicates the occurrence of a fault but does not inform which fault it is. The designed observer could be improved to achieve the fault isolation.
3. More actuator faults and component faults could be simulated for RBF neural network FDI. In this study, three different fault types only cover 38.4% of the total fault types and there are still many fault types could be studied.
4. A multi-layer perceptron (MLP) neural network could be developed and simulated for WTS FDI. The MLP neural network is another most commonly used type of neural network and has been widely used in many fault detection and isolation fields.

REFERENCE

ACKERMANN, T. 2012. *Wind Power in Power Systems*, Wiley.

AMIRAT, Y., BENBOUZID, M. E. H., BENSAKER, B. & WAMKEUE, R. Condition Monitoring and ault Diagnosis in Wind Energy Conversion Systems: A Review. 2007 IEEE International Electric Machines & Drives Conference, 3-5 May 2007 Antalya, Turkey. 1434-1439.

AMJADY, N. & REZAEY, A. A new power transformer fault diagnosis system and its application for wind farms. 2012 Proceedings of 17th Conference on Electrical Power Distribution, 2-3 May 2012 Tehran, Iran. 1-5.

ANAYA-LARA, O., JENKINS, N., EKANAYAKE, J., CARTWRIGHT, P. & HUGHES, M. 2009. *Wind energy generation: modelling and control*, US, Wiley.

ASSOCIATION, G. W. E. n. d. *The Structure of a Modern Wind Turbine - An Overview* [Online]. WWEA. Available: http://www.wwindea.org/technology/ch01/estructura-en.htm [Accessed 27th July 2011].

ATHANS, M., FEKRI, S. & PASCOAL, A. Issues on robust adaptive feedback control. Preprints of the 16th IFAC world congress, 3-8 July 2005 Prague, Czech Republic. 9-39.

BASSEVILLE, M. 1988. Detecting changes in signals and systems—a survey. *Automatica*, 24**,** 309-326.

BEARD, R. V. 1971. *Failure accommodation in livear system through self reorganization.* PhD thesis, MIT.

BHAGWAT, A., SRINIVASAN, R. & R. KRISHNASWAMY, P. 2003. Multi-linear model-based fault detection during process transitions. *Chemical Engineering Science,* 58**,** 1649-1670.

BIANCHI, F. D., BATTISTA, H. D. & MANTZ, R. J. 2007. *Wind turbine control systems: principles, modelling and gain scheduling design*, Springer.

BIN, L., YAOYU, L., XIN, W. & YANG, Z. A review of recent advances in wind turbine condition monitoring and fault diagnosis. Power Electronics and Machines in Wind Applications, 24-26 June 2009 Lincoln, NE, USA. 1-7.

BLAKE, D. & BROWN, M. Simultaneous, Multiplicative Actuator and Sensor Fault Estimation using Fuzzy Observers. 2007 IEEE International Fuzzy Systems Conference, 23-26 July 2007 London, United Kingdom. 1-6.

BOUNO, T., YUJI, T., HAMADA, T. & HIDEAKI, T. 2005. Failure forecast diagnosis of small wind turbine using acoustic emission sensor.

BURTON, T., JENKINS, N., SHARPE, D. & BOSSANYI, E. 2011. *Wind Energy Handbook*, Wiley.

CAO, W., XIE, Y. & TAN, Z. 2012. *Wind turbine generator technologies.*

CASELITZ, P., GIEBHARDT, J. & MEVENKAMP, M. On-line fault detection and prediction in wind energy converters. Institut fur Solare Energieversorgungstechnik (ISET) e.V.

CASELITZ, P., GIEBHARDT, J. & MEVENKAMP, M. On-line fault detection and prediction in wind energy converters. Proceedings of the EWEC, 10-14 October 1994 Macedonia, Greece. 623-627.

CHANG, D.-H. & ISLAM, S. 2000. Estimation of Soil Physical Properties Using Remote Sensing and Artificial Neural Network. *Remote Sensing of Environment,* 74**,** 534-544.

CHEE PIN, T. & EDWARDS, C. Multiplicative fault reconstruction using sliding mode observers. 2004 5th Asian Control Conference, 20-23 July 2004 Melbourne, Victoria, Australia. 957-962 Vol.2.

CHEN, C., SUN, C., ZHANG, Y. & WANG, N. Fault diagnosis for large-scale wind turbine rolling bearing using stress wave and wavelet analysis. 2005 International Conference on Electrical Machines and Systems, 27-29 Sept. 2005 Nanjing, China. 2239-2244 Vol. 3.

CHEN, J. & PATTON, R. J. 2012. *Robust Model-Based Fault Diagnosis for Dynamic Systems,* Springer Publishing Company, Incorporated.

CHEN, J., PATTON, R. J. & ZHANG, H. Y. 1996. Design of unknown input observers and robust fault detection filters. *International Journal of Control,* 63**,** 85-105.

CHIANG, L. H., RUSSELL, E. L. & BRAATZ, R. D. 2012. *Fault Detection and Diagnosis in Industrial Systems,* Springer London.

CHNG, E. S., CHEN, S. & MULGREW, B. 1996. Gradient radial basis function networks for nonlinear and nonstationary time series prediction. *IEEE Transactions on Neural Networks,* 7**,** 190-194.

CHOW, E. & WILLSKY, A. 1984. Analytical redundancy and the design of robust failure detection systems. *IEEE Transactions on Automatic Control,* 29**,** 603-614.

CHRISTENSEN, J. J., ANDERSSON, C. & GUTT, S. 2009. Remote condition monitoring of Vestas turbines. *Technical Track—Operation & Maintenance, Proceedings EWEC, Marseille, France*.

CLANCEY, W. J. & SHORTLIFFE, E. H. 1984. Introduction: Medical artificial intelligence programs. *Clancy and Shortliffe*.

DANESHI-FAR, Z., CAPOLINO, G. A. & HENAO, H. 2010. Review of Failures and Condition Monitoring in Wind Turbine Generators. *XIX International Conference on Electrical Machines.* Rome.

DELMAIRE, G., CASSAR, J. P. & STAROSWIECKI, M. Identification and parity space techniques for failure detection in SISO systems including modelling errors. Proceedings of the 33rd IEEE Conference on Decision and Control, 14-16 Dec 1994 Lake Buena Vista, FL, USA. 2279-2285 vol.3.

DIAO, Y. & PASSINO, K. M. 2002. Intelligent fault-tolerant control using adaptive and learning methods. *Control Engineering Practice,* 10**,** 801-817.

DODGE, D. M. n. d. *Illustrated History of Wind Power Development* [Online]. Darrell Dodge and TelosNet Web Development. Available: http://www.telosnet.com/wind/early.html [Accessed 4th July 2011].

DUTTON, A. Thermoelastic stress measurement and acoustic emission monitoring in wind turbine blade testing. Proc. European Wind Energy Conference 2004 (EWEC 2004), 22-25 Nov 2004 London.

ECHAVARRIA, E., TOMIYAMA, T. & BUSSEL, G. J. W. V. 2007. Fault Diagnosis approach based on a model-based reasoner and a functional designer for a wind turbine. An approach towards self-maintenance. *Journal of Physics: Conference Series,* 75**,** 012078.

ECHAVARRIA, E., TOMIYAMA, T., HUBERTS, H. & VAN BUSSEL, G. Fault diagnosis system for an offshore wind turbine using qualitative physics. EWEC 2008, 31 March - 4 April 2008 Brussels, Belgium. Citeseer.

ELLABBAN, O., ABU-RUB, H. & BLAABJERG, F. 2014. Renewable energy resources: Current status, future prospects and their enabling technology. *Renewable and Sustainable Energy Reviews,* 39**,** 748-764.

FENG, G., DAPING, X. & YUEGANG, L. Pitch-control for large-scale wind turbines based on feed forward fuzzy-PI. WCICA 2008. 7th World Congress on Intelligent Control and Automation, 25-27 June 2008 Chongqing, China. 2277-2282.

FRANK, P. & KELLER, L. 1980. Sensitivity discriminating observer design for instrument failure detection. *IEEE Transactions on Aerospace and Electronic Systems,* 4**,** 460-467.

FRANK, P. M. 1990. Fault diagnosis in dynamic systems using analytical and knowledge-based redundancy: A survey and some new results. *Automatica,* 26**,** 459-474.

FRANK, P. M. Advances in observer-based fault diagnosis. International Conference on Fault Diagnosis: TOOLDIAG'93, 5-7 April 1993 Toulouse, France. 817-36.

FRANK, P. M. 1996. Analytical and qualitative model-based fault diagnosis - A survey and some new results. *European Journal of Control,* 2**,** 6-28.

FRANK, P. M. & K PPEN-SELIGER, B. 1997. Fuzzy logic and neural network applications to fault diagnosis. *International Journal of Approximate Reasoning,* 16**,** 67-88.

FREDRICKSON, S., ROBERTS, S., TOWNSEND, N. & TARASSENKO, L. Speaker identification using networks of radial basis functions. Proc. of the VII European Signal Processing Conference, 13-16 September 1994 Edinburgh, Scotland, U.K. 812-815.

GAO, C., ZHAO, Q. & DUAN, G. R. Multiplicative fault estimation for a type of nonlinear uncertain system. Proceedings of the 30th Chinese Control Conference, 22-24 July 2011 Yantai, China. 4355-4360.

GARCIA, M. C., SANZ-BOBI, M. A. & DEL PICO, J. 2006. SIMAP: Intelligent System for Predictive Maintenance: Application to the health condition monitoring of a windturbine gearbox. *Computers in Industry,* 57**,** 552-568.

GATZKE, E. P. & DOYLE III, F. J. 2002. Use of multiple models and qualitative knowledge for on-line moving horizon disturbance estimation and fault diagnosis. *Journal of Process Control,* 12**,** 339-352.

GELB, A. 1974. *Applied optimal estimation,* MIT press.

GENTIL, S., MONTMAIN, J. & COMBASTEL, C. 2004. Combining FDI and AI approaches within causal-model-based diagnosis. *Systems, Man, and Cybernetics, Part B: Cybernetics, IEEE Transactions on,* 34**,** 2207-2221.

GERTLER, J. 1997. Fault detection and isolation using parity relations. *Control Engineering Practice,* 5**,** 653-661.

GERTLER, J. & SINGER, D. 1990. A new structural framework for parity equation-based failure detection and isolation. *Automatica,* 26**,** 381-388.

GERTLER, J. J. & MONAJEMY, R. 1995. Generating directional residuals with dynamic parity relations. *Automatica,* 31**,** 627-635.

GHOSHAL, A., SUNDARESAN, M. J., SCHULZ, M. J. & FRANK PAI, P. 2000. Structural health monitoring techniques for wind turbine blades. *Journal of Wind Engineering and Industrial Aerodynamics,* 85**,** 309-324.

GLAUERT, H. 1935. Airplane Propellers. *Aerodynamic Theory.* Berlin: Springer Berlin Heidelberg.

GOMM, J. B., WILLIAMS, D., EVANS, J. T., DOHERTY, S. K. & LISBOA, P. J. G. 1996. Enhancing the non-linear modelling capabilities of MLP neural networks using spread encoding. *Fuzzy Sets and Systems,* 79**,** 113-126.

GUANG-BIN, H., SARATCHANDRAN, P. & SUNDARARAJAN, N. 2005. A generalized growing and pruning RBF (GGAP-RBF) neural network for function approximation. *IEEE Transactions on Neural Networks,* 16**,** 57-67.

HANSEN, M. H., HANSEN, A. D., LARSEN, T. J., ØYE, S., S RENSEN, P. & FUGLSANG, P. 2005. *Control design for a pitch-regulated, variable speed wind turbine*.

HATCH, C. 2004. Improved wind turbine condition monitoring using acceleration enveloping. *Orbit,* 61**,** 58-61.

HUANG, Q., JIANG, D., HONG, L. & DING, Y. 2008. Application of Wavelet Neural Networks on Vibration Fault Diagnosis for Wind Turbine Gearbox. *In:* SUN, F., ZHANG, J., TAN, Y., CAO, J. & YU, W. (eds.) *Advances in Neural Networks - ISNN 2008: 5th International Symposium on Neural Networks, ISNN 2008, Beijing, China, September 24-28, 2008, Proceedings, Part II.* Berlin, Heidelberg: Springer Berlin Heidelberg.

HWAS, A. & KATEBI, R. Model-based fault detection and isolation for wind turbine. Proceedings of 2012 UKACC International Conference on Control, 3-5 Sept. 2012 Cardiff, United Kingdom. 876-881.

HWAS, A. & KATEBI, R. Nonlinear observer-based fault detection and isolation for wind turbines. 2014 22nd Mediterranean Conference of Control and Automation (MED), 16-19 June 2014 Palermo, Italy. 870-875.

HYERS, R. W., MCGOWAN, J. G., SULLIVAN, K. L., MANWELL, J. F. & SYRETT, B. C. 2006. Condition monitoring and prognosis of utility scale wind turbines. *Energy Materials,* 1**,** 187-203.

IGBA, J., ALEMZADEH, K., DURUGBO, C. & HENNINGSEN, K. 2015. Performance assessment of wind turbine gearboxes using in-service data: Current approaches and future trends. *Renewable and Sustainable Energy Reviews,* 50**,** 144-159.

INSEOK, H., SUNGWAN, K., YOUDAN, K. & SEAH, C. E. 2010. A Survey of Fault Detection, Isolation, and Reconfiguration Methods. *Control Systems Technology, IEEE Transactions on,* 18**,** 636-653.

ISERMANN, R. 1984. Process fault detection based on modeling and estimation methods—A survey. *Automatica,* 20**,** 387-404.

ISERMANN, R. 2005. Model-based fault-detection and diagnosis – status and applications. *Annual Reviews in Control,* 29**,** 71-85.

JIHONG, L., DAPING, X. & XIYUN, Y. Sensor fault detection in variable speed wind turbine system using H_ /H∞ method. 2008 7th World Congress on Intelligent Control and Automation, 25-27 June 2008 Chongqing, China. 4265-4269.

JONKMAN, J., BUTTERFIELD, S., MUSIAL, W. & SCOTT, G. 2009. Definition of a 5-MW reference wind turbine for offshore system development. National Renewable Energy Lab.(NREL), Golden, CO (United States).

JOSELIN HERBERT, G. M., INIYAN, S., SREEVALSAN, E. & RAJAPANDIAN, S. 2007. A review of wind energy technologies. *Renewable and Sustainable Energy Reviews,* 11**,** 1117-1145.

KALMAN, R. E. 1960. A new approach to linear filtering and prediction problems. *Journal of basic Engineering,* 82**,** 35-45.

KAMAL, M. & YU, D. 2011. Model-based fault detection for proton exchange membrane fuel cell systems. *International Journal of Engineering, Science and Technology,* 3**,** 1-15.

KAMAL, M. M. & YU, D. Fault detection and isolation for PEMFC systems under closed-loop control. Proceedings of 2012 UKACC International Conference on Control, 3-5 Sept. 2012 Cardiff, United Kingdom. 976-981.

KAMAL, M. M., YU, D. W. & YU, D. L. 2014. Fault detection and isolation for PEM fuel cell stack with independent RBF model. *Engineering Applications of Artificial Intelligence,* 28**,** 52-63.

KASHANINEJAD, M., DEHGHANI, A. A. & KASHIRI, M. 2009. Modeling of wheat soaking using two artificial neural networks (MLP and RBF). *Journal of Food Engineering,* 91**,** 602-607.

LI, M., HE, S. & LI, X. 2009. Complex radial basis function networks trained by QR-decomposition recursive least square algorithms applied in behavioral modeling of nonlinear power amplifiers. *International Journal of RF and Microwave Computer-Aided Engineering,* 19**,** 634-646.

LIGHTBODY, G. & IRWIN, G. W. 1997. Nonlinear control structures based on embedded neural system models. *IEEE Transactions on Neural Networks,* 8**,** 553-567.

LU, D., QIAO, W. & GONG, X. 2017. Current-Based Gear Fault Detection for Wind Turbine Gearboxes. *IEEE Transactions on Sustainable Energy,* PP**,** 1-1.

MANWELL, J. F., MCGOWAN, J. G. & ROGERS, A. L. 2010. *Wind Energy Explained: Theory, Design and Application*, Wiley.

MAYBECK, P. S. 1982. *Stochastic models, estimation, and control*, Academic press.

MEHRA, R. K. & PESCHON, J. 1971. An innovations approach to fault detection and diagnosis in dynamic systems. *Automatica,* 7**,** 637-640.

MING, Y., GENGYIN, L., MING, Z. & CHENGYONG, Z. Modeling of the Wind Turbine with a Permanent Magnet Synchronous Generator for Integration. Power Engineering Society General Meeting, 2007. IEEE, 24-28 June 2007 Tampa, FL, USA. 1-6.

MIRONOVSKII, L. A. 1979. Functional diagnosis of linear dynamic systems. *Avtomatika i Telemekhanika***,** 120-128.

MOUSTAFA, A. A., ALQADI, Z. A. & SHAHROURY, E. A. 2011. Performance evaluation of artificial neural networks for spatial data analysis.

MUYEEN, S. M., TAMURA, J. & MURATA, T. 2008. *Stability Augmentation of a Grid-connected Wind Farm*, Springer London.

NARENDRA, K. S. & PARTHASARATHY, K. 1990. Identification and control of dynamical systems using neural networks. *IEEE Transactions on Neural Networks,* 1**,** 4-27.

NAZARI, J. & ERSOY, O. K. 1992. Implementation of back-propagation neural networks with MatLab.

NELLES, O. 2002. Nonlinear system identification. IOP Publishing.

NELSON, V. 2009. *Wind Energy: Renewable Energy and the Environment*, CRC Press.

NG, C. & RAN, L. 2016. *Offshore Wind Farms: Technologies, Design and Operation*, Elsevier Science.

NORVILAS, A., NEGIZ, A., DECICCO, J. & ÇINAR, A. 2000. Intelligent process monitoring by interfacing knowledge-based systems and multivariate statistical monitoring. *Journal of Process Control,* 10**,** 341-350.

ODGAARD, P. F., STOUSTRUP, J. & KINNAERT, M. Fault Tolerant Control of Wind Turbines - a Benchmark Model. 7th IFAC Symposium on Fault Detection, Supervision and Safety of Technical Processes, 30 June - 3 July 2009 Barcelona, Spain. 155 - 160.

OGATA, K. 2010. *Modern Control Engineering*, Pearson.

OKEDU, K. E. 2012. Effects of Drive Train Model Parameters on a Variable Speed Wind Turbine. *International Journal of Renewable Energy Research (IJRER),* 2**,** 92-98.

OU, S. & ACHENIE, L. E. K. 2005. A hybrid neural network model for PEM fuel cells. *Journal of Power Sources,* 140**,** 319-330.

PARK, J. & RIZZONI, G. A closed-form expression for the fault detection filter. Proceedings of the 32nd IEEE Conference on Decision and Control, 15-17 Dec 1993 San Antonio, Texas, USA. 259-264 vol.1.

PATAN, K. 2008. *Artificial neural networks for the modelling and fault diagnosis of technical processes*, Springer.

PATTON, R. & CHEN, J. A review of parity space approaches to fault diagnosis. IFAC Safeprocess Conference, 1991a. 65-81.

PATTON, R., CLARK, R. & FRANK, P. M. 1989. *Fault diagnosis in dynamic systems: theory and applications*, Prentice Hall.

PATTON, R. J. & CHEN, J. Robust fault detection using eigenstructure assignment: a tutorial consideration and some new results. Proceedings of the 30th IEEE Conference on Decision and Control, 11-13 Dec 1991b Brighton, ENGLAND. 2242-2247 vol.3.

PATTON, R. J. & CHEN, J. 1994. Review of parity space approaches to fault diagnosis for aerospace systems. *Journal of Guidance, Control, and Dynamics,* 17**,** 278-285.

PATTON, R. J. & CHEN, J. 1997. Observer-based fault detection and isolation: Robustness and applications. *Control Engineering Practice,* 5**,** 671-682.

PATTON, R. J., CHEN, J. & SIEW, T. M. Fault diagnosis in nonlinear dynamic systems via neural networks. Control '94. International Conference on Control, 21-24 March 1994 Coventry, UK. 1346-1351 vol.2.

PATTON, R. J., LOPEZ-TORIBIO, C. J. & UPPAL, F. J. Artificial intelligence approaches to fault diagnosis. IEE Colloquium on Condition Monitoring: Machinery, External Structures and Health, 23-22 April 1999 Birmingham, UK. 5/1-518.

PAU, L. F. 1981. *Failure diagnosis and performance monitoring*, M. Dekker.

PLOIX, S. & ADROT, O. 2006. Parity relations for linear uncertain dynamic systems. *Automatica,* 42**,** 1553-1562.

PORFíRIO, C. R., ALMEIDA NETO, E. & ODLOAK, D. 2003. Multi-model predictive control of an industrial C3/C4 splitter. *Control Engineering Practice,* 11**,** 765-779.

PRASAD, P. R., DAVIS, J. F., JIRAPINYO, Y., JOSEPHSON, J. R. & BHALODIA, M. 1998. Structuring diagnostic knowledge for large-scale process systems. *Computers & Chemical Engineering,* 22**,** 1897-1905.

PRICE, T. J. 2005. James Blyth: Britain's first modern wind power pioneer. *Wind Engineering,* 29**,** 191-200.

PUIG, V., QUEVEDO, J., ESCOBET, T. & DE LAS HERAS, S. Passive robust fault detection approaches using interval models. Proceeding of the 15th IFAC World Congress, 21 - 26 July 2002 Barcelona, Spain.

QIAO, W. & LU, D. 2015. A Survey on Wind Turbine Condition Monitoring and Fault Diagnosis - Part I: Components and Subsystems. *IEEE Transactions on Industrial Electronics,* 62**,** 6536-6545.

RAFIQ, M. Y., BUGMANN, G. & EASTERBROOK, D. J. 2001. Neural network design for engineering applications. *Computers & Structures,* 79**,** 1541-1552.

RAO, M., SUN, X. & FENG, J. 2000. Intelligent system architecture for process operation support. *Expert Systems with Applications,* 19**,** 279-288.

REN21 2011. Renewables 2011 Global Status Report. *In:* SECRETARIAT, P. R. (ed.).

REN21 2014. Renewables 2014 Global Status Report. Paris.

REZAEI, V. & JOHNSON, K. E. Robust fault tolerant pitch control of wind turbines. 2013 IEEE 52nd Annual Conference on Decision and Control (CDC), 10-13 Dec 2013 Firenze, Italy. 391-396.

RIBRANT, J. & BERTLING, L. Survey of failures in wind power systems with focus on Swedish wind power plants during 1997-2005. Power Engineering Society General Meeting, 2007. IEEE, 24-28 June 2007 Tampa, FL, USA. 1-8.

RODRIGUES, M., THEILLIOL, D., ADAM-MEDINA, M. & SAUTER, D. 2008. A fault detection and isolation scheme for industrial systems based on multiple operating models. *Control Engineering Practice,* 16**,** 225-239.

RODRIGUEZ, L., GARCIA, E., MORANT, F., CORRECHER, A. & QUILES, E. Application of latent nestling method using Coloured Petri Nets for the Fault Diagnosis in the wind turbine subsets. 2008 IEEE International Conference on Emerging Technologies and Factory Automation, 15-18 Sept 2008 Hamburg, Germany. 767-773.

RUMELHART, D. E., HINTON, G. E. & WILLIAMS, R. J. 1985. Learning internal representations by error propagation. DTIC Document.

SALMAN, S. K. & TEO, A. L. J. 2003. Windmill modeling consideration and factors influencing the stability of a grid-connected wind power-based embedded generator. *Power Systems, IEEE Transactions on,* 18**,** 793-802.

SCHNEIDER, R. & FRANK, P. M. Fuzzy logic based threshold adaption for fault detection in robots. Proceedings of the Third IEEE Conference on Control Applications, 24-26 Aug 1994 Glasgow. 1127-1132 vol.2.

SHEN, W. Z., ZAKKAM, V. A. K., S RENSEN, J. N. & APPA, K. 2007. Analysis of counter-rotating wind turbines. *Journal of Physics: Conference Series,* 75**,** 012003.

SHI, F. & PATTON, R. J. A robust adaptive approach to wind turbine pitch actuator component fault estimation. 2014 UKACC International Conference on Control (CONTROL), 9-11 July 2014 Loughborough, United Kingdom. 468-473.

SLOOTWEG, J. G., POLINDER, H. & KLING, W. L. Dynamic modelling of a wind turbine with doubly fed induction generator. Power Engineering Society Summer Meeting, 17 July 2001 Vancouver, Canada. 644-649 vol.1.

SORSA, T., KOIVO, H. N. & KOIVISTO, H. 1991. Neural networks in process fault diagnosis. *Systems, Man and Cybernetics, IEEE Transactions on,* 21**,** 815-825.

STAROSWIECKI, M., CASSAR, J. P. & COCQUEMPOT, V. Generation of optimal structured residuals in the parity space. IFAC 12th World Congress, 18 -23 July 1993 Sydney, Australia. 535-542.

SUNDARESAN, M. J., SCHULZ, M. J. & GHOSHAL, A. 2002. Structural health monitoring static test of a wind turbine blades. National Renewable Energy Laboratory.

TAVNER, P. J., BUSSEL, G. J. W. V. & SPINATO, F. Machine and converter rehabirifles in wind turbines. The 3rd IET International Conference on Power Electronics, Machines and Drives, 2006, 4-6 April 2006 Dublin, Ireland. 127-130.

URAIKUL, V., CHAN, C. W. & TONTIWACHWUTHIKUL, P. 2007. Artificial intelligence for monitoring and supervisory control of process systems. *Engineering Applications of Artificial Intelligence,* 20**,** 115-131.

VENKATASUBRAMANIAN, V., RENGASWAMY, R. & KAVURI, S. N. 2003a. A review of process fault detection and diagnosis: Part II: Qualitative models and search strategies. *Computers & Chemical Engineering,* 27**,** 313-326.

VENKATASUBRAMANIAN, V., RENGASWAMY, R., KAVURI, S. N. & YIN, K. 2003b. A review of process fault detection and diagnosis: Part III: Process history based methods. *Computers & chemical engineering,* 27**,** 327-346.

VENKATASUBRAMANIAN, V., RENGASWAMY, R., YIN, K. & KAVURI, S. N. 2003c. A review of process fault detection and diagnosis: Part I: Quantitative model-based methods. *Computers & chemical engineering,* 27**,** 293-311.

VRIES, O. D. 1979. Fluid dynamic aspects of wind energy conversion. DTIC Document.

WALFORD, C. A. 2006. Wind Turbine Reliability: Understanding and Minimizing Wind Turbine Operation and Maintenance Costs. United States.

WANG, S. W., YU, D. L., GOMM, J. B., PAGE, G. F. & DOUGLAS, S. S. 2006. Adaptive neural network model based predictive control for air–fuel ratio of SI engines. *Engineering Applications of Artificial Intelligence,* 19**,** 189-200.

WATTON, J. 2007. *Modelling, Monitoring and Diagnostic Techniques for Fluid Power Systems,* Springer London.

WELCH, G. F. 2014. Kalman Filter. *Computer Vision.* Springer.

WHELAN, M. J., JANOYAN, K. D. & QIU, T. Integrated monitoring of wind plant systems. SPIE Smart Structures and Materials + Nondestructive Evaluation and Health Monitoring, 9-13 MARCH 2008 San Diego, United States. 69330F-69330F-3.

WHITE, J. & SPEYER, J. 1987. Detection filter design: Spectral theory and algorithms. *Automatic Control, IEEE Transactions on,* 32**,** 593-603.

WIGGELINKHUIZEN, E., VERBRUGGEN, T., BRAAM, H., RADEMAKERS, L., XIANG, J. & WATSON, S. 2008. Assessment of Condition Monitoring Techniques for Offshore Wind Farms. *Journal of Solar Energy Engineering,* 130**,** 031004-031004-9.

WILKINSON, M. R., SPINATO, F. & TAVNER, P. J. Condition Monitoring of Generators & Other Subassemblies in Wind Turbine Drive Trains. 2007 IEEE International Symposium on Diagnostics for Electric Machines, Power Electronics and Drives, 6-8 Sept 2007 Cracow, Poland. 388-392.

WILLSKY, A. & JONES, H. 1976. A generalized likelihood ratio approach to the detection and estimation of jumps in linear systems. *IEEE Transactions on Automatic Control,* 21**,** 108-112.

WILLSKY, A. S. 1976. A survey of design methods for failure detection in dynamic systems. *Automatica,* 12**,** 601-611.

WILSON, R. E. & LISSAMAN, P. B. 1974. Applied aerodynamics of wind power machines. Oregon State Univ., Corvallis (USA).

WILSON, R. E., LISSAMAN, P. B. & WALKER, S. N. 1976. Aerodynamic performance of wind turbines. Oregon State Univ., Corvallis (USA).

XIA, Q. & RAO, M. 1999. Dynamic case-based reasoning for process operation support systems. *Engineering Applications of Artificial Intelligence,* 12**,** 343-361.

YAGER, R. R. 1987. Using approximate reasoning to represent default knowledge. *Artificial Intelligence,* 31**,** 99-112.

YANG, W., TAVNER, P. J., CARBTRE, C. J. & WILKINSON, M. 2008. Research on a Simple, Cheap but Globally Effective Condition Monitoring Technique for Wind turbines. 2008. 18th International Conference on Electrical Machines, 6-9 Sept 2008 Vilamoura, Portugal. 1-5.

YANG, W., TAVNER, P. J., CARBTRE, C. J. & WILKINSON, M. 2010. Cost-Effective Condition Monitoring for Wind Turbines. *IEEE Transactions on Industrial Electronics,* 57**,** 263 - 271

YANG, W., TAVNER, P. J. & WILKINSON, M. R. 2009. Condition monitoring and fault diagnosis of a wind turbine synchronous generator drive train. *IET Renewable Power Generation,* 3**,** 1-11.

YI, L., TIE QI, C. & HAMILTON, B. 2000. A fuzzy system for automotive fault diagnosis: fast rule generation and self-tuning. *IEEE Transactions on Vehicular Technology,* 49**,** 651-660.

YILMAZ, A. S. & ÖZER, Z. 2009. Pitch angle control in wind turbines above the rated wind speed by multi-layer perceptron and radial basis function neural networks. *Expert Systems with Applications,* 36**,** 9767-9775.

YU, D. & SHIELDS, D. Fault diagnosis in bi-linear systems-A survey. Proceeding of The third European Control Conference, 5-8 September 1995 Roma, Italy. 360-366.

YU, D. & SHIELDS, D. N. 1997. A bilinear fault detection filter. *International Journal of Control,* 68**,** 417-430.

YU, D. L., CHANG, T. K. & YU, D. W. 2005. Adaptive neural model-based fault tolerant control for multi-variable processes. *Engineering Applications of Artificial Intelligence,* 18**,** 393-411.

YU, D. L. & GOMM, J. B. 2003. Implementation of neural network predictive control to a multivariable chemical reactor. *Control Engineering Practice,* 11**,** 1315-1323.

YU, D. L., GOMM, J. B. & WILLIAMS, D. 1999. Sensor fault diagnosis in a chemical process via RBF neural networks. *Control Engineering Practice,* 7**,** 49-55.

YUJI, T., BOUNO, T. & HAMADA, T. 2006. Suggestion of temporarily for forecast diagnosis on blade of small wind turbine. *IEEJ Transactions on Power and Energy,* 126**,** 710-711.

Z. HAMEED, Y. S. H., Y. M. CHO, S. H. AHN, C. K. SONG 2009. Condition monitoring and fault detection of wind trubines and related algorithms: A review. *Renewable and Sustainable Enerty Reviews,* 13**,** 1 - 39.

ZADEH, L. A. 1971. Similarity relations and fuzzy orderings. *Information Sciences,* 3**,** 177-200.

ZAHER, A. S. & MCARTHUR, S. D. J. A Multi-Agent Fault Detection System for Wind Turbine Defect Recognition and Diagnosis. 2007 IEEE Lausanne Power Tech, 1-5 July 2007 Lausanne, Switzerland. 22-27.

ZHAI, Y. & YU, D. 2008. Radial-basis-function-based feedforward—feedback control for air—fuel ratio of spark ignition engines. *Proceedings of the Institution of Mechanical Engineers, Part D: Journal of Automobile Engineering,* 222**,** 415-428.

ZHANG, X., HE, S., ZHO, P. & WANG, W. 2008. Summerization and study of fault diagnosis technology of the main components of wind turbine generator system. *IEEE International Conference on Sustainable Energy Technologies.*

ZHANG, X., POLYCARPOU, M. M. & PARISINI, T. 2002. A robust detection and isolation scheme for abrupt and incipient faults in nonlinear systems. *Automatic Control, IEEE Transactions on,* 47**,** 576-593.

ZHANG, X., POLYCARPOU, M. M. & PARISINI, T. 2010. Fault diagnosis of a class of nonlinear uncertain systems with Lipschitz nonlinearities using adaptive estimation. *Automatica,* 46**,** 290-299.

ZHI, T., BELL, K. L. & TREES, H. L. V. 2001. A recursive least squares implementation for LCMP beamforming under quadratic constraint. *IEEE Transactions on Signal Processing,* 49**,** 1138-1145.

ZHOU, K. & DOYLE, J. C. 1998. *Essentials of robust control*, Prentice Hall.

ZHOU, Y., WANG, D., HUANG, H., LI, J. & YI, L. 2011. *Fuzzy Logic Based Interactive Multiple Model Fault Diagnosis for PEM Fuel Cell Systems*, INTECH Open Access Publisher.

ZIMMERMAN, H. 1991. Fuzzy Set Theory and Its Applications.

APPENDIX 1

WIND TURBINE SIMULINK MODEL

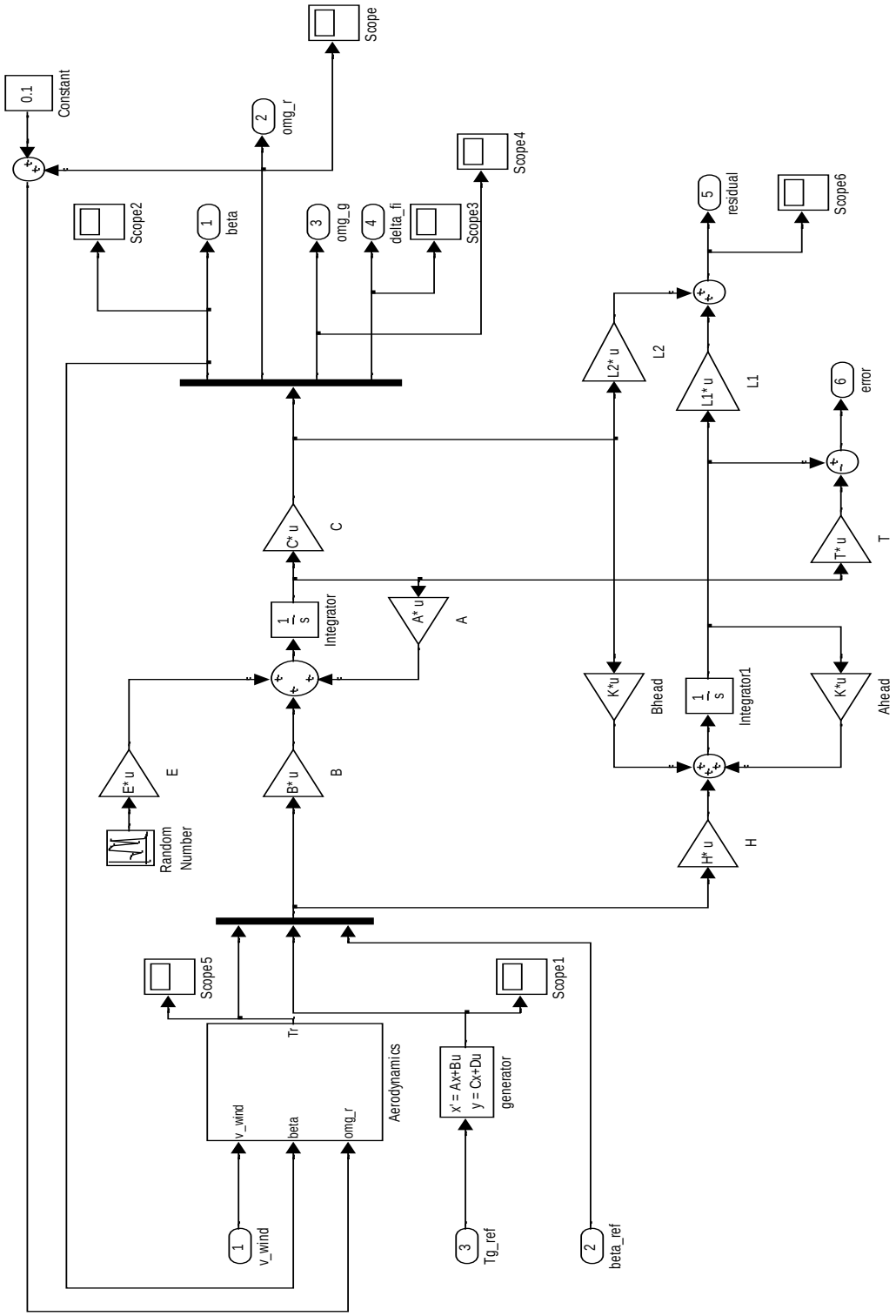

APPENDIX 2

WIND TURBINE MATLAB CODE

```
clear all

pi    = 3.1415;
R     = 63;                  % m      rotor disc radius
rho   = 1.225;               % kg/m3  mass density of air
N     = 97;                  %        gear ratio
Ir    = 5.9154e7;            % kg m2  inertia of rotor
Ig    = 500;                 % kg m2  inertia of generator
Ds    = 6.215e6;             % N/m s  Driveshaft damping constant
Ks    = 8.6763e8;            % N/m s  Driveshaft spring constant
Prate = 5e6;                 % W      Rated Power
omgrate=12.1;                % rpm    Tated rotor speed in rpm
omgr_rate= (2*pi*omgrate)/60;  % rad/s  Rated rotor speed in rad/s
tau=0.1;                     %        Generator actuator time constant
Tg_ref = Prate/(omgr_rate*N);
beta_ref=35;
vw=20;                       % m/s    Wind Speed
wn    = 0.88;                % rad/s  pitch actuator natural frequency
zeta  = 0.9;                 %        pitch actuator damping


A=[0 0 0 0 1;
   0 -Ds/Ir Ds/(Ir*N) -Ks/Ir 0;
   0 Ds/(Ig*N) -Ds/(Ig*N^2) Ks/(Ig*N) 0;
   0 1 -1/N 0 0;
   -wn^2 0 0 0 -2*zeta*wn];

B=[0 0 0;
   1/Ir 0 0;
   0 -1/Ig 0;
   0 0 0;
   0 0 wn^2;];

C=[1 0 0 0 0;
   0 1 0 0 0;
   0 0 1 0 0];

E=[0 ;1/Ir ;0 ;0 ;0 ];
```

```
F=[0; 0; -1/Ig; 0; 0];

G=[ 0; 0; 0; 0; -2*zeta*wn];

Q=[1;1;1];

n=5;
m=3;
p=4;
r=n-rank(E)

[U,S,V]=svd(E)
U0=mat2cell(U,5,[2 3])

Uz2=U0{1,2}

Uz2T=Uz2'
Uz2T0=mat2cell(Uz2T,3,[3 2])
N1=Uz2T0{1,1}
N2=Uz2T0{1,2}

T1=N1
T2=N2

A0=mat2cell(A,5,[3 2])
A1=A0{1,1}
A2=A0{1,2}

As=Uz2T*A2*pinv(N2)

Id=eye(3,3)
Cs=Id-N2*pinv(N2)

rank([Cs;Cs*As;Cs*As*As;Cs*As*As*As])
rank([Cs As*Cs As*As*Cs As*As*As*Cs])

Po=[-1;-20;-30]
W=(place(As',(-Cs)',Po))'

Ahead=As+W*Cs

W1=eye(3,3)
[U1,S1,V1]=svd(T2)
U10=mat2cell(U1,4,[1 3])
```

```
Un2=U10{1,2}
L1=W1*Un2'
L2=-L1*T1

T=[T1 T2]
Bhead=T*A1-Ahead*T1
H=T*B

Ts=0.1;
Tm=100;
Ns=Tm/Ts;
tt=[0:Ts:Ts*Ns]';
u1=[ones(Ns+1,1)*vw];
u2=[ones(Ns+1,1)*beta_ref];
u3=[ones(Ns+1,1)*Tg_ref];
u4=[zeros(Ns+1,1)];
u5=[zeros(Ns+1,1)];
u6=[zeros(Ns+1,1)];
u7=[zeros(Ns+1,1)];
u8=[zeros(Ns+1,1)];

[Tm,X,beta,omg_r,omg_g,res,sta_e]= ...

sim('RubustObserver_system_fault170803',tt,[],[tt,u1],[tt,u2],[tt,u3]
,[tt,u4],[tt,u5],[tt,u6],[tt,u7],[tt,u8]);

figure(1)
subplot(3,1,1)
plot(Tm,beta)
grid on
title('Blade Angle')
xlabel('Time(sec)')
ylabel('Degree')

subplot(3,1,2)
plot(Tm,omg_r)
grid on
title('Rotor Speed')
xlabel('Time(sec)')
ylabel('Rad/s')

subplot(3,1,3)
plot(Tm,omg_g)
grid on
```

```
title('Generator Speed')
xlabel('Time(sec)')
ylabel('Rad/s')

figure(2)
subplot(5,1,1)
plot(Tm,u4)
grid on
title('Pitch System Fault')
xlabel('Time(sec)')
ylabel('Fault')

subplot(5,1,2)
plot(Tm,u5)
grid on
title('Drive-train System Gearbox Fault')
xlabel('Time(sec)')
ylabel('Fault')

subplot(5,1,3)
plot(Tm,u6)
grid on
title('Sensor Fault 1')
xlabel('Time(sec)')
ylabel('Fault')

subplot(5,1,4)
plot(Tm,u7)
grid on
title('Sensor Fault 2')
xlabel('Time(sec)')
ylabel('Fault')

subplot(5,1,5)
plot(Tm,u8)
grid on
title('Sensor Fault 3')
xlabel('Time(sec)')
ylabel('Fault')

figure(3)
plot(Tm,res)
grid on
axis([0 100 -0.5 0.5])
```

```
title('Residual')
xlabel('Time(sec)')
ylabel('Residual')


%simulate Component fault

u4=[zeros(100,1);ones(100,1)*zeta;zeros(801,1)];
u5=[zeros(Ns+1,1)];
u6=[zeros(Ns+1,1)];
u7=[zeros(Ns+1,1)];
u8=[zeros(Ns+1,1)];

[Tm,X,beta,omg_r,omg_g,res,sta_e]= ...

sim('RubustObserver_system_fault170803',tt,[],[tt,u1],[tt,u2],[tt,u3]
,[tt,u4],[tt,u5],[tt,u6],[tt,u7],[tt,u8]);

figure(4)
subplot(3,1,1)
plot(Tm,beta)
grid on
title('Blade Angle')
xlabel('Time(sec)')
ylabel('Degree')

subplot(3,1,2)
plot(Tm,omg_r)
grid on
title('Rotor Speed')
xlabel('Time(sec)')
ylabel('Rad/s')

subplot(3,1,3)
plot(Tm,omg_g)
grid on
title('Generator Speed')
xlabel('Time(sec)')
ylabel('Rad/s')

figure(5)
plot(Tm,u4)
grid on
title('Pitch System Fault')
```

```
axis([0 100 -0.3 1.1])
xlabel('Time(sec)')
ylabel('Fault')


figure(6)
subplot(2,1,1)
plot(Tm,u4)
grid on
title('Pitch System Fault')
axis([0 100 -0.3 1.1])
xlabel('Time(sec)')
ylabel('Fault')

subplot(2,1,2)
plot(Tm,res)
grid on
axis([0 100 -0.003 0.015])
title('Residual')
xlabel('Time(sec)')
ylabel('Residual')

%simulate actuator fault
u4=[zeros(Ns+1,1)];
u5=[zeros(200,1); ones(100,1)*(Tg_ref*0.1); zeros(701,1)];
u6=[zeros(Ns+1,1)];
u7=[zeros(Ns+1,1)];
u8=[zeros(Ns+1,1)];

[Tm,X,beta,omg_r,omg_g,res,sta_e]= ...

sim('RubustObserver_system_fault170803',tt,[],[tt,u1],[tt,u2],[tt,u3]
,[tt,u4],[tt,u5],[tt,u6],[tt,u7],[tt,u8]);

figure(7)
subplot(3,1,1)
plot(Tm,beta)
grid on
title('Blade Angle')
xlabel('Time(sec)')
ylabel('Degree')

subplot(3,1,2)
plot(Tm,omg_r)
```

```
grid on
title('Rotor Speed')
xlabel('Time(sec)')
ylabel('Rad/s')

subplot(3,1,3)
plot(Tm,omg_g)
grid on
title('Generator Speed')
xlabel('Time(sec)')
ylabel('Rad/s')


figure(8)
plot(Tm,u5)
grid on
title('Actuator Fault')
axis([0 100 -1000 5000])
xlabel('Time(sec)')
ylabel('Delta Tg')

figure(9)
subplot(2,1,1)
plot(Tm,u5)
grid on
title('Drive-Train Gearbox Fault')
axis([0 100 -1000 5000])
xlabel('Time(sec)')
ylabel('Delta Tg')

subplot(2,1,2)
plot(Tm,res)
grid on
title('Residual')
xlabel('Time(sec)')
ylabel('Residual')

%simulate sensor faults 1
u1=[ones(Ns+1,1)*vw];
u2=[ones(Ns+1,1)*beta_ref];
u3=[ones(Ns+1,1)*Tg_ref];
u4=[zeros(Ns+1,1)];
u5=[zeros(Ns+1,1)];
u6=[zeros(400,1);ones(100,1)*1;zeros(501,1)];
```

```
u7=[zeros(Ns+1,1)];
u8=[zeros(Ns+1,1)];

[Tm,X,beta,omg_r,omg_g,res,sta_e]= ...

sim('RubustObserver_system_fault170803',tt,[],[tt,u1],[tt,u2],[tt,u3]
,[tt,u4],[tt,u5],[tt,u6],[tt,u7],[tt,u8]);

figure(10)
plot(Tm,beta)
grid on
title('Blade Angle')
xlabel('Time(sec)')
ylabel('Degree')

figure(11)
plot(Tm,beta)
grid on
title('Blade Angle')
xlabel('Time(sec)')
ylabel('Degree')

figure(12)
subplot(2,1,1)
plot(Tm,beta)
grid on
title('Measured Blade Angle')
xlabel('Time(sec)')
ylabel('Degree')

subplot(2,1,2)
plot(Tm,res)
grid on
title('Residual')
xlabel('Time(sec)')
ylabel('Residual')
axis([0 100 -0.3 0.3])

%simulate sensor faults 2
u4=[zeros(Ns+1,1)];
u5=[zeros(Ns+1,1)];
u6=[zeros(Ns+1,1)];
u7=[zeros(600,1);-ones(100,1)*0.5;zeros(301,1)];
u8=[zeros(Ns+1,1)];
```

```
[Tm,X,beta,omg_r,omg_g,res,sta_e]= ...

sim('RubustObserver_system_fault170803',tt,[],[tt,u1],[tt,u2],[tt,u3]
,[tt,u4],[tt,u5],[tt,u6],[tt,u7],[tt,u8]);

figure(13)
plot(Tm,omg_r)
grid on
title('Rotor Speed')
xlabel('Time(sec)')
ylabel('Rad/s')

figure(14)
plot(Tm,u7)
grid on
title('Sensor Fault 2: omg_r')
xlabel('Time(sec)')
ylabel('Fault')

figure(15)
subplot(2,1,1)
plot(Tm,omg_r)
grid on
title('Measured Rotor Speed')
xlabel('Time(sec)')
ylabel('Rad/s')

subplot(2,1,2)
plot(Tm,res)
grid on
title('Residual')
xlabel('Time(sec)')
ylabel('Residual')

%simulate sensor faults 3
u4=[zeros(Ns+1,1)];
u5=[zeros(Ns+1,1)];
u6=[zeros(Ns+1,1)];
u7=[zeros(Ns+1,1)];
u8=[zeros(800,1);ones(100,1)*1.5;zeros(101,1)];

[Tm,X,beta,omg_r,omg_g,res,sta_e]= ...
```

```
sim('RubustObserver_system_fault170803',tt,[],[tt,u1],[tt,u2],[tt,u3]
,[tt,u4],[tt,u5],[tt,u6],[tt,u7],[tt,u8]);

figure(16)
plot(Tm,omg_g)
grid on
title('Generator Speed')
xlabel('Time(sec)')
ylabel('Rad/s')

figure(17)
plot(Tm,u8)
grid on
title('Sensor Fault 3: omg_g')
xlabel('Time(sec)')
ylabel('Fault')

figure(18)
subplot(2,1,1)
plot(Tm,omg_g)
grid on
title('Measured Generator Speed')
xlabel('Time(sec)')
ylabel('Rad/s')

subplot(2,1,2)
plot(Tm,res)
grid on
title('Residual')
xlabel('Time(sec)')
ylabel('Residual')
axis([0 100 -50 50])
```

APPENDIX 3

NEURAL NETWORK MATLAB CODE

```
clear all;


pi    = 3.1415;
R     = 63;                  % m      rotor disc radius
rho   = 1.225;               % kg/m3  mass density of air
N     = 97;                  %       gear ratio
Ir    = 5.9154e7;            % kg m2  inertia of rotor
Ig    = 500;                 % kg m2  inertia of generator
Ds    = 6.215e6;             % N/m s  Driveshaft damping constant
Ks    = 8.6763e8;            % N/m s  Driveshaft spring constant
Prate = 5e6;                 % W      Rated Power
omgrate=12.1;                % rpm    Tated rotor speed in rpm
omgr_rate= (2*pi*omgrate)/60;  % rad/s  Rated rotor speed in rad/s
tau=0.1;                     %       Generator actuator time constant
Tg_reff = Prate/(omgr_rate*N);
beta_ref=35;
vw=20;                       % m/s    Wind Speed
wn    = 0.88;                % rad/s  pitch actuator natural frequency
zeta  = 0.9;                 %       pitch actuator damping


A=[0 0 0 0 1;
   0 -Ds/Ir Ds/(Ir*N) -Ks/Ir 0;
   0 Ds/(Ig*N) -Ds/(Ig*N^2) Ks/(Ig*N) 0;
   0 1 -1/N 0 0;
   -wn^2 0 0 0 -2*zeta*wn;];

B=[0 0 0;
   1/Ir 0 0;
   0 -1/Ig 0;
   0 0 0;
   0 0 wn^2;];

C=[1 0 0 0 0;
   0 1 0 0 0;
   0 0 1 0 0];

E=[0 ;1/Ir ;0 ;0 ;0 ];
```

```
F=[0; 0; -1/Ig; 0; 0];
G=[ 0; 0; 0; 0; -2*zeta*wn];
Q=[1;1;1];

vw_min=5;
vw_max=40;

beta_ref_min=10;
beta_ref_max=35;

Tg_ref_min=0.1*Prate/(omgr_rate*N);
Tg_ref_max=1*Prate/(omgr_rate*N);

Nn=1000;

%******************************* Generate vw as the first input

%*********************************random input
 ll=ceil(20*rand(2000,1));
 ll=20*ones(2000,1);
 vw=zeros(0,1);
 for i=1:2000
     uu=vw_min+(vw_max-vw_min)*rand;
     if uu>15 && uu<30
         uu=uu+5*(rand+1)/2;
     end
     for j=1:ll(i)
         vw=[vw;uu];
     end
 end
 vw=vw(1:Nn,1);



figure(1)
plot(vw)
grid on
title('Generate input Wind Speed')
xlabel('Time(sec)')


%******************************* Generate beta_ref as the second
input
 ll=ceil(20*rand(2000,1));
```

```
 beta_ref=zeros(0,1);
 for i=1:2000
    uu=beta_ref_min+(beta_ref_max-beta_ref_min)*rand;
    if uu>15 && uu<30
       uu=uu+2*(rand+1)/2;
    end
    for j=1:ll(i)
       beta_ref=[beta_ref;uu];
    end
 end
 beta_ref=beta_ref(1:Nn,1);




figure(2)
plot(beta_ref)
grid on
title('Generate input beta_ref')
xlabel('Time(sec)')


%****************************** Generate Tg_ref as the third input
ll=ceil(20*rand(2000,1));
 Tg_ref=zeros(0,1);
 for i=1:2000
    uu=Tg_ref_min+(Tg_ref_max-Tg_ref_min)*rand;
    if uu>0.3*Prate/(omgr_rate*N) && uu<0.6*Prate/(omgr_rate*N);
       uu=uu+1000*(rand+1)/2;
    end
    for j=1:ll(i)
       Tg_ref=[Tg_ref;uu];
    end
 end

 Tg_ref=Tg_ref(1:Nn,1);


figure(3)
plot(Tg_ref)
grid on
title('Generate input Tg_ref')
xlabel('Time(sec)')
```

```
Ts=0.1;
Tm=100;
Ns=Tm/Ts;
tt=Ts*(1:Ns)';
u1=vw;
u2=beta_ref;
u3=Tg_ref;
u4=[zeros(Ns,1)];
u5=[zeros(Ns,1)];
u6=[zeros(Ns,1)];
u7=[zeros(Ns,1)];
u8=[zeros(Ns,1)];

[Tm,X,beta,omg_r,omg_g]= ...

sim('WTmdl',tt,[],[tt,u1],[tt,u2],[tt,u3],[tt,u4],[tt,u5],[tt,u6],[tt
,u7],[tt,u8]);

figure(4)
plot(beta)
grid on
title('Blade Angle')
xlabel('Time(sec)')
ylabel('Degree')

figure(5)
plot(omg_r)
grid on
title('Rotor Speed')
xlabel('Time(sec)')
ylabel('rad/s')

figure(6)
plot(omg_g)
grid on
title('Generator Speed')
xlabel('Time(sec)')
ylabel('rad/s')

%******************************** Prepare data
u=[vw beta_ref Tg_ref];
y=[beta omg_r omg_g];
Nu=length(u);
```

```
nh=10;

minu=min(u);maxu=max(u);
miny=min(y);maxy=max(y);
su=(u-ones(Nu,1)*minu)./(ones(Nu,1)*(maxu-minu));
sy=(y-ones(Nu,1)*miny)./(ones(Nu,1)*(maxy-miny));



x=[sy(3:Nu,:) sy(2:Nu-1,:) sy(1:Nu-2,:) su(3:Nu,:) su(2:Nu-1,:)
su(1:Nu-2,:)];


[c,ro]=kmeansg(x',nh);
ro=ro*24;

%****************************** Recursive training
lam=0.99;
w=1e-8*rand(nh,3);
P=1e8*eye(nh);
%yh=sy;
yh(1:5,:)=sy(1:5,:);

for i=4:Nu-300
    x=[yh(i-1,:) yh(i-2,:) yh(i-3,:) su(i-1,:) su(i-2,:) su(i-3,:)]';

    for j=1:nh
        fi(j,1)=exp(-(x-c(:,j))'*(x-c(:,j))/ro(j)/ro(j));
    end
    yh(i,:)=fi'*w;
    L=P*fi/(lam+fi'*P*fi);
    w=w+L*(sy(i,:)-fi'*w);
    P=(P-P*fi*fi'*P/(lam+fi'*P*fi))/lam;
end

for i=Nu-300:Nu
    x=[yh(i-1,:) yh(i-2,:) yh(i-3,:) su(i-1,:) su(i-2,:) su(i-3,:)]';

    for j=1:nh
        fi(j,1)=exp(-(x-c(:,j))'*(x-c(:,j))/ro(j)/ro(j));
    end
    yh(i,:)=fi'*w;
end
```

```
mae=mean(abs(sy(1:Nu-300)-yh(1:Nu-300)));
mae1=mean(abs(sy(Nu-300:Nu)-yh(Nu-300:Nu)));

res0=sy-yh;

MAE_beta=sum(abs(res0(:,1)))/Nu
MAE_omg_r=sum(abs(res0(:,2)))/Nu
MAE_omg_g=sum(abs(res0(:,3)))/Nu

figure(7)
subplot(311)
plot(1:Nu,sy(:,1),1:Nu,yh(:,1))
subplot(312)
plot(1:Nu,sy(:,2),1:Nu,yh(:,2))
subplot(313)
plot(1:Nu,sy(:,3),1:Nu,yh(:,3))

figure(8)
subplot(311)
plot(1:Nu,res0(:,1))
axis([0 1000 -1 1]);
subplot(312)
plot(1:Nu,res0(:,2))
axis([0 1000 -1 1]);
subplot(313)
plot(1:Nu,res0(:,3))
axis([0 1000 -1 1]);


%************************************************

vw=20*ones(5000,1);

beta_ref=20*ones(5000,1);

Tg_ref=0.8*Tg_reff*ones(5000,1);

Ts=0.1;
Tm=500;

Ns=Tm/Ts;
tt=Ts*(1:Ns)';
u1=vw;
u2=beta_ref;
```

```
u3=Tg_ref;
u4=[zeros(Ns,1)];
u5=[zeros(Ns,1)];

u6=[zeros(1000,1);1.2*ones(500,1);zeros(3500,1)];    %sensor fault 1

u7=[zeros(2500,1);1.5*ones(500,1);zeros(2000,1)];    %sensor fault 2

u8=[zeros(4000,1);1.3*ones(500,1);zeros(500,1)];     %sensor fault 3


[Tm,X,beta,omg_r,omg_g]= ...

sim('WTmdl',tt,[],[tt,u1],[tt,u2],[tt,u3],[tt,u4],[tt,u5],[tt,u6],[tt
,u7],[tt,u8]);


u1=[vw beta_ref Tg_ref];
y1=[beta omg_r omg_g];
Nt=length(u1);

minu=min(u);maxu=max(u);
miny=min(y);maxy=max(y);
su1=(u1-ones(Nt,1)*minu)./(ones(Nt,1)*(maxu-minu));
sy1=(y1-ones(Nt,1)*miny)./(ones(Nt,1)*(maxy-miny));

yh1(1:5,:)=sy1(1:5,:);

for i=4:Nt
    x=[yh1(i-1,:) yh1(i-2,:) yh1(i-3,:) su1(i-1,:) su1(i-2,:) su1(i-
3,:)]';

    for j=1:nh
        fi(j,1)=exp(-(x-c(:,j))'*(x-c(:,j))/ro(j)/ro(j));
    end
    yh1(i,:)=fi'*w;
end

[Tm,X,sy2,yh2]= ...
    sim('fault_dis',tt,[],[tt,sy1],[tt,yh1]);


res1=sy2(:,1)-yh2(:,1);
res2=sy2(:,2)-yh2(:,2);
```

```
res3=sy2(:,3)-yh2(:,3);

figure(9)
subplot(311)
plot(1:Nt,sy2(:,1),1:Nt,yh2(:,1))
subplot(312)
plot(1:Nt,sy2(:,2),1:Nt,yh2(:,2))
subplot(313)
plot(1:Nt,sy2(:,3),1:Nt,yh2(:,3))

figure(10)
subplot(311)
plot(1:Nt,res1)
subplot(312)
plot(1:Nt,res2)
subplot(313)
plot(1:Nt,res3)
axis([0 5000 -0.5 1]);

figure(11)
title('Faults MFs')
subplot(311)
plot(1:Nt,u6)
axis([0 5000 -0.5 1.5])
subplot(312)
plot(1:Nt,u7)
axis([0 5000 -1.75 0.5])
subplot(313)
plot(1:Nt,u8)
axis([0 5000 -0.5 1.5])

figure(12)
plot(1:Nt,res1)
title('Model Prediction Error for Blade Pitch Angle Sensor Fault')


figure(13)
plot(1:Nt,res2)
title('Model Prediction Error for Rotor Speed Sensor Fault')


figure(14)
plot(1:Nt,res3)
title('Model Prediction Error for Generator Speed')
```